THE UNIVERSITY OF ALBERTA

Seismic Stability Studies near the Middle America Trench

by

Antonio Uribe Carvajal

A THESIS

SUBMITTED TO THE FACULTY OF GRADUATE STUDIES AND RESEARCH

IN PARTIAL FULFILMENT OF THE REQUIREMENTS FOR THE DEGREE

OF Doctor of Philosophy

IN

Geophysics

Department of Physics

EDMONTON, ALBERTA

Fall 1984

THE UNIVERSITY OF ALBERTA

RELEASE FORM

NAME OF AUTHOR Antonio Uribe Carvajal

TITLE OF THESIS Seismic Stability Studies near the Middle America Trench

DEGREE FOR WHICH THESIS WAS PRESENTED Doctor of Philosophy

YEAR THIS DEGREE GRANTED Fall 1984

Permission is hereby granted to THE UNIVERSITY OF ALBERTA LIBRARY to reproduce single copies of this thesis and to lend or sell such copies for private, scholarly or scientific research purposes only.

The author reserves other publication rights, and neither the thesis nor extensive extracts from it may be printed or otherwise reproduced without the author's written permission.

(SIGNED) ....

PERMANENT ADDRESS:

Sur 71B #319
Col. Justo Sierra. 09460
Mexico 13, D.F., Mexico

DATED ....June 20......1984

THE UNIVERSITY OF ALBERTA

FACULTY OF GRADUATE STUDIES AND RESEARCH

The undersigned certify that they have read, and recommend to the Faculty of Graduate Studies and Research, for acceptance, a thesis entitled Seismic Stability Studies near the Middle America Trench submitted by Antonio Uribe Carvajal in partial fulfilment of the requirements for the degree of Doctor of Philosophy in Geophysics.

Ed. Nyland

Supervisor

E. R. Kanasewich

Anton Z. Capri

R. St J. Lambert

H. Hasegawa

External Examiner

Date June 15, 1984

Dedication

To

Salvador, Eva Natalia,

Margarita,

Claudia and Adriana.

Abstract

Stress estimates obtained from modelling various regions near the Middle America trench have been combined with rock failure criteria expressed in statistical terms to yield probabilistic measures of seismic risk in these areas. These measures allow the study of different geodynamic processes, in such a way that the probable location of seismic failure can be estimated. Repetitive modelling of a system evolving in time can suggest the most likely time of failure.

A new measure of seismic instability has been developed which combines the stress components into a unique measure of seismic risk. This function depends on the material properties, and the geological structures involved in a particular problem.

The results obtained here for the Valley of Mexico are in agreement with the observed seismicity and the geodynamic knowledge of the area. This seismic activity seems to be triggered by the reduction of water in the aquifer that underlies Mexico City.

The distance at which the stress drop due to the occurrence of an earthquake can affect the seismic behaviour of distant locations is linked to the thickness of the elastic part of the tectonic plate at the epicentral location. This variation on the possible range of seismic activity supports the existence of long term precursors for distances up to 10^3km.

The high risk areas derived from the models can be identified with seismic active areas. This is done with simple models of the geodynamic processes involved. The material properties used are in general the elastic parameters and their variation with temperature. The external forces applied to the models are those that have the potential to change the overall distribution of seismic instability such as the gravitational pull of the downgoing slab, the viscous drag of the mantle and the frictional force between plates. Therefore, these distributions are regional in nature.

In spite of these simplifications, the distributions of seismic instability calculated for the Middle America trench region are in accordance with the observed seismic behaviour of the area. Shallow activity (depth≤70 km) along both sides of the trench is more frequent than in the North America-Caribbean plate boundary. Deep earthquakes are more likely to occur in the trench south of the Tehuantepec ridge. Events in this southern branch have a smaller range of effects than those to the north of the ridge due to the difference in the cohesion between the plates and the subducting angle.

Acknowledgements.

I would like to express my gratitude to my supervisor Prof. Edo Nyland for his patience, guidance and friendship. To him I owe many thanks for reinforcing my interest in Geodynamics and focusing my efforts in the direction that has resulted in this document.

This work is a product of the combined efforts of many authors, which I have referred to throughout the text, and from the lectures I have recieved from many professors. To all of them, I am in debt.

I take this opportunity to thank Prof. N. Morgenstern and the Geotechnical Engineering group of this University for allowing me to share their computational resources.

I would like to thank all my colleagues for many useful discussions, particularly those who helped me with the proofreading of the thesis.

I am grateful to the National Council of Science and Technology of Mexico (CONACYT) and to the Department of Physics of the University of Alberta for their financial support during my studies here.

I thank my wife Margarita and my parents Salvador and Eva Natalia for their unconditional support, and my daughters Claudia and Adriana for making this one of the most enjoyable periods of my life.

Table of Contents

Chapter Page

1. Introduction. 1

1.1 The Problem. 3

1.2 Stress and Strain in the Earth Sciences. 3

1.3 Stresses and Earthquakes. 10

1.4 Stress modelling in geodynamics. 13

1.5 Methods For Determining Tectonic Stress States. 21

1.6 Some Earthquake Related Phenomena 29

2. Types of failure and stability studies. 35

2.1 Rock Failure. 35

2.2 The Stability of Earth Materials. 42

2.3 General definition of stability. 46

2.4 Instability function in three dimensions. 50

2.5 Residual Stability Function. 54

2.6 The Probability Function. 57

2.7 General comments on the instability functions. ..63

3. Elastic models of seismic failure and its application to the Valley of Mexico 65

3.1 Introduction 66

3.2 Previous Seismo-Geodynamical Studies 72

3.3 Seismic instrumentation inside the area 75

3.4 State of stress 78

3.5 Discussion of Elastic Models 90

3.6 Porous media modelling 98

3.7 Conclusions 104

4. Thermo-elastic Behaviour of the Subducting Lithosphere, and its Relation to Long Range Precursors. 107

4.1 Introduction. 108

4.2 The Method. 114

4.3 The subduction zone models. 126

4.4 Discussion of results. 141

4.5 Conclusions. 149

5. Earthquake risk studies for the problem of induced seismicity on water reservoirs applied to the Itzantun site. 151

5.1 Evaluation of the risk of induced seismicity. ..152

5.2 General concepts on induced seismicity 155

5.3 The Itzantun site 160

5.4 Natural seismicity levels 162

5.5 Model studies 167

5.6 The approach 169

5.7 Discussion of Results 171

5.8 Conclusions about instability at Itzantun. 178

6. Discussion of results and further studies proposed .181

6.1 The Cocos-North America-Caribbean triple junction. 182

6.2 Stress determination on seismic active areas. ..193

6.3 Concluding remarks. 195

References. 197

Appendix A. Introduction to Finite Elements. 211

Appendix B. Calculation of stress increments in porous media. 225

Table Captions.

Table Page

1. Dependence of the material properties on temperature of the thermo-elastic models studied.................................... 125

2. Effect of the thickness of an elastic plate on the distance from an applied force at which a given displacement takes place................ 144

3. Variation of the stability function for different rates of filling of the Itzantun reservoir.................................. 175

4. Input data that originated Figure 46 using the procedure described by equations (B.25) to (B.32)..................................... 239

Figure Captions.

Figure Page

1. Seismicity of the earth (Richter,1958)........ 11
2. Earthquake recurrence patterns................ 31
3. Mohr-Coulomb failure criterion in a shear stress vs normal stress diagram (a) and in principal stresses diagrams in two dimensions (b) and in three dimensions (c).............. 37
4. Drucker-Prager failure criterion.............. 39
5. Examples of Hoek and Brown's (1980)empirical failure criterion for a) sandstones and b)for granites.................................. 41
6. General definition of instability as the minimum distance from the surface of the Mohr circle to the failure criterium............... 48
7. Definition of the instability function in three dimensions............................ 52
8. Definition of residual instability as the minimum distance between the Mohr circle and the Coulomb failure envelope................. 55
9. Definition of the probability function........ 59
10. Earthquake locations inside the Valley of Mexico. The numbers in this figure indicate known locations; 1 Ciudad Universitaria, 2 Chapultepec,3 Alameda and 4 Texcoco........... 69
11. Number of events recorded in the Valley of Mexico vs time (modified from Figueroa, 1971). 74
12. Location of the seismic stations of the SISMEX network.................................. 77

13. a) Resulting instability distribution in bars. b) Shows in the bottom the displacement suffered due to the gravitational load........ 81

c)Stress components and the corresponding residual instability distribution for a gravitational model of the Valley of Mexico... 83

14. Residual instability distributions in bars, resulting from varying the slope angle. a) For a slope of 60° and b) For a slope of 30°...... 86

15. Residual instability distribution in bars for the following variations: a) a cone has been introduced in the bottom b) the left side of the valley has roughened...................... 87

16. Residual stability distribution for a cross-section on the line AB (figure 17). The shaded area represents the location of observed seismicity.......................... 89

17. Observed piezometric drop in the valley given in meters. The shaded area represents the location of observed seismicity.............. 93

18. Stability changes due to the change in the gravitational load for different stress environments. a) normal faulting, b) thrust faulting and c) strike-slip faulting environment................................. 95

19. Observed subsidence of the valley given in meters. The shaded area represents the location of observed seismicity.............. 97

20. Change in pore pressure given in bars, calculated due to the pumping of water from the underlying formations of the Valley of Mexico..................................... 101

21. Different types of subducting zones resulting from plate coupling considerations (modified from Kanamori, 1977)......................... 115

22. Nodal distribution used in the initial models. 128

23. Elastic modelling of a subducting zone. a, b are the probability distributions before and after the occurrence of an earthquake at *.... 129

24. Thermoelastic model of a subducting zone at 45°. a and b the same as in figure 23......... 133

25. Probability distributions for a trench with a slab subducting at 10°. a and b as before..... 136

26. Probability distributions for a trench with a slab subducting at 60°. a and b as before..... 137

27. Probability distributions for a trench with a long slab subducting at 45°. a and b as before....................................... 139

28. Probability distributions for a trench with a long slab subducting at 60°. a and b as before....................................... 140

29. Calculated deformation of a shear fractured lithosphere subject to a horizontal compressive stress of 10^9 dynes/cm^2, (modified from Gunn, 1947)............................ 154

30. Location map of the study area............... 161

31. Major geologic features of the area of Itzantun................................. 163

32. Seismic stations and epicentral determinations 165

33. Deep events located by the Itzantun network... 166

34. Deep events from figure 33 in a depth vs their distance to the Middle America trench diagram. 168

35. The upper graph shows a loading history, where the total load is reached after 2 years of loading. The bottom graph shows the instability at 1 km depth.................... 173

36. The upper graph shows a loading history, where the total load is reached after 16 years of loading. The bottom graph shows the instability at 1 km depth.................... 174

37. The upper graph shows a loading history in which an unload takes place before the total load is attained. The bottom graph shows the instability at 1 km depth.................... 177

38. The upper graph shows the same loading history as that of figure 37. The bottom graph shows the instability at 4 km depth................. 179

39. Tectonic features and epicentral locations recorded in the triple junction area. a) Shows the shallow earthquakes (depth< 70 km) and b) the intermediate and deep events (modified from Molnar and Sykes, 1969).................. 183

40. Two dimensional model of the area............ 185

41. Element distribution used for the three dimensional model............................ 188

42. Probability function distributions for horizontal cross-sections at depths of a) 25, b) 50, c) 100 and d) 150 km.................. 190

43. Probability distribution at the upper surface of the slab with depth...................... 191

44. Instability of a model of a magmatic intrusion. a) no buoyancy forces are applied. b)Buoyancy forces are applied at the bottom of the intruding body........................... 194

45. Subdivision of a continuum material into finite elements............................. 216

46. Loading history with several exponential segments.................................... 238

1. Introduction.

Earthquakes can be treated as mechanical instabilities. They occur when the rock is unable to support an increase of stress. Therefore, seismic risk studies are approached here by determining how stable the rocks are under various stress conditions.

Many failure criteria exist for rocks and it is not obvious that any of them are representative for the geological scales used here. Nevertheless, it is possible to overcome this problem by using a generalized definition of seismic instability independent of the type of failure envelope used. This will allow the failure criteria to be changed without losing any generality.

Different geodynamic processes will be treated throughout this work in which it will be necessary to vary the material properties and the stress-strain relations that describe the behaviour of the materials involved. These different exercises will provide an insight into the geodynamical processes occurring in the Middle America trench region, as well as illustrate what kind of studies can be done with these kinds of procedures.

The results obtained can be generalized to other areas. Explanations of some observed seismic phenomena can be derived, (eg. Why does the range of long term precursors vary?). Instability distributions will be shown as predictors of the possible location of failure initiation or as time predicting functions for particular locations.

Individual studies of different seismically active areas related geodynamically to the different parts of the Middle America trench give an overall picture of the region. Stresses calculated by means of the finite elements technique will be used in some cases, analytical methods will be applied in others.

The determination of the stability of state of stress in the earth is of vital importance in understanding any of the different processes which occur in the interior of the earth. In this chapter the current knowledge of the propagation of stresses in the upper part of the earth is reviewed. I briefly mention the different techniques that exist for measuring these stresses, I explore the possible relation between earthquakes and stresses; between the tectonic models of the earth and the location of the observed seismic activity; and the consequences that the different kinds of seismic behaviour observed might have in our understanding of the earth.

In chapter 2, I connect these stress arguments to the occurrence of seismic failures by means of a definition of seismic stability. Once defined this concept can undergo several variations which are discussed in sections 2.3 to 2.6. These individual forms are applied throughout chapters 3 to 6.

1.1 The Problem.

Geodynamics is the quantitative study of the processes that take place in the real earth. A major problem that it has to overcome is that direct observations of these processes in the interior of the earth are impossible; knowledge relies on the interpretation of a series of geophysical observables, from which reasonable deductions may be made. This thesis deals with the geodynamical mechanical state of the earth and this mechanical state can be studied through the distribution and propagation of stresses and strains throughout the different materials that constitute the earth. In particular, the way the stress state may be related to seismic instability is examined here.

1.2 Stress and Strain in the Earth Sciences.

The concepts of stress and strain are fundamental to the interpretation of earthquake mechanisms, and any study of structural geology needs them for any description of rock behaviour. The stresses that exist in a given rock mass or geological area control the processes that result in the mechanical state of this material, and allow us to make predictions of the changes that might occur in the future.

Strains and displacements are frequently measured, and from these the stresses can be deduced. The stresses at a point in the interior of a body are determined by the system of forces that act in the vicinity of that given point. The deformation of the body in the vicinity of such point is termed strain (Richter, 1958). The analysis of strain is fundamental for studies of the deformation of any material (Jaeger and Cook, 1979). The study of stress is in itself a pure static analysis, independent of the properties assumed for the material which may be elastic, plastic or any other. This means that in order to state the amount of stress on a given point inside a body it is not necessary to specify the physical properties of the body itself.

Knowledge of the history of the stress state is also fundamental to the understanding of the tectonic processes that occur in the earth. However stress values are very difficult to obtain even for a single location of the earth lithosphere; Wyss (1977) mentions this difficulty and points out that of the six components of the stress tensor usually only a few can be estimated.

Rock behaviour under stress changes is poorly understood, since it depends on many factors like the forces that have been applied previously, the duration of such forces, the confining pressure and the temperature. In geodynamical terms the state of stress is linked to causes (loading and unloading, heating and cooling, plate motions and driving forces, etc.), to consequences (creep deformation, and seismic failure), and to rheology (the depth over which stress can be supported and the time dependence of material properties). None of these links has been characterized in sufficient detail to define the constitutive equation for any part of the lithosphere without making many assumptions (Solomon et al., 1980).

Due to the lack of understanding of the earth processes and the relation between the strains and stresses at depth, the constitutive relationship is poorly understood. Several ways to relate them have been proposed; it has been found from laboratory tests that strain in rocks increases in a linear way when they are subjected to small external stresses. This kind of linear dependence between stress and strain is named linear elasticity and is characterized by the generalized Hooke's law

$$\sigma_{ij}=C_{ijmn}\epsilon_{mn} \tag{1.1}$$

where σ_{ij} are the cartesian components of the stress tensor, C_{ijmn} the elastic modulus components. The components ϵ_{mn} of the infinitesimal strain tensor are defined in terms of **u** by

$$\epsilon_{mn}=(u_{n,m}+u_{m,n})/2 \tag{1.2}$$

where $\mathbf{u}(\mathbf{x})$ is the distortion suffered by a body at point x when a set of forces is applied to it, the displacement of a particle originally at **x**, from the initial state to the distorted one. The initial state need not be stress free.

While this kind of constitutive relation seems adequate for many geophysical and engineering purposes, there is need for a more sophisticated formulation to account for the non-linear behaviour observed in rocks when the temperature and confining pressure increase. One equation that seems to describe these observations is that of a viscous or visco-elastic material (Jaeger and Cook, 1979),

$$\dot{\epsilon} = E^{-1}\dot{\sigma} + \sigma/\eta \tag{1.3}$$

where E is the Young's modulus and η the viscosity of the material.

The dependence of equation 1.3 on temperature and confining pressure is implied in the viscosity. It is important to note that this equation predicts that:

1. For high stress rate ($\dot{\sigma}$) the first term will dominate and the material will behave elastically.
2. For small $\dot{\sigma}$ values the second term will dominate giving the material a viscous behaviour.
3. As the confining pressure and the temperature increase, the material becomes gradually less viscous until it reaches a "fluid" state.

Savage and Prescott (1978), proposed this kind of behaviour to model depth dependence of the stresses in the earth. Ringwood (1975), also suggested a non-linear kind of stress variation with depth for ocean and continental rocks. Kirby (1977), explains that in experiments conducted in cylinders of rock subject to a uniaxial stress state $\sigma_{11} \neq \sigma_{22} = \sigma_{33} = P$ where the x_1 direction is parallel to the cylinder axis and P is the confining pressure, the differential stress $\sigma=|\sigma_{11}-P|$ is related to the strain rate $\dot{\epsilon}$, temperature T and pressure P for most earth materials by the non-linear expression

$$\dot{\epsilon}=A'[\sinh(a\sigma]^{n}\exp[-(E'+PV')/RT] \qquad (1.4)$$

where A',E',a,η and V' are material properties and R is the gas constant. Equation 1.4 for large temperature and pressure becomes the exponential law

$$\dot{\epsilon}=A\ \exp(\beta\sigma)\ \exp[-(E'+PV')/RT] \qquad (1.5)$$

where A=A'/2 and $\beta=\eta a$. This type of equation (1.5) is taken by Kirby (1977) and Savage and Prescott (1978) and others, as representative of the upper part of the mantle. In this thesis the elastic behaviour of the upper part of the crust and the viscoelastic nonlinear behaviour of the stresses in depth and temperature will be used extensively.

It seems probable that earthquakes are mechanical instabilities evidenced by a sudden failure of the rock to sustain the shear stress acting across a surface; the surface is usually an already existing fault but may be one newly created by the failure. Due to the large time scales in which geologic processes take place it is possible to picture the earth in equilibrium at any time. This implies that the rate of accumulation of stress in the earth's upper layers is relatively small.

Nevertheless, when the accumulated stress overcomes the strength of the rocks, failure occurs. Stability values can measure the probability that failure will occur in a particular location within a given volume. This volume could contain several materials and may contain discontinuities. The only constraint is that the stress-strain relationships throughout the whole body have to be known or at least assumed.

Stability is then a function of the state of stress at particular locations, it compares this state of stress with the overall stress, to obtain a measure of how stable these locations are with respect to the surrounding areas. The stability functions that have been developed will be discussed in chapter 2 of this thesis.

The reason why earthquakes occur only at particular locations of the earth's lithosphere is due to concentrations of stresses at weakened areas; The combination results in unstable areas. These concentrations are likely to occur if forces are applied at particular locations of a body within the neighbourhood of the application point. They also appear in the vicinity of any kind of discontinuity, which can be a sharp boundary or other change in physical properties. A simple example can be stated. If a force is applied at the surface of an elastic plate, the plate will deform in the vicinity of the point of application. At locations away from the force the plate has not suffered any distortion at all. This distortion is linked to the stresses by the relations in section 1.1, therefore, the stresses due to this force diminish with the distance to the applied force. The rate of attenuation is determined by the stress-strain relationship characteristic for the material.

The degree of instability is given by the system of forces acting in the area and the geological structures and type of material present in it, and its "strength". All these things combine in such a way that the smaller the stability of a location is, the greater probabilty it has to be the origin of a seismic event.

It is the purpose of this thesis to demonstrate how simple notions of rock mechanics can combine with what is known about earthquakes to develop a simple stability criterion. This criterion may give us insight into aspects of earthquake generation, and probable causes for some of the earthquake related phenomena observed. Application to particular problems will be demonstrated throughout the following chapters. In order to attack each of these problems the stability criterion will suffer small changes that will be explained in the corresponding parts of this thesis. However, the general features of stability will remain valid. In chapter 2 these generalities are presented.

1.3 Stresses and Earthquakes.

An earthquake can be thought of as a sudden release of energy that takes place at a particular location, and is associated with faulting or other dynamic processes. Hypocenter is a term used since the 1850's when Mallet and others believed that an earthquake originated in a small volume that could be represented by a point for most purposes (Richter, 1958), and used to designate the location of the origin of the earthquake. The term is now thought of as the location of the initial rupture of the rocks, where the earthquake originates.

Richter (1958), also recognized that the energy source for a tectonic earthquake is energy stored within the earth during a long period of growth of strain. If the associated stresses accumulate continuously they will reach the peak strength of the rock and failure will generally occur. He also concluded that fracture will occur along preexisting weaknesses and that the active faults are weakness planes where fractures occur one after the other.

The seismic belts on the surface of the earth are where most earthquakes are located (figure 1), (Richter,1958). This observation was made by Gutenberg (1949), and he suggested that the stress in these belts somehow is accumulating and as result of this, earthquakes are being produced.

There are two main types of activity occurring within the seismic plate. One type results from stresses due to the

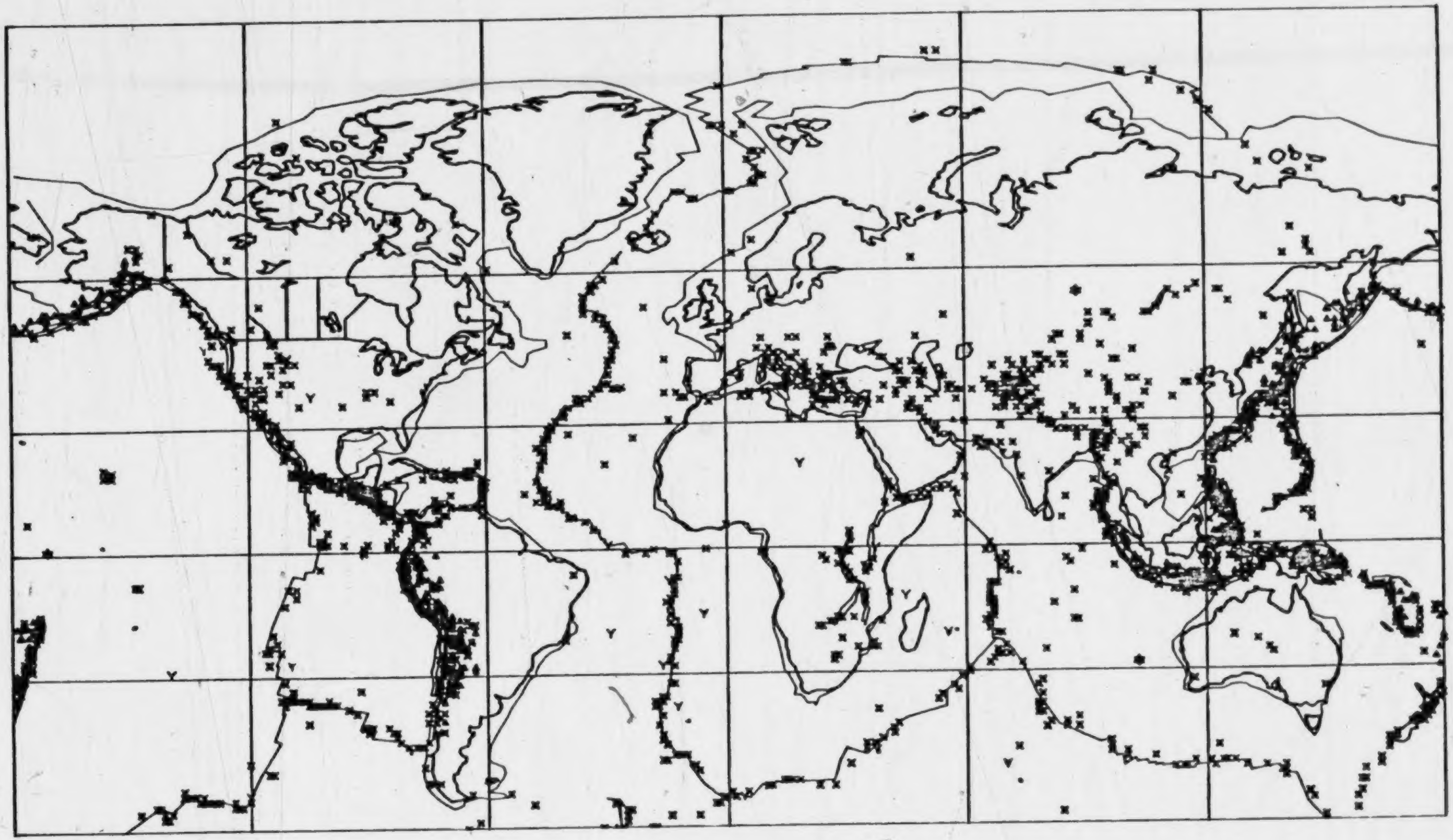

Figure 1.... seismicity of the earth-seismic belts.

deformation of the plate itself; these are earthquakes that take place close to the plate boundaries. They are due to the bending of the plate (Isacks et al., 1968). There are also earthquakes that result from stresses transmitted through the plate away from its boundaries (Isacks and Molnar, 1971).

The implications of seismic observations are that the generation of earthquakes in a subduction zone is governed by the distribution of stresses within the lithosphere and by changes in the physical properties of the material due to the presence of the subducting slab (Isacks and Molnar,1971). Several hypotheses exist to explain shear fractures observed at intermediate depths. The one that suggests a high pressure, high temperature mechanical instability (Byerlee and Brace, 1969) seems to be the most appropriate. It is expected that the cold slab remains cooler than the surrounding medium (which was already at higher temperatures, when the process started), down to a depth where the slab cannot exist as a solid. This model of a cold subducting slab has been generaly accepted and the temperatures in it have been calculated with several models (i.e. McKenzie, 1969; Minear and Toksoz, 1970; Griggs, 1972).

These thermal induced stresses have no significant effect on the mechanisms of shallow earthquakes. The presence of this kind of seismic activity, may not be necessarily related to the plate boundaries but to local geological phenomena. For the study of this kind of earthquakes viscous behaviour of the surrounding medium is not to be expected due to the shallow depths at which they originate.

1.4 Stress modelling in geodynamics.

'The plate-tectonics hypothesis explains the tectonic and seismic activity now occurring within the upper layers of the earth as resulting from the interaction of a small number of large rigid plates whose boundaries are the seismic belts of the world. The plates outlined by these belts are not actively deformed except along their borders and the motion occurring within them is mostly limited to broad epirogenic movements. These plates may contain continental as well as oceanic surfaces. The seismic belts are zones where differential movements between plates take place' (Le Pichon, 1973).

Plate boundaries are zones of concentration of stress because they represent the discontinuities in the lithosphere. This means they are unstable in the sense used in this thesis. That physical properties of the lithosphere vary sharply has been inferred from the geophysical observations. If the plates also collide with each other, inter-plate forces generate concentrations of stress on their boundaries.

Cox (1973) points out that plate tectonics is a unifying hypothesis which provides a kinematic model of the upper layer of the earth, and that it can be used to make quantitative predictions about most phenomena studied by the different disciplines of the earth sciences. Plate tectonics links all these phenomena by postulating the existence of moving plates. Where two plates are moving apart, new oceanic floor is formed by solidification of molten rock in the opening crack. Where two converge, one of them is usually thrust beneath the other, forming oceanic trenches, generating earthquakes and as the descending plate melts rise to form volcanoes.

The basis of this hypothesis has been developed since the beginning of the century. It integrates the idea of continental drift and the idea of sea-floor spreading (Hess, 1962). However, the hypothesis itself was defined during the late nineteen sixties (Le Pichon, 1973) when the implications of the following ideas were understood:

1. The primary rheological stratification of the upper mantle and the crust into lithosphere and asthenosphere governs the mechanical behaviour of the upper layers of the earth (Isacks et. al.,1968).
2. Most of the mechanical energy of the surface of the earth is spent within a few narrow seismic belts (Richter, 1958).
3. There are geometrical constraints imposed on the displacements of rigid bodies at the surface of the earth (Wilson, 1965 and Bullard, 1965).

In the development of the plate tectonics hypothesis, there are many other important contributions, however, it is not the purpose of this work to present a complete review of how it has reached its present form, nor to go into the detailed description of all the phenomena that contribute to it. Nevertheless, the aspects mentioned above are of vital importance to what will be treated in this thesis. In particular, the rheological stratification of the mantle and lithosphere, and the different mechanical properties of the diverse intraplate boundaries are important.

The following concepts must be underlined:

1. The lithosphere,which includes the crust and the uppermost mantle, has significant strength and may be up to several hundred kilometers in thickness (Isacks et al., 1968).
2. The asthenosphere extends from the base of the lithosphere to a depth of a few hundred kilometers and is a layer of effectively little strength (Isacks et al., 1968).
3. A transfom fault is the interplate boundary where the relative velocity of one plate with respect to another is parallel to the boundary itself (Wilson, 1965). Turcotte (1974), explained this type of faults as the result of thermal contraction of the earth's crust, and suggest that they might be associated with the formation of a solid layer due to the cooling of a nonelastic "fluid". Another possible explanation is that transform

faults are a product of intraplate geometrical evolution (McKenzie and Morgan, 1969).

4. Converging zones are the intraplate boundaries where two plates collide with each other. If two plates of the same constitution meet, they deform and can produce mountain belts, like the Himalayas produced by the collision between India and Asia.

   If an oceanic plate collides with a continental one then the heavier oceanic plate subducts beneath the lighter continental one. This subduction zone is a consuming plate margin called a trench (i.e. McKenzie and Morgan, 1969), or an arc (i.e. Wilson, 1965) which are defined as lines of relative motion along which surface is destroyed asymmetrically. The surface is destroyed only on one side of the line.

5. Diverging zones or mid-ocean ridge crests, are lines of relative motion along which surface is produced symmetrically. The actual relative direction of motion need not be perpendicular to this line, but it often is (Le Pichon, 1973).

6. Triple junctions are points on the surface of the earth where three plates meet. The relations between the relative velocities of the plates determine the evolution of the triple junction in time. If the evolution of the triple junction is possible without a change in geometry, then the vertex is defined as a stable junction. If the junction can exist for an

instant only it is defined as unstable (McKenzie and Morgan, 1969). The junction of three transform faults is always unstable whereas the junction of three ridges spreading perpendicularly to their axis is always stable. Junctions with two boundaries in a straight line, fixed with respect to the plate they bound, are also always stable (Le Pichon, 1973). An unstable triple junction evolves to a more stable kind of triple junction.

It is also necessary to differentiate between oceanic and continental lithosphere because their material properties are different. Most investigators who have tried to define the detailed mechanical properties of the lithosphere have converged to a model of oceanic lithosphere that is consistent with the thermal models of the upper mantle, experimental rock mechanics, gravity and bathymetry surveys, and patterns of seismicity and focal mechanisms. In this model the lower oceanic lithosphere is visco-elastic and will not support loads for long time periods, but its stiffness may be important for transient loads or in the initial response to loading.

The upper lithosphere is elastic and is able to support loads for 10^9 years without appreciable relaxation (Forsyth, 1979). At a high state of stress it deforms elastically, yielding brittle fracture. The transition from the brittle regime of the upper lithosphere to the ductile regime of the lower layer is predominantly thermally controlled, thus the flexural rigidity increases as the lithosphere cools. This means that near a trench brittle failure may occur at greater depths than is possible near the ridges.

This pattern of higher rigidity for the cooler lithosphere would imply that for continental lithosphere, which is older, we should expect higher rigidity values than those for ocean basins provided temperature is the dominant parameter. Nevertheless, the flexural rigidity values obtained for samples of continental materials are smaller than those from oceanic lithosphere. The explanation (e.g. Forsyth,1979; McNutt, 1980) lies in the mineralogic composition of the continental rocks which in general are weaker and subjected to continuous isostatic movements. Therefore, the ductile regime in continental areas may in general be reached at a shallower depth than in the oceanic crust.

Observations of the dispersion of Rayleigh waves have shown a significant heterogeneity in the structure of the upper mantle beneath the Pacific Ocean. The heterogeneity is well correlated with lithospheric age. The lid to the low-velocity zone is very thin near the ridge crest and becomes thicker as it moves away from the ridge, reaching a thickness of about 60 km after 50 million years and about 85 km after 100 million years (Leeds et. al., 1974).

Hanks and Rayleigh (1980) introduce the notion of differentiation between the lithosphere and the "elastic plate", the upper part of the lithosphere. They point out that away from the major plate boundaries, the elastic plate can support several kilobars of deviatoric stress, in response to local or regional loads. Thatcher et al. (1980) by looking at the time-dependent aseismic deformation of the lithosphere resulting from large earthquakes suggest a thickness of the elastic plate of 30 to 60 km; which is done by modelling the lithosphere as an elastic plate overlying a viscoelastic half space.

McNutt (1980) concluded from gravity observations that the upper several tens of kilometers of both oceanic and continental intraplate regions can support a kilobar or so of deviatoric stress for roughly 10^9 years for intact rock. Turcotte et al. (1980) suggest that there is no significant difference in elastic strength between the elastic plates of both continental and oceanic lithosphere, at least in the orogenically stable areas. Moreover, in both areas the elastic plate has significant strength and a thickness of several tens of kilometers, on a time scale of billions of years.

The thickness of the lithosphere derived from flexural rigidity studies is the equivalent thickness of a plate with uniform properties, responding to a load applied on it (Cazenave et al., 1980). The values derived in this way for the thickness of the oceanic lithosphere are considerably less than those determined through seismic wave propagation studies (Leeds et al., 1974). A comparison between elastic and seismic thickness values for lithosphere of the same age suggest a ratio of about 1/3 (Cazenave et al., 1980).

There are many estimates of lithosphere thickness and they need not be the same. Seismic lithosphere is defined as the layer of high velocities and low attenuation of seismic waves. Another definition of lithosphere thickness is the thermal thickness, which separates the region where the conductive heat transport dominates from lower regions where convection is the principal mechanism of heat transport (Parsons and Sclater, 1977).

Based on the existence of the elastic plate described earlier, the determination of stresses in the upper few tens of kilometers of the earth can be approached by analysing elastic models, if the region under study is away from the interplate boundaries (Solomon et al., 1980). The modelling of regions within these boundaries should be done by taking into account the thermal dependence of the stresses that may be present in these areas. This approach will be followed for the different geodynamic problems in the next chapters. Kirby (1977) looks into this problem and gives the following suggestions:

1. A significant portion of the lithosphere could be described using a nonlinear strain-stress relation. At greater depths $\dot{\epsilon} \simeq \sigma^3$.
2. The upper part of the lithosphere should deform in the brittle failure. He mentions that in particular, in a subduction zone the upper 25 km of the plate should be under brittle deformation.

3. The stresses at the base of the lithosphere have a large range of variation due to change in the thickness of the plates.

It is also of prime importance to include the presence of fluids in the materials modelled, since it has been long recognized that variations in the pressure of these internal fluids can, and in fact do, change the state of stresses in a given region. This has been observed primarily in the induced seismic activity that has occurred in some artificial lakes after the impounding of the water reservoir had started as shown by Gough (1978), Simpson (1976, 1981), Withers and Nyland (1976, 1978), Bell and Nur (1978) and many others. The importance of this pore pressure is dependent on the porosity and permeability of the rocks in each model.

1.5 Methods For Determining Tectonic Stress States.

The seismic behaviour of different geodynamic systems varies widely from relatively small microearthquakes only detectable with highly sensitive instruments to large destructive earthquakes. The kind of seismic manifestations observed in a particular region must be representative of the state of stress that prevails in it. Different seismic behaviour should then characterize locations under different stress distributions.

For this reason I have started this thesis with a description of those aspects of earthquake seismology that will allow the definition of a stability criterion representative of the risk of an earthquake. This criterion should be such that it can be modified to become representative of the different stress enviroments which occur in the upper part of the lithosphere.

The use of materials with a linear elastic stress-strain relationship will prove to be a good first approximation in the selected cases. This will help in the treatment of more complicated situations. Elastic analysis combined with the hydrological characteristics of the site can result in reasonable conclusions about the distribution of risk in some areas. The modelling of materials with thermoelastic stress-strain relationships will enable us to get an insight into the physics behind the observed long range precursors of some large earthquakes. The use of a porous media will strongly suggest that the geometry of an applied water load, its loading history and the presence of weakness planes are the parameters that very well determine the presence of induced seismicity in particular areas. This last exercise will set the background necessary to analyse the classical approach to consolidation problems in water reservoir engineering in order to seek the time delays which are often observed in induced seismicity cases. The usual analysis does not predict these time delays in a satisfactory way.

In order to accomplish any of these goals, it is necessary to estimate the stresses at the location of interest. A logical way to proceed is to try to make some sense of the state of stress from observed measurable phenomena; this is the case of the seismic behaviour which can be quantified.

Two admittedly imperfect methods exist for assessing some but not all aspects of seismic risk, by microseismicity studies and by inference of the stress states. The occurrence of microseismicity reflects stress release on the faults on which it occurs. The frequency and size of such activity must depend to a large extend on available energy. However, the ambient stress level after the occurrence of an earthquake, which can exist without being reflected in seismic activity, remains unknown. This level is controlled by fault strength and can vary with geology, and external influences such as dams.

The magnitude-frequency distribution of most earthquake sequences follows the empirical rule

$$\text{Log } N=a-bM \tag{1.6}$$

where N is the number of shocks of magnitude greater than or equal to M. "a" and "b" are constants determined for each region. The constant a is uncertain since it depends on the sampling time and is subject to large errors. The value usually used to represent the state of stress of the region is "b". Values of b have been reported from 0.5 to 1.5, but usually lie between 0.7 and 1.0 for tectonic regions.

If the slope of equation 1.6 is large (b large) it predicts a smaller ratio of large to small earthquakes. This suggests the presence of many cracks and a weak material. Due to the logarithmic nature of equation 1.6 a small b value, representative of a zone with fewer small earthquakes but perhaps more large ones will indicate a stronger (more homogeneous) material, since in general there are fewer large seismic events than small ones. The b values for aftershock sequences at lakes have been observed to be about 1.0, and they are much higher than the normal b values of the same region. The b values of the foreshocks are even larger for large induced events.

The b value of earthquakes has been extensively studied (Gupta and Rastogi,1976; Gough,1978) and has been found to be characteristic of the seismicity within a given region. A region of high strength and variable stress distribution is often characterized by low values of the slope b, whereas a source region in which there are existing fractures near critical stress has high values of b (Gough, 1978)

Scholz (1968) relates high b-values to zones under spatially heterogeneous stress distributions and lower b-values to more homogeneous distributions. He concludes that the state of stress plays the most important role in determining the value of b. This means that for an area with high tectonic activity we are to expect a high b-value. Gupta and Rastogi (1976) and Simpson (1976) explain that the high b-values observed at lake sites are due to the heterogeneous nature of the stresses induced by the reservoir depending on the geological structures present.

The major limitation of empirical seismological relations derived from the study of seimic catalogues is that these are not by any means complete; that is the recording network is only capable of registering all the events of magnitude greater than a given threshold. Even in the best studied areas the period when records are available is a small sample in geological time scales. Nevertheless, that is all we have to go on. Lamoreaux et al. (1983) studied this problem of incomplete data in their study of the occurrence of seismic patterns in the Middle-America trench. Discussions about the validity of statistical seismic studies have been done by many independent researchers (ie. Lomnitz, 1966; Lamoreaux, 1982; Rikitake, 1977). They all concluded that due to the short history of recording, statistics may be misleading, nevertheless, that is all we have to go on. Rikitake (1977), points out that it is possible to use statistics in seismology only if a series of seismic observations over a period of several decades or longer is available for that particular region.

Geologic investigation in the late Quaternary might provide valuable data on recurrence periods of damaging earthquakes (Allen, 1975). Such investigations appear to help overcome many of the statistical shortcomings of instrumental and historical records. It may be expected that the dangerous large events (M>7) will leave geologic traces, from which not only their occurrence, but also, the amount of slip and thus their magnitude can be derived. These investigations may provide the "maximum credible earthquake" data required for hydroelectric project design, for other large engineering projects and is desired in the assesment of earthquake risk in geodynamical modelling.

A third method of stress analysis is to attempt a direct measurement of stress. Several methods exist for routine determination of formation stress (Haimson and Fairhurst, 1970). The most useful appears to be that used by the U.S. Bureau of Mines (Obert et al., 1962). This method involves placing a diameter gauge in a borehole of approximately 3 cm diameter. This is usually a low modulus inclusion which consists of a piston in a brass barrel. The piston measures the borehole diameter by deflection of a bar fitted with a strain-gauge. The resistance of the gauge can be monitored with normal strain gauge equipment.

Once the borehole gauge is in place a large diameter coring bit (≃ 20 cm) can be used to drill out the rock containing the gauge. A fairly simple application of elasticity theory relates the observed relaxation of the rock to stresses in the plane perpendicular to the borehole. Three measurements of this type in 3 independent directions are used to deduce the complete stress tensor. All that is required is a competent rock drilling crew with equipment capable of cutting large diameter cores. It is crucial that the drilling crew be experienced for the large diameter core must be retrieved in one piece. Borehole gauges can be constructed by any qualified machinist and strain monitoring equipment is a standard item. The problem is that these measurements are local and shallow, and not necessarily representative on a regional scale. The seismic behaviour on the other hand is regional in character and can be thought as a way of determining the average behaviour of a given zone.

Flat jack tests are not as reliable for these stress analyses. The results can be severely contaminated by geometric influences due to the excavation from which they are made. High modulus inclusion methods (Hast, 1958) might have a place in competent rock but seem ruled out in sedimentary basins or heavily fractured materials.

Hydrofracturing (Hubbert and Willis, 1957; Haimson and Fairhurst, 1970) is probably the only way to acquire stress data at depth but it requires the drilling of several deep wells. Such wells would however serve a useful purpose in monitoring fluid pressure behaviour during loading of a reservoir. This technique has limitations

1. One principal stress must be vertical.
2. Drill hole must be near vertical.
3. Cracks can introduce considerable uncertainty in results.

The orientation of the principal stresses in the upper few kilometers of the earth's crust has also been determined by analysing the direction of oil-well breakouts (i.e. Gough and Bell, 1981). This is done with a 4-arm dipmeter, which records the magnitude and azimuth of two orthogonal diameters of the hole. A breakout occurs when when one of the diameters fits the original drill and the other is greater. The observed direction of the breakouts is consistent within a single well, and seems to be independent of the geological structures through which the hole has been drilled. The consistency of breakout orientation throughout a single geologic province (Bell and Gough, 1979), suggests that the systematically oriented azimuths are products of stress concentrations near the hole in a regional stress field where the two horizontally oriented principal stresses are different.

Well breakouts give no measure of the magnitude of the stresses and if they are to be useful in the determination of the regional orientation of the principal stresses we require the presence of many wells in the area.

Finally, one of the methods for estimating stresses in the lithosphere is by modelling, using the major geophysical observables of heat flow, seismic wave propagation data, gravity, radioactivity, electric conductivity, magnetometry, and the plate velocities as constraints. The link between the geophysical observables and the stress in the lithosphere is through the different constitutive equations mentioned earlier in this chapter. These are equations that relate the rate of strain to the applied stress, temperature, pressure or any other parameter that might influence this strain rate. Unfortunately almost all these parameters must be estimated. Model calculations are discussed later in this thesis.

1.6 Some Earthquake Related Phenomena

Several aspects of the earth's seismic behaviour, that are of importance to the understanding of this work and are the necessary background to the following chapters must be outlined.

Recurrence patterns.

The study of the seismic catalogs for the different parts of the earth has resulted in several empirically derived observations. One of these is that large destructive earthquakes tend to repeat themselves in location and in time (i.e. McNally and Minster, 1981; Singh et al., 1981). For simple plate boundaries the average recurrence time T can be calculated from

$$T=u/\alpha v \qquad (1.7)$$

where u is the average displacement that takes place at a location due to seismic activity, α is the ratio of seismic slip to the total slip and v is the relative plate velocity (Sykes and Quittmeyer, 1981).

Two assumptions are implicit in this kind of formulation, one is that the major part of the slip at the location is due to large earthquakes and the other is that the plate velocities can be treated as constant over large periods of time (Sykes and Quittmeyer,1981). This has lead to the development of three different type of recurrence patterns (Shimazaki and Nakata, 1980). These patterns (figure 2) are:

1. The time recurrence model shown in figure 2.a assumes that the stress required to fracture a given location is constant as indicated by the horizontal line at T_1 level of stress on this figure. This is not necessarily true since fractures decrease the strength of the material and modifies its frictional resistance. The model implies that stress is accumulated until it reaches level T_1. Then an earthquake takes place and the stress level drops to a smaller level and the cycle starts again. This pattern enables us, in principle, to predict when is an earthquake going to occur based on the size of the previous one.
2. Figure 2.b describes the Slip predictable model. It assumes that the level of stress after the occurrence of any seismic event is the same, that if an earthquake is going to occur today, its magnitude can be predicted from the time lag from the previous one. This kind of modelling is not in good agreement with the seismic catalogues from Japan (Shimazaki and Nakata, 1980) California (Bufe, 1977) and the Middle America Trench (Singh et al., 1983).
3. The strictly repetitive model shown in figure 2.c is the combination of the previous two, the levels T_1 and T_2

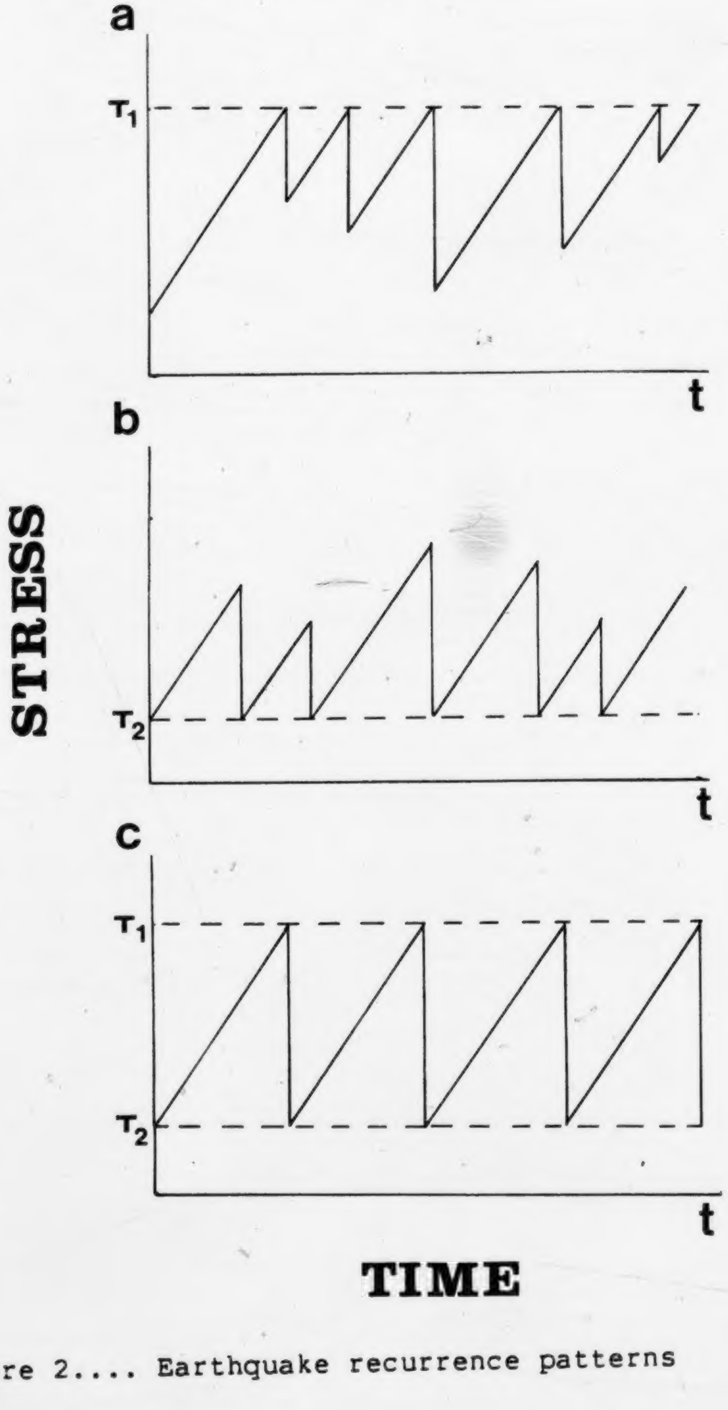

Figure 2.... Earthquake recurrence patterns

are fixed, the time of recurrence is always the same and the earthquake is of the same magnitude every time. This one has all the defects of the other two combined, and is considered a limiting ideal case.

The common assumption of all these models, that the rate of accumulation of stress is constant, has been used extensively in many other geophysical studies (i.e. Newman and Knopoff, 1982; Singh et al.,1983). This concept of a continually increasing stress will permit the study of the variation of the stability function due to an earthquake (Chapter 3). Therefore, I have assumed that earthquakes represent a sharp reduction in stress and are the only natural way in which stress can change abruptly.

Observed recurrence times at a given location are irregular enough that for most regions the knowledge of this average time interval between succesive earthquakes does not greatly constrain future times of occurrence (Rikitake, 1977).

Seismicity Patterns.

Another observation from historical seismicity records is that sometimes large earthquakes appear to affect the seismic behaviour of zones which are very far away, and some large events seem to be preceded by anomalous seismic behavior. All these types of peculiar seismic behaviour have been grouped as Seismicity Patterns or Long Range Precursors.

Most of the observed seismicity patterns can be interpreted as a combination of quiescence and activation (Lamoreaux, 1982). Quiescence is understood as a decrease in the seismic activity of a region in comparison to normal activity. Activation is then an increase in the seismicity of a region, an increase in the total energy release rate there, or both.

Many of these patterns have been identified, some of them involve activation only. Foreshocks are the most obvious of this kind of precursors, they are swarms or small events close in time and space that occur just before a major earthquake takes place in the region. Successful predictions have been made by recognizing this pattern i.e. the Haicheng magnitude 7.3 earthquake of 1975 (Scholz, 1977). Pattern 'swarms' (Keilis-Borok and Rotvain, 1979) refers to a group of small magnitude events closly grouped in space and time occurring during a time interval when the overall seismicity is not below average, and takes place several years before a major earthquake takes place in the area. McNally (1977) observed this pattern in California, Ohtake (1976) reported similar findings in Japan.

Keilis-Borok et al. (1980 a,b,c) have proposed three related seismicity patterns which deal with the activation of a region. These three patterns have been collectively termed "Bursts of seismicity". They consist of abnormal clustering in time, energy and space before a major earthquake. These are, pattern 'swarms', pattern 'bursts of aftershocks', which consist of an anomalous number of aftershocks concentrated at the beginning of the aftershock sequence, and pattern 'Sigma' which consists of an increase in the cumulative seismic energy released to the 2/3 power over a sliding time window, pattern sigma is identified as the peak of the summation.

Some of the observed seismicity patterns are superposition of quiescence and activation. Evison (1977), suggested a pattern of premonitory swarms followed by a quiescent period in the epicentral region. Mogi (1969) identified a doughnut pattern for some large earthquakes in Japan. Keilis-Borok and Rotvain (1979), suggest a similar algorithm, pattern 'A-Q' (activation-quiescence). Pattern 'A-Q' combines two activation areas at opposite sides of an earthquake prone site with a quiescent area in the middle.

There is no satisfactory physical explanation for the occurrence of these patterns, although some theories exist. Two major approaches have been developed

1. They are a result of the actual distribution of physical properties of the earth.
2. They are the result of the processes of crack population growth, independent of what material these cracks are on.

The right answer will probably link both of these explanations. In chapter 4 this is explored by using the stability functions.

2. Types of failure and stability studies.

A major aim of this work is to link together what is known about the earth processes from direct in-situ measurements and experimental results with the variation of the geophysical observables such as seismological behaviour.

To accomplish this it is convenient to review some concepts of rock mechanics which are fundamental to the further understanding of what is expected from the earth. This analysis will set up the rules that must be followed in any kind of description of rock failure.

Once the mechanical background has been presented, the chapter proceeds to explore different ways to determine seismic risk. Applications to time dependent phenomena are analysed first. This is modified for the determination of seismic risk isolines in active areas. The chapter concludes with a method in which the seismic risk is represented by probability of seismic failure in particular areas.

2.1 Rock Failure.

It is important to recall the different types of failure criteria that are applied in rock mechanics. All these are functions of the internal distribution of stress in the material. However, the internal stress of small laboratory samples may not be representative of the stress distribution in real geological environments. Nevertheless, all the criteria assume that the "average" stress is representative and can be used to describe this behaviour.

Von Mises criterion suggests that yielding of *ductile* material occurs when the limit value of the octahedral shear stress (τ_0) is achieved (Jaeger and Cook, 1979). τ_0 as a function of the principal stresses σ_1, σ_2 and σ_3 is given as:

$$\tau_0=1/3\{(\sigma_1-\sigma_2)^2+(\sigma_2-\sigma_3)^2+(\sigma_3-\sigma_1)^2\}^{1/2} \tag{2.1}$$

Another yielding criterion is that due to Tresca, which states that ductile yielding will occur when the maximum shear stress τ_{mx} is reached (Jaeger and Cook, 1979), where:

$$\tau_{mx}=(\sigma_1-\sigma_3)/2 \tag{2.2}$$

The most widely used but not necessarily the most appropriate failure criterion is the one known as Mohr-Coulomb. This criterion implies that failure occurs when the critical shear stress τ, given as $\tau=S_0+\sigma\tan\phi$, is reached. S_0 and ϕ are material constants. This criterion (figure 3), will be discussed extensively in the following parts of this chapter. In this figure are shown the classical ways in which this criterion can be represented, a) In shear stress vs normal stress in cartesian coordinates, and b) in a principal stress diagram, where $m=(1+\sin\phi)/(1-\sin\phi)$ and $b=2S_0\cos\phi/(1-\sin\phi)$.

In three dimensions the stress envelope of figure 3.b is given by the hexagonal pyramid shown in 3.c.

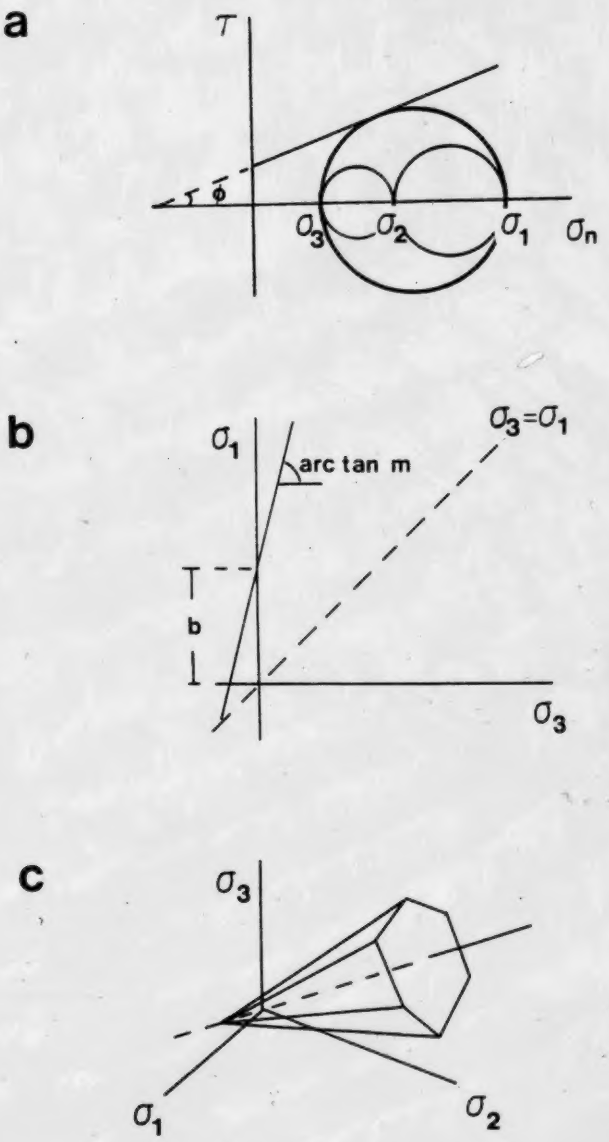

Figure 3.... Mohr-Coulomb failure criterion in a shear stress vs normal stress diagram (a) and in principal stresses diagrams in two dimensions (b) and in three dimensions (c).

The Drucker-Prager criterion is based on the replacement of the pyramid of figure 3.c from the Mohr-Coulomb method by a circular cone inside the pyramid. This results in the following failure criterion

$$F=\alpha J_1+\sqrt{J_2}-k=0 \qquad (2.3)$$

where J_1 and J_2 are the first and second stress invariants

$\alpha=\tan\phi/(9+12\tan^2\phi)^{1/2}$

and

$k=3S_0/(9+12\tan^2\phi)^{1/2}$

The importance of this kind of criterion (figure 4), is that it takes into account the intermediate principal stress σ_2, which is neglected in the Mohr-Coulomb criteria.

All these criteria have been postulated on the basis of theoretical considerations and have been extensively tested. Except for the Mohr-Coulomb their application in geophysics is rare since they all imply assumptions about the behaviour of the materials of interest. A failure criterion based on the actual physical process leading to failure was suggested by Griffith in 1924. A material contains a number of randomly oriented zones of potential failure in the form of weak grain boundaries, fissures, cracks or open flaws. These flaws can be approximated by long thin elliptical openings and one can assume that there is no interference between

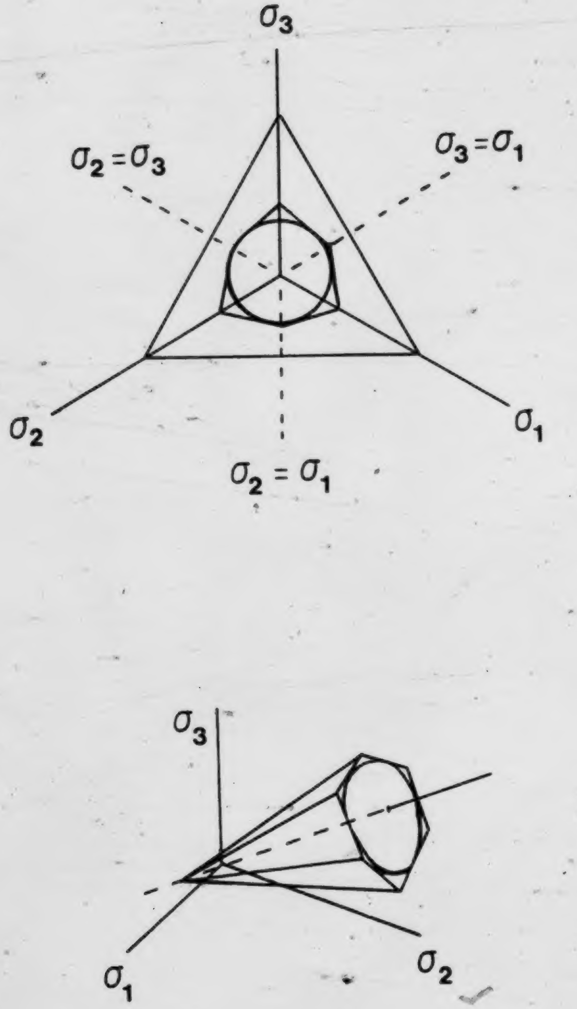

Figure 4.... Drucker-Prager failure criterion.

flaws in an idealized elastic material. In this case even under high compressive states of stress, tension stresses occur in the boundaries of these openings and fracture must initiate at that boundary when the tensile strength is exceeded.

The maximum tangential stress (σ_{tn}) near the tip of the elliptical opening is

$$\sigma_{tn}\cdot m=\sigma_y\pm(\sigma_y^2+\tau_{xy}^2)^{1/2} \tag{2.4}$$

where m=a/b.

This criterion implies several characteristics of the crack (Stagg and Zienkiewicz, 1968):

1. It propagates out of the plane of the flaw.
2. It propagates to infinity if it is not confined (tensile splitting rupture).
3. It propagates towards the major principal axis.
4. No rupture occurs when σ_1 and σ_3 are compressive (stable crack propagation).
5. The final length of the crack depends on the ratio σ_3/σ_1 and the initial flaw length.
6. Depending on the crack density, cracks may merge and a failure may occur due to this crack coalescence (creation of a shear fault).

Hoek and Brown (1981) have made an empirical attempt to put all the information available together (figure 5), and develop an empirical strength criterion:

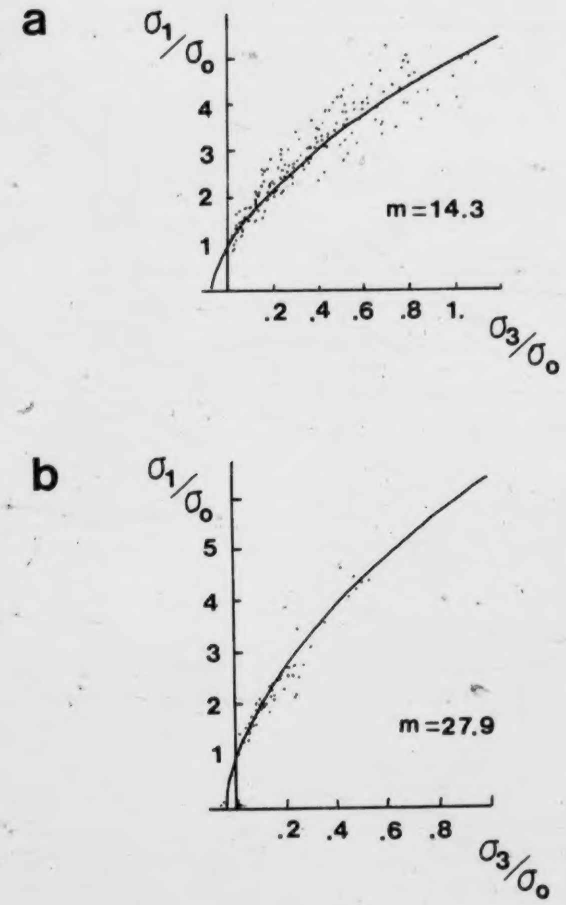

Figure 5.... Shows some examples of Hoek and Brown's empirical failure criterion for a) sandstones and b)for granites.(modified from Hoek and Brown, 1981)

$$\sigma_1/\sigma_0=\sigma_3/\sigma_0+(M\sigma_3/\sigma_0+S)^{1/2} \tag{2.5}$$

where M and S are constants which depend on the rock. For intact rock S=1 and $M=\sigma_0/\sigma_t$, σ_t being the tensile strength of the material and σ_0 the confining pressure. M will decrease rapidly as the degree of prior fracturing increases.

2.2 The Stability of Earth Materials.

The concept of stability has been used in rock engineering to predict failure. In major engineering projects, it is of great importance to determine the strength of the rocks at a site and avoid the collapse of the geological structures that may be present there. This is done by making several assumptions about the strength of the materials, discontinuities, and other local features. In general, these calculations demonstrate the amount of strengthening required in the area. Introducing artificial supports will locally increase the material strength and permit the work to be done with a safety factor.

The simplest example, involving this type of reasoning is the determination of the average cohesion necessary to maintain the equilibrium of an open pit (Brown and King, 1966). They determine the components of stress and make use of the Coloumb failure envelope to determine the STABILITY of a slope model, by looking at the toe of the slope, and calculating the plane of possible failure by using

$$\theta = \tan^{-1} 2\sigma_{xy} / 2(\sigma_{xx}-\sigma_{yy}) + \pi/4 + \phi/2 \qquad (2.6)$$

for σ_{xx} greater than σ_{yy} as a function of the angle of internal friction of the material ϕ.

Once the potential slip surface has been given then the average cohesion S_0 for each path L can be calculated as:

$$S_0=[\int \tau dL+\int (\sigma-P)\tan\phi \cdot dL]/\int dL \qquad (2.7)$$

where τ is the shear stress, σ the normal stress and P the pore water pressure. The Couloumb failure envelope is given as:

$$|\tau|>S_0-(\sigma-P)\tan\phi \qquad (2.8)$$

The calculation assumes that rock behaviour is linear-elastic and that failure will occur in the direction of an angle θ for which the corresponding value of S_0 is minimum. This engineering approach works. In this thesis we extend the analysis to the study of stability of large geologic structures in order to connect seismicity and rock mechanics in a quantitative way.

In geodynamical studies of the elastic plate, instabilities represent seismic events and nothing can be done to increase the mechanical strength of the material. Turcotte et al. (1980), studied instabilities due to fault weakening caused by frictional work. Stuart (1979) points out that the subject of earthquake mechanics viewed as a boundary problem in continuum mechanics reduces to the study of

1. constitutive properties and geological structures present in the surroundings, and
2. remotely applied boundary conditions.

These concepts must lead to the observed nature of the earthquake cycle. The stages of this cycle are

1. slow increase of stress due to remote loading,
2. the onset, propagation and cessation of the rupture and
3. post seismic adjustment.

To this, it should be added, that fast stress changes may occur in the upper few kilometers of the earth. This inclusion will in fact integrate the engineering approach and the more general geophysical studies of the earth's crust and upper mantle.

Earth instability models require a precise statement of the dependence of the stability on the material properties of the models. The instability criterion depends on the stiffness of the material and the stiffness of discontinuities present in the model. It is given as the possibility of a fault slip due to a remote displacement or stress release. Stuart (1979) points out that physically, this condition corresponds to a sudden, finite fault slip caused by an arbitrarily small progressive change on regional stress. The unstable slip during faulting is driven by the release of elastic energy stored in the surroundings as proposed in the elastic rebound theory. Then, any constitutive law in which stress can decrease rapidly during deformation can be used to create an instability criterion.

Failure represents the actual stress release and originates at the location in which the ratio of the strength of the material to the stress stored in it is minimum. The crack will propagate through the rock until it reaches a location where the stresses are not enough to overcome the rock strength. Therefore, the size of the stress concentration will determine the size of the crack. Very localized concentrations then are expected to produce small cracks, while regional concentrations are more likely to produce large cracks.

The stress concentration due to the propagation of the seismic waves ahead of the tip of a crack can cause the fault slip. The cohesive force of the material where the rupture occurs, determines what happens when the rupture propagates along a fault plane with obstacles or barriers. These barriers may be thought of as localized high values of the cohesive force of the material. Aki and Richards (1980) suggest that three different things may occur when the tip of a crack passes through such a barrier, depending on how strong the barrier is with respect to the initial stress:

1. If the initial stress is relatively high, the barrier is broken immediately.
2. If the barrier strength is relatively high, the barrier is left behind unbroken.

3. If they both are similar, the barrier is not broken when the crack tip passes, but it may eventually break due to later stress increases.

2.3 General definition of stability.

The determination of zones of seismic risk in geosciences is a subject in which several items must be taken into account:

1. Concentration of stresses due to geological structures in the region of interest, that is, sudden changes in material properties occurring inside the model under study.
2. External forces acting on the medium, like plate driving forces, volcanic activity, igneous intrusions, changes in water content or in pore pressure on the rock mass.
3. Evidence of previous seismic activity in the area.
4. Location of the site with respect to the active seismic belts of the earth.

Once all the above factors have been considered, assumptions about the constitutive equations that regulate the stress propagation in the model can be made. The next step is to calculate the stress tensor components. This can be done by solving the boundary value problem with analytical methods or numerical techniques. The detailed development examples of both approaches can be found in appendices A and B.

If the variation of the stress tensor throughout the model is known, its components can be combined in such a way that a measurement of stability at each point of the model can be calculated. This is done by applying the Mohr circle principle to the resulting principal stresses and relating it to a failure criterion.

The physical significance of using a Coulomb failure envelope is that the rock is taken to have a linear relationship between the critical shear stress τ_{13} and the critical maximum stress diference $\sigma_1-\sigma_3$, that is required to reach failure. A solid exhibiting this kind of behaviour is characterized by a linear relation between the components of stress and strain as described in section 1.1 and implies reversibility of the stress strain relations. This assumption for the upper few kilometers of the earth is plausible if the constraints mentioned through chapter 1 are observed.

If the envelope of the Mohr circles at failure has the form of a straight line (figure 6), it is given by equation (2.8), which can be rewritten as:

$$\Delta\tau=S_0+\Delta\sigma_n\tan\phi \tag{2.9}$$

where $\Delta\tau$, is the shear strength increment of the rock. ϕ, is the angle of shear resistance, $\Delta\sigma_n$, is the normal effective stress increment on the plane of fracture, and S_0 is the shear strength increment of the material under zero normal

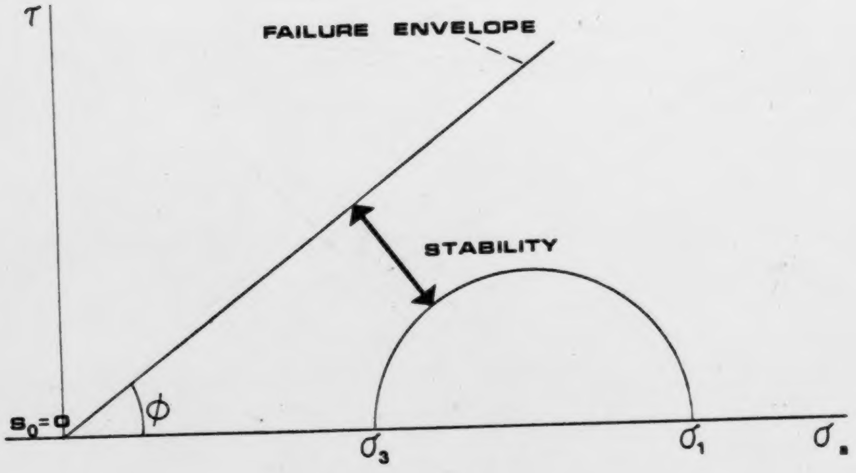

Figure 6.... Shows the general definition of instability as the minimum distance from the surface of the Mohr circle to the failure criterion.

pressures.

'S_0' varies considerably from zero in fractured material to ≃ 50 bars for sedimentary rocks and up to several hundreds of bars for igneous rocks in intact material (Withers, 1977). In the case of our geological situation, we have the presence of fractures and 'S_0' is expected to be small. The shear angle ϕ lies between 25° and 45°, therefore the coefficient of friction is between 0.47 and 1.0. This one is usually around 0.6 (ϕ=30°).

Since the value of 'S_0' is unknown, fixing it to zero, and determining the variation of the minimum distance between this failure envelope and the Mohr circle will result in a measurement of the stabilty of the system at a given time. This is equivalent to the introduction of a reference frame. That is, at the beginning of the calculation, the model was taken in equilibrium, and then by making some physical change, increments on the principal stresses are calculated. These will result in a unique measurement that will denote if the corresponding location in the model has increased or decreased in stability with respect to the original situation.

This kind of reference frame can only be used if there is a physical change in the conditions of the area from one time to another. The risk of a seismic event should depend on the minimum distance between the failure envelope and the resulting Mohr circle. Some of its applications will be seen in the succeding chapters of this thesis.

Although the definition of stability functions requires the precise definition of a failure criterion, it is not restricted to the use of a linear envelope. In order to apply this kind of stability analysis to greater depths than those for which elastic behaviour is justified the failure criterion must be changed. In Chapter 4 a different type of envelope has been used since the stress-strain relations dealt with there are not always linear, and the material is allowed to become somewhat ductile. Therefore the envelope there will describe the yielding of rocks.

The shapes of the reference failure envelopes used throughout the following chapters are derived from the physical characteristics that will be described for each model. In general the materials are assumed to have zero tensile strength, to behave elastically in the upper few kilometers of the earth's lithosphere and the shear stress angle ϕ is taken as 30°. As the temperature of the model reaches 300°C plastic behaviour is assumed.

2.4 Instability function in three dimensions.

In the Mohr's circle representation in three dimensions, the normal and shear stress across a plane of weakness whose normal has direction cosines l, m, n, are given by Jaeger and Cook (1979, p27). Fixing two of the direction cosines (say n and l) two equations can be obtained. Each of them represents one family of Mohr's circles in two dimensions and for a fixed value of the corresponding direction cosine each represents a unique circle. Therefore, by fixing n and 1, two circles can be drawn such that their intersection will lie at a point on the surface of a three dimensional Mohr representation, and will be a unique location for these two circles whose centers are $(\sigma_1+\sigma_2)/2$ and $(\sigma_2+\sigma_3)/2$ and whose radii are AC and BD respectively (figure 7).

With the previous procedure it is possible to determine the values of σ and τ for every combination of stresses. That is, the location of the point P from figure 9 can be determined for any time using the simple Mohr-Coulomb failure envelope. This criterion suggests that failure occurs when the minimum shear on a failure plane exceeds the shear strength of the rock.

If fractures are present in the material S_0 is probably small. Therefore since the value of S_0 is unknown, I set it to zero. Now the variation of the minimum distance between the failure envelope and the point 'P', defines the changing stability of the system.

By fixing the angles θ and ψ, the plane of weakness of the material is determined. The variation with time of the distance between the corresponding point P on the surface of the Mohr's circles and the failure envelope will result in an "INSTABILITY" history for a given location of coordinates X, Y, Z. This risk history can be represented as a curve in an instability value vs time diagram. This curve is then referred to as an instability function.

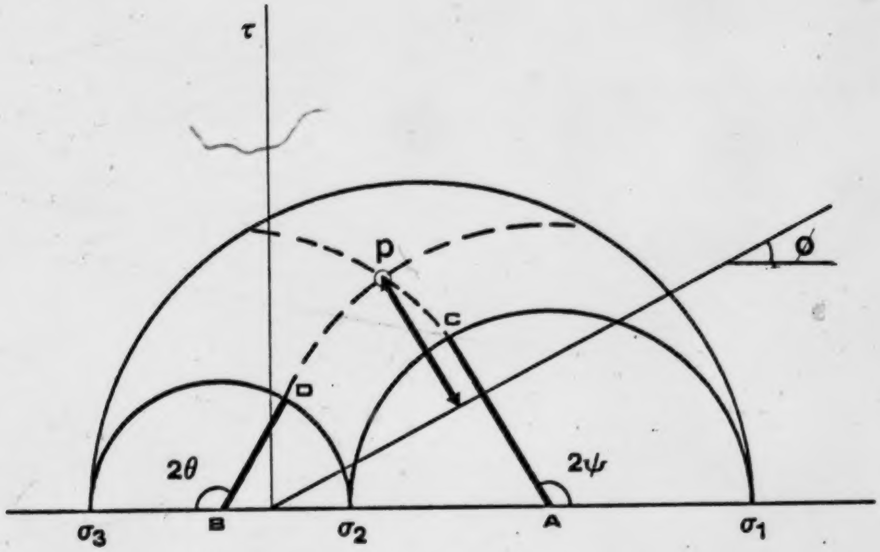

Figure 7.... Definition of the instability function in three dimensions as the distance between P and the failure envelope.

This kind of risk function can be used to study induced seismicity at water reservoirs (Uribe-Carvajal and Nyland, 1983), in such a way that this function will depend only on the loading history of the reservoir, the known geological structures (that will determine the angles θ and ψ), and the geometry or the bathymetry of the lake. Stability has been defined as a function proportional to the minimum distance between the failure envelope and 'P'.

The use of a Coulomb failure criterion is applicable when rocks behave in an elastic way and that fracture occurs in a brittle way. Although rocks behave in a more complicated way, the assumption of elastic materials is often made in geophysics. Solomon et al. (1980) and many others have suggested that the upper few tens of kilometers of the earth's crust can be treated as elastic materials; Turcotte (1974), determined that the upper bound for this pseudo-elastic behaviour is 300°C. This temperature acts as the limititation to the applicability of this kind of linear failure envelope.

Assuming Mohr-Coulomb failure is consistent with the assumption that the incremental stresses cause elastic deformation particularly near failure, the assumption of brittle failure may not be true for all faults, but it is a reasonable, tractable hypothesis.

In the case of the application to a water reservoir (chapter 5), we acknowledge that the treatement of the earth as porous halfspace consisting of an elastic matrix saturated with water is a simplistic model. However, the stability functions are relative, and only serve as indicators of how the risk of inducing seismic activity is changing with respect to a reference initial value.

2.5 Residual Stability Function.

The determination of the state of regional stress itself can be approached by determining the stress field in a two dimensional finite element model. A constraint on this model is that observed seismicity occurs in areas of high shear stress. These areas are referred to as being unstable. The stability of a given location has been determined by the distance of a Mohr circle from a Coulomb type of failure envelope. Since the values obtained represent the stress increment that is required to reach failure, this is an instability measure (Uribe-Carvajal and Nyland, 1983).

In the previous section, I introduced the notion that a measure of the seismic stability of a geologic structure was the minimum distance between the envelope describing failure in shear and the Mohr circle for the stress state. This notion is applied here. A large value for this quantity implies a low risk of failure or high stability. Note that stability behaves inversely to risk. Another geometric measure of the relative position of the stress with respect to the failure envelope might be reasonable.

I introduce in this part a measure of risk of failure I call residual instability (figure 8). This residual

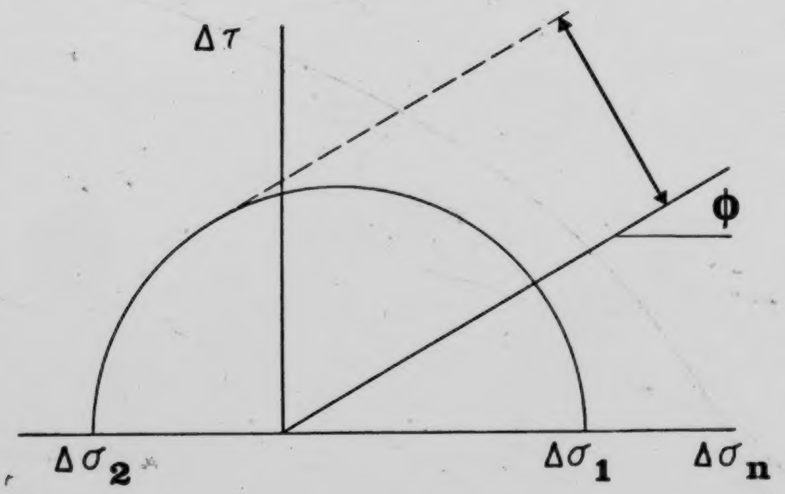

Figure 8.... Shows the definition of residual instability as the minimum distance between the Mohr circle and the Coulomb failure envelope.

instability is derived by first estimating some form of average stress in the area under investigation and then determining the stress in an anomalous zone, subtracting from this stress the ambient background stress and calculating the distance of the Mohr circle for the residual stress from the failure envelope. The normal (lithostatic) stress is usually that which would result from a gravitating uniform half-space, the anomalous stress is derived from the gravitational stresses that would be present when a particular geodynamic structure is included. In chapter 3 this residual instability is applied to the study of seismic behaviour and the determination of high risk areas.

The residual instability behaves rather differently from our previous measure. Residual principal stresses can be negative. This means that the Mohr circle that corresponds to these stresses could cross a failure criterion that intersects the origin as in figure 8. This does not mean that failure will occur, it merely means that the distance from the Mohr circle for the total stress to the failure envelope has decreased and failure is more likely. Strictly, failure will not occur until the Mohr circle for the residual stress is as far above the failure envelope as that for the normal stress is below the failure envelope. The residual instability can be negative. This will occur when the Mohr circle for the residual stress is completely below the failure envelope. What is important is whether this residual measure is larger in one location than another for if it is, the location with the larger measure is more unstable.

This relative treatment of the problem is necessary. Although the assumption that the strength in tension of rocks is small appears justified it cannot be verified on the scales we consider here. The sign of the instability measure depends on the point where the failure envelope intersects the zero normal stress axis on the Mohr diagram. Note that the instability values considered here are distances on a Mohr diagram. This means that instability has the same units as stress. Keep in mind however that an ambiguity exists. The actual intercept of the failure envelope, that is, the strength in tension of the formation is an unknown. As a result of this residual instability values for any model are nonunique to an additive constant.

The contours of equal residual instability show specific areas where the resulting stresses combine in such a way that it is possible to denote them as minimum stability areas.

2.6 The Probability Function.

The concept of instability has been discussed previously as a comparative measure between two states of stress and represents a measure of the risk of the occurrence of a seismic event. It deals essentially with the determination of the principal stresses and its interpretation in form of a Mohr circle, and the minimum distance between this circle and an envelope determined by a failure criterion. In order to take this instability function one step further and to be able to talk in a clear language about risk, I introduce here a change to the instability or risk function by linking it to the probabilty of failure at a particular location of a model with respect to the rest of the model when a system of forces is applied to it.

This probability distribution (figure 9) is also relative. It indicates that some areas will be closer to failure than others but does not mean that at a high probability valued location an earthquake must occur. It is not a comparative measure of stability for a point at two different times, but rather, a comparative measure for all the different parts of the model at a particular stage.

To calculate the probability function, first it is necessary to calculate the principal stress distribution at every point of the model. With these stresses Mohr circle diagrams can be constructed. In figure 9 circle 1 is the Mohr diagram that corresponds to the node of highest stability or minimum risk, which as seen previously is proportional to the minimum distance between the Mohr circle and the failure envelope. This distance can be negative and in the figure is indicated as d_{min}. Circle 2 corresponds to that node for which the resulting distance d is maximum.

The failure criterion specified by a single envelope on a Mohr-Coulomb diagram prescribes an absolute condition for

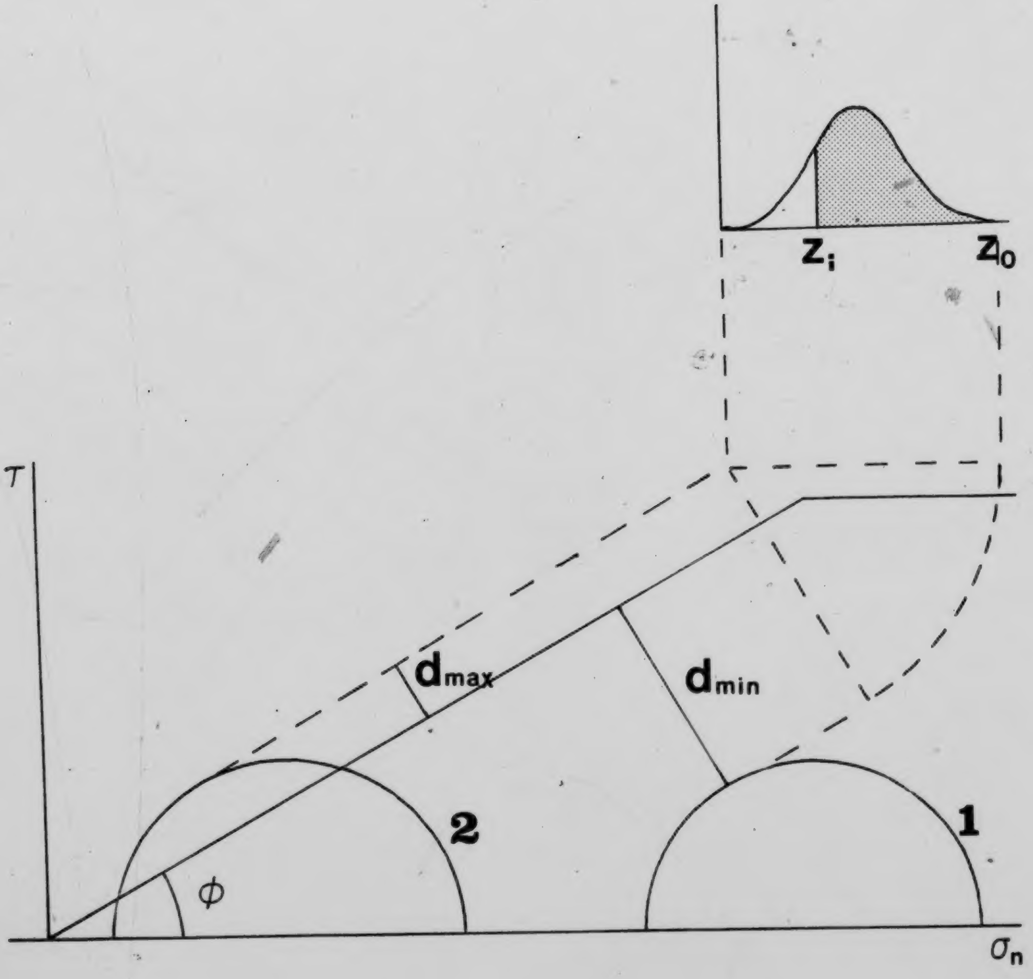

Figure 9.... Definition of the probability function.

failure. It is my view that this is simplistic for earthquakes. I prefer to think of a probability of failure concentrated in the neighbourhood of the failure envelope. In what follows we make an intuitive argument about the way the finite element estimates of instability could be mapped into a probability function describing risk of failure.

Stresses can be calculated at every node in a finite element model. This produces a set of numbers, call them $\{d_i\}$ for the distance between the failure envelope and the Mohr Circle at the ith node in the system. Suppose now that each value d can be mapped onto a probability distribution $\lambda(d)$ in a unique way.

This suggests that an association can be made between the position of the Mohr Circle and a probability of failure. The idea is illustrated in figure 9. The problem to solve is the determination of the form of $\lambda(d)$.

The set of numbers $\{d_i\}$ will contain both small and large values. It need not be obviously a set of probabilities, it does however provide a link to the probabilities. I argue first that a normal distribution is a reasonable form for λ. All probability distributions tend to a normal distribution near their peak (the central limit theorem; Reichl, 1980). If this is so the parameters of the distribution must be determined. In particular a rule must be devised whereby a probability of the form

$$y(z)=(2\pi)^{-1/2}\int_{z_0}^{z_i}\exp(-x^2/\sigma^2)dx \qquad (2.10)$$

can be used to assess the risk of failure. The choice of the integrand is governed by the requirements of a normal distribution and the integration is present to contain the notion that the risk of failure is cumulative from a threshold z_0. Physically one can think of the failure criterion as being controlled by the density of cracks of varying size. The creation of a catastrophic cascade crack is described by a probability density like y(z).

The identification is complete once x, σ, z_0, and z have been identified. Let d_{mx} be the largest and d_{min} the smallest members of $\{d_i\}$. Then define $R_{mx}=d_{mx}-d_{min}$ and $R_i=d_{mx}-d_i$. Then $x_i=R_i/R_{mx}$. Since the variables x_i range from 0 to 1 I choose $\sigma=1$ and then calculate the y corresponding to d_i from the integral

$$y(z)=(2\pi)^{-1/2}\int_{z_0}^{z_i}\exp(-x^2)dx \tag{2.11}$$

This integral is easy to do and can be evaluated rapidly when z_i is between 0 and 1.

Observe that the integration is only over a portion of the normal distribution. Choosing the lower limit of the integral at z_0 ensures that the probability of a seismic event at the most stable node is zero. This is to some extend arbitrary, but seems justified on observational grounds. Earthquakes do after all show strong clustering. The choice of a normal distribution is now dictated by the fact that we are 'near' the high probability regions. Since we never integrate over the entire normal distribution no probability will become 1. This is also reasonable.

A question now arises about the use of $\sigma=1$. Since the interpretation done is relative, I compare probabilities at different points, the value of σ does not really matter. An improved approach to this problem could involve both fitting σ to data from models and examine whether other than normal distributions could work better. I have not done so because normal distributions give excellent results, as will be shown later in this thesis.

Knopoff (1971), relates the probability for the occurrence of earthquakes to the state of strain of the material. However, a comparison between his work and the definitions presented here is not easy. He defines a mathematical algorithm that depends on three different types of probabilities: The probability that the stored energy of deformation is at a certain level $P(E,t)dE$; the probability that, if this energy is at a given level, an earthquake will occur $\lambda(E)$; and the transition probability that, if the earthquake occurs at an energy state X the final energy state will be at a given level E, which is given by $T(X|E)dE$. These are used to predict if rupture can take place at a particular time at a given location.

My probability function could be seen as a particular case of the $\lambda(E)$ of Knopoff. Here I assume that the model is at a given energy level. Then the analysis of all parts of the model is necessary, which is a static exercise highly dependent on the material properties. To predict changes on the distribution of probability due to the occurrence of earthquakes it is necessary to introduce stress drops at the focal locations and recalculate the whole model.

It should be noted that due to the nature of this probability distribution a zone with a value of 1 indicates where the model is most unstable. This does not means that an earthquake will take place there, but rather that if an event should occur in the model at the state of stresses modelled, fracture would initiate there.

2.7 General comments on the instability functions.

Stability functions that compare all the parts of a model at a particular stage (as in the cases of the residual instability and the probability functions), can be used to predict the probable place of rupture initiation. To be able to do this it is necessary that significant differences exist in the instability distribution within the model. Once rupture takes place the crack will propagate until it reaches a zone of sufficient stability to stop this propagation. This will occur where the strength of the material increases. The final length of the crack could then be linked to the length of the high risk areas. It is possible that if an earthquake occurs it might propagate to other high risk areas if the stable bridges between these areas and the one in which the event took place are narrow. These kinds of predictions are demonstrated in chapters 3 and 4 of this thesis.

In instability functions dealing with several stages it will be possible to predict in which stage failure might occur. This is shown in chapter 5.

3. Elastic models of seismic failure and its application to the Valley of Mexico

The observation that near boundaries between continents and oceans there tend to exist mountain belts (Gunn, 1947), that in general are parallel to subduction arcs, has one exception (Molnar and Sykes, 1969). The Mexican volcano chain known as the Neovolcanic axis (which is the mountain belt associated with the Middle America Trench, north of the Tehuantepec Ridge) is located anomalously far back from the trench and is not situated above the focus of intermediate depth earthquakes. The strike of this mountain belt differs by about 15° from that of the trench. However, it is difficult to believe that the volcanoes are unrelated to the subduction zone. Molnar and Sykes (1969) suggest that factors that could explain this anomalous distribution of volcanoes may be:

1. Magmas in this region are not generated near the dipping seismic belt.
2. Magmas follow an indirect path to the surface due to the existence of previous zones of weakness.
3. The slip rate of the downgoing slab may have changed during the last few million years, as Mexico approached the East Pacific rise.

This third hypothesis might lead to a decrease in seismic activity before the volcanism stopped (Molnar and Sykes,1969). One problem with this mechanism is that shallow activity is still frequent near the trench.

Other factors to consider in search of the probable mechanism that might be responsible for this anomalous volcanic distribution is the absence of volcanism between 18° and 15° N and the possibility that the Tehuantepec ridge may have been active in the past 10 million years. This will be dealt with in chapter 6 of this work.

In this chapter the residual instability function presented in section 2.5 is applied to a site which is seismically active and could be related to the Middle American island arc north of the Tehuantepec ridge. Thus the behaviour of this kind of instability under different circumstances can be monitored and the role of the subduction mechanism on the local seismicity detected in this location can be tested. This chapter is an expanded version of *Elastic models of seismic failure in the Valley of Mexico* by Uribe-Carvajal and Nyland published in Pure and Applied Geophysics, vol 120, 1982 in which it was proven that the regional stresses in the plate have little effect on the distribution of shallow unstable zones compared to the effects of local geologic structures and localized changes of stress.

3.1 Introduction

Restricted parts of the valley of Mexico have been plagued by swarms of small earthquakes during recent years. The cause of these events is puzzling, but they may relate to massive artificial changes in the hydrology of the lake-bed which underlies most of Mexico City. The valley is located at approximately 250 km inland of the Cocos-North American plate boundary.

If the valley responds elastically, plane strain finite element calculations can be used to relate geologic and seismic structure to observed seismicity and overall stability of the valley. These calculations show that unstable zones and areas of local seismicity coincide if the triggering mechanism of the seismicity is related to variations of pore pressure and water load.

In order to make such a connection it is necessary to ascribe the generating mechanism of the seismicity to the density and elastic modulus anomalies associated with the valley structure, and to suggest that the phenomenon that triggers this seismicity is related to changes in water content of the near surface formations. Calculations of the change in pore pressure due to the pumping of water from the system show that the unstable areas are indeed concentrated within the valley and in general tend to confirm the conclusions drawn from the elastic analysis.

The valley of Mexico is located in the central portion of the Neovolcanic axis of Mexico and it contains Mexico City. The seismic characteristics of the valley of Mexico (Figueroa, 1971) are a result of the geological conditions that prevail in the valley; a particularly unfavourable geologic condition is the old lake-bed that underlies Mexico City and its surrounding areas. The seismic behaviour of the valley is characterized by high shallow microseismic activity and frequent local earthquakes of small magnitude with depth in the 2 to 8 km range (figure 10)

This seismicity is probably a symptom both of the geological processes which caused the valley itself and the artificial changes in the area since the beginning of the construction of the city (Oviedo, 1967). In the valley there has been and still is volcanic activity and there are also great changes in hydrological conditions. These processes have occurred continuously and have created multiple faults, fractures, volcanoes and barriers that have closed some of the natural drainage channels of the valley. As a result there has been an accumulation of a variety of materials with different mechanical properties in the valley. These heterogeneities in the thickness and type of material are responsible for the variety of geological processes that have been observed. Since the beginning of the 20th century, the expansion of the city and the lack of drainage has made it necessary to pump water out of the underlying formations. This is a probable cause of the observed changes of the piezometric levels (Cruickskank et al., 1979) and of the sinking suffered in some areas of the valley.

Many faults have been located from geologic evidence and some have been inferred from seismic activity but many are probably covered by lava flows inside the valley or by the layer of sediments (which in some locations can exceed 2 km of thickness).

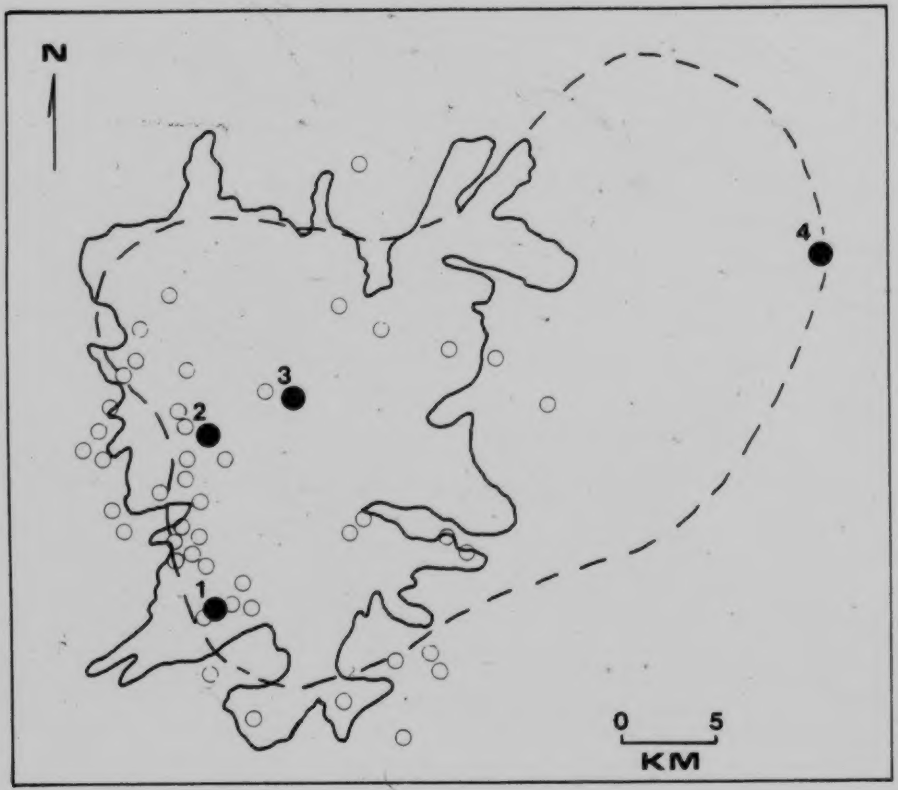

Figure 10.... Earthquake locations inside the Valley of Mexico. The numbers in this figure indicate known locations; 1 Ciudad Universitaria, 2 Chapultepec,3 Alameda and 4 Texcoco. The broken line outlines the valley and the continuous one Mexico City

Any investigation of the geodynamics of the valley of Mexico must consider the probable cause of the local seismicity. I do not believe that it is directly attributable to volcanic activity. The seismicity is observed in the South Western part of the city and there is no evidence of thermal activity other than that which caused the Chichinautzin lava flow which is of early pleistocene age, and constitutes the southern limit of the valley. There has been more recent activity in the valley, but the nearest recent activity is about 70 km East of the area in which the seismicity was observed. The region of Popocatepetl is active now. A connection between the seismicity observed in South West Mexico City and volcanic manifestations in the South East is probable but it is suggested here that triggering by pore pressure changes due to pumping of water in the valley is a more plausible explanation. In this chapter the relationship between the geologic and hydrologic structure of the valley of Mexico and its seismic behaviour is investigated.

Little is known about the geodynamic characteristics of the valley. The importance of these data comes from the fact that the seismic activity detected inside the city seems concentrated at a few locations, and that the damage suffered by the structures of the city varies greatly in locations only a few hundred meters apart. Methods of obtaining information about the tectonic state of stress of the valley from the knowledge of its geological characteristics will be investigated in this chapter. This stress state obviously will help to delineate the earthquake generating mechanism.

Solomon et al. (1980) pointed out that the state of tectonic stress in a given location is linked to the rheology of the material and to the history of application of a system of forces. None of this information is known in sufficient detail to enable the determination of an unique state of stress. Nevertheless, it is important to estimate this stress state because the tectonic stresses cause crustal deformation and control many tectonic processes.

In this study an elastic model of the crust in a two dimensional cross section will be used. It is assumed that the only force acting in the vertical direction is the weight of the material itself. This elastic treatment is in accordance with Lambeck (1980), who pointed out that the usual elastic theory approximation to determine stresses in the earth's crust may not be entirely adequate, unless the region in study is sufficiently far away from the plate boundaries and other sources, so that the lithosphere has cooled and elastic forces become the dominant support mechanism for the isostatic load. This is the case in the valley of Mexico.

3.2 Previous Seismo-Geodynamical Studies

The seismic characteristics of the valley have been recognized since the begining of this century. Scientists have focused their efforts on earthquake problems related to seismic engineering. This perhaps is the main problem to overcome when more general geophysical studies are intended. Although the area has been monitored continuously since at least 1909, the reports are more concerned with intensities than magnitudes, the location and reasons for the events are of secondary importance to the effects on the civil structures of the city and the determination of safe building codes for the different areas of the valley. Only recently have geodynamical studies also been recognized as also of importance. This is understandable if one considers the human factors involved.

All this implies that although the seismic catalog that is available is complete to a magnitude threshold of approximately 1.0, the magnitude listing in the catalog is incomplete. However, the original smoked paper records from the Tacubaya seismic station are available for anyone interested in completing the task and from these at least coda magnitude determinations are possible. The major problem in this catalog is that during most of its length the only seismic station available is Tacubaya, which makes the epicentral locations and the depths inaccurate. Nevertheless, for most of the local events the effects of the earthquake in the valley were restricted to a zone of small radius (1 km); this supports the locations to ± 2 km, and the epicentral depths for these local events can also be generalized; they are shallow.

The seismic instrumentation of the Tacubaya National Observatory has been recording without interruption since 1909 (figure 11). In this period it has registered more than 1900 local events inside the valley, most of them less than 25 km from the observatory. Figueroa (1971) calculated that the total energy released in these local earthquakes is of the order of $10^{17.5}$ ergs.

Figueroa (1971) noted that a common feature of all these events is a dominant short period, not greater than .5 sec, independent of the intensity of the earthquake. The time of duration or Coda length (T) is less than 5 sec for most of these earthquakes. This results in a magnitude of 0.5 at the most, using the formula (3.1) for coda magnitude:

$$M = A - B \log T \tag{3.1}$$

and the constants A and B determined for California (Richter, 1958). A magnitude of 0.25 is obtained from applying the constants for Rangely Colorado (O'Neill and Healy, 1973). A magnitude of 0.4 is the result when using the constants determined for the central part of Chiapas in southern Mexico (Uribe-Carvajal, 1979). These calculations reinforce the previous inference that the Tacubaya seismic catalog is complete at least from a magnitude of 1.0 for the

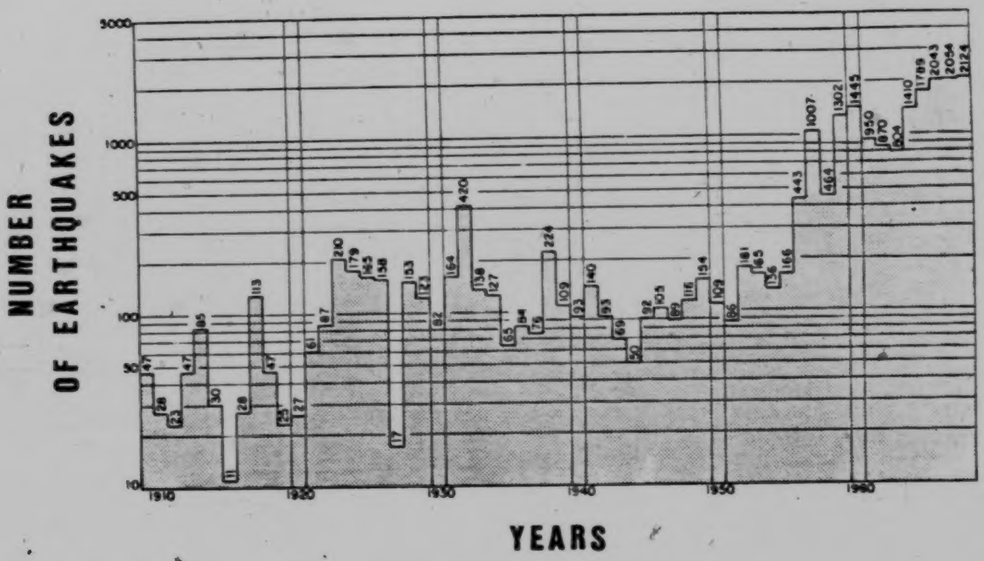

Figure 11.... Number of events recorded in the Valley of Mexico vs time (modified from Figueroa, 1971).

whole valley.

Figure 11 shows without any doubt that the amount of local seismicity recorded inside the valley has been slowly increasing during most of this century. It is reasonable then to assume that it is directly related to the growth of Mexico City and to the amount of water pumped out of the subsoil in the area.

The region has been monitored for more than 70 years and the recurrence times for large earthquakes in the Middle America trench zone are of the order of 35 years. If the region of interest is a tectonic feature of the subduction of the Cocos plate beneath the North American plate it can be expected that the recurrence time will be of the same order in the valley. However, due to the discrepancy between the strike of the mountain belt and the trench, the assumption that no large tectonic earthquakes occurred in the area after two periods is weak. Nevertheless, no evidence of a large earthquake is found in the past 200 years.

3.3 Seismic instrumentation inside the area

As mentioned in the previous section, most of what is known about the seismic characteristics of the valley are due to the records obtained at the Tacubaya seismic observatory. The observatory has three horizontal seismometers and one Weichert vertical seismometer with a mass of 17 tons, a period of 1.5 sec, and a maximum amplification of 2000 times. All this intrumentation belongs to the past generation of mechanical seismometers, of which there are few still in operation. Records on smoked paper are stored and any event of interest might be located on them.

In 1967 an electromagnetic seismic station began to operate in the old Institute of Geophysics of the University of Mexico (UNAM) and has been in intermittent operation since then.

Since 1961 the Institute of Engineering of the same university has set a network of seismic equipment throughout the entire valley. By 1971 it included 8 strong motion recording instruments (accellerographs) and 3 seismoscopes (figure 12) (Figueroa, 1971).

A seismic telemetering network was installed in 1976 with the specific goal of studying the seismic behaviour of the valley. In cooperation with the UNESCO the Institute of Engineering started the Sistema de Informacion Sismo-Telemetrica de Mexico (SISMEX). By 1978 this had four seismic stations in full operation (figure 12), each with a short period (1 sec) vertical seismometer. The analog signal from these stations is sent to a central location in the institute itself where the signals are recorded on magnetic tape at the same time as ink galvanometer seismograms of each station are drawn. The events are selected from these records and then digitized by means of a NOVA 800 minicomputer. The data are stored in digitized form on

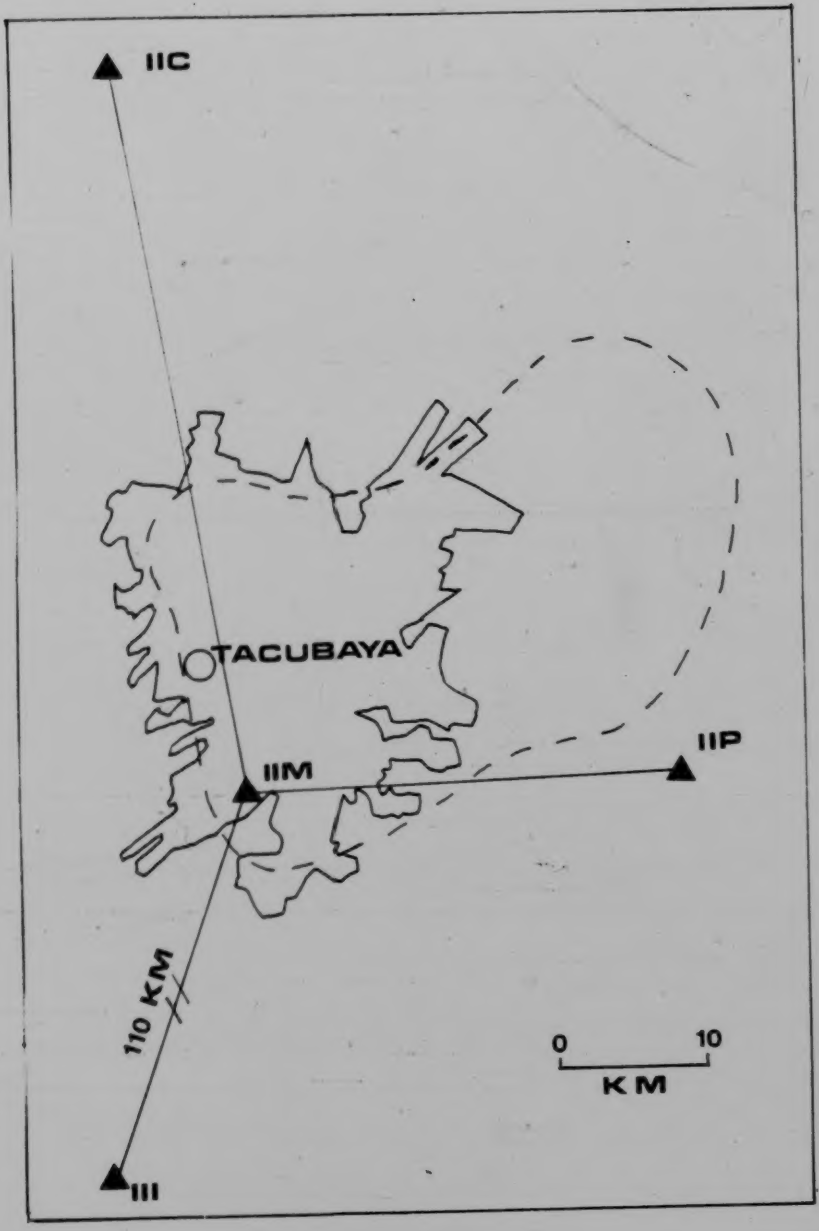

Figure 12.... Shows the location of the seismic stations of the SISMEX network.

permanent magnetic tapes which allows manipulation for any kind of seismic study.

This network has been integrated into a nationwide network since 1979, which allows large earthquakes to be studied more accurately. The local events in the valley are rarely, if ever, detected by seismic stations outside the valley.

The SISMEX network has improved enormously the quality of the seismic information recorded within the valley and has made apparent the completeness of the previous catalog obtained from the records from the Tacubaya seismic observatory and the potential for high accuracy seismic studies is now available. This network has operated without interruption and information derived mainly from its records is now being analysed to understand the seismic behaviour of the Valley of Mexico.

3.4 State of stress

The determination of the state of regional stress itself can be approached by determining the stress field in a two dimensional finite element model. A constraint on this model is that observed seismicity occurs in areas of high shear stress. These areas have been referred to as unstable (Chapter 2). The stability for this elastic model at any given location can be determined by the distance of a Mohr circle from a Coulomb type of failure envelope as shown in figure 8 (Chapter 2). The precise instability criterion used in this chapter will be the Residual Instability Function as described in section 2.5 of this thesis.

To be able to calculate the desired instability function one must specify a model. For this study a seismically determined model of the valley of Mexico (Havskov, 1982 b) was initially adopted. The regional structure of the area is modelled as a set of horizontal layers shown in figure 13. This model was obtained from an earthquake swarm that occurred in February 1981, and is an extension of one based on refraction profiles (Havskov and Singh, 1978).

The structure of the upper 200 meters of sediments is well known since numerous wells have been drilled in the valley. Unfortunately, only one has gone to a depth of 2000 meters (Oviedo, 1967). However, since the regional state of stress is the main concern here, the details of this structure are of secondary importance. The general conclusions of detailed studies (Cruickshank et al., 1979) will be taken to fix the average behaviour at shallow depths.

The models will deal at the most with the upper 20 km of the lithosphere. For the elastic models a finite element program that works with linear elements of three and four sides has been developed. The results obtained have been reproduced also by applying the program ADINA (Bathe,1978). A general description of ADINA can be found in chapter 4. The porous media analysis was done with the help of the program ADINAT (Bathe, 1981) which is a complementary finite element program to ADINA allowing the modelling of consolidation problems.

The grids of finite elements used in the initial models have in common that for the upper 6 km the elements taken are cubes of approximately 1 km per side while below this depth the elements have a dimension of 2 km in the vertical direction. This rule was changed for the final models due to the complicated geology and the node distribution used can be seen in figure 16a.

The initial model (figure 13) is a modification of Havskov's model in the sense that the horizontal layers have been placed inside half of a valley shaped structure. The dip of the walls in the valley was initially taken as 45°. The variation of the stability function can then be observed as a function of this angle.

The boundary conditions taken are as follows: on the bottom, no vertical displacement can take place. The valley is taken to be symmetrical, that is, the model is restricted to move in the vertical direction only on the right side. On the left, a horizontal stress of 0.8 of the gravitational load is applied. The value 0.8 is used because the maximum shear stress calculated with this criterion gives values similar to those determined by the maximum shear stress curve for hard rock (McGarr, 1980), and those determined from hydrofracturing experiments by Haimson (1978). It is in agreement with the few available measurements, from which

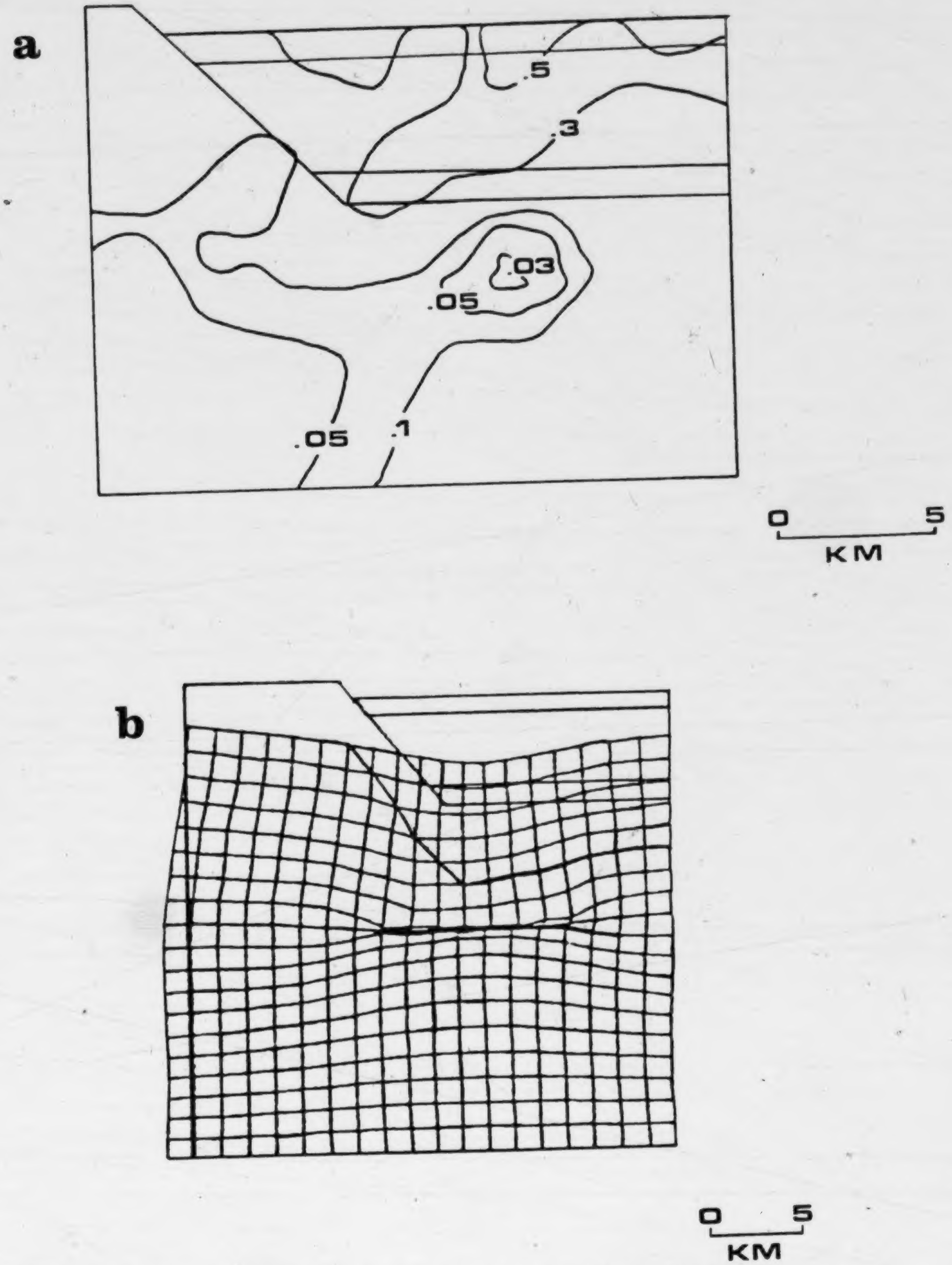

Figure 13.... a) Shows the resulting instability distribution in bars. b) Shows at the bottom, the displacement suffered due to the gravitational load.

McGarr (1980) indicated that the shear stress increases with depth in the upper 3 to 5 km, and there is no sign of a reduction in its gradient with depth.

The elastic moduli used were calculated by fixing a Poisson ratio of .25 for all the layers and giving the following densities for each of the strata from above downwards: 2.2, 2.6, 2.65, and 2.8 g/cm^3 for the basin structure.

Figure 13c shows the relation between the different components of the stress tensor and the resulting residual instability distribution for a model similar to the previous one. The same densities are used in this exercise, however, the boundary conditions at the vertical walls of the model differ from the other models used in this chapter. The nodes at these boundaries can not move in the horizontal direction. That is, the only force that is acting in the model is gravity.

The measure defined as residual instability (chapter 2) will be explored in this chapter. The residual stress will be derived from the change in gravitational stresses that results from the introduction of the structure of the Valley of Mexico in the homogenous halfspace. Detailed observations of the regional stress in the Valley of Mexico are not available but it is known that thrust earthquakes have been observed there (Havskov, 1982.b). The present model permits such events because of the inclusion of horizontal compression by constraining the boundaries of the finite

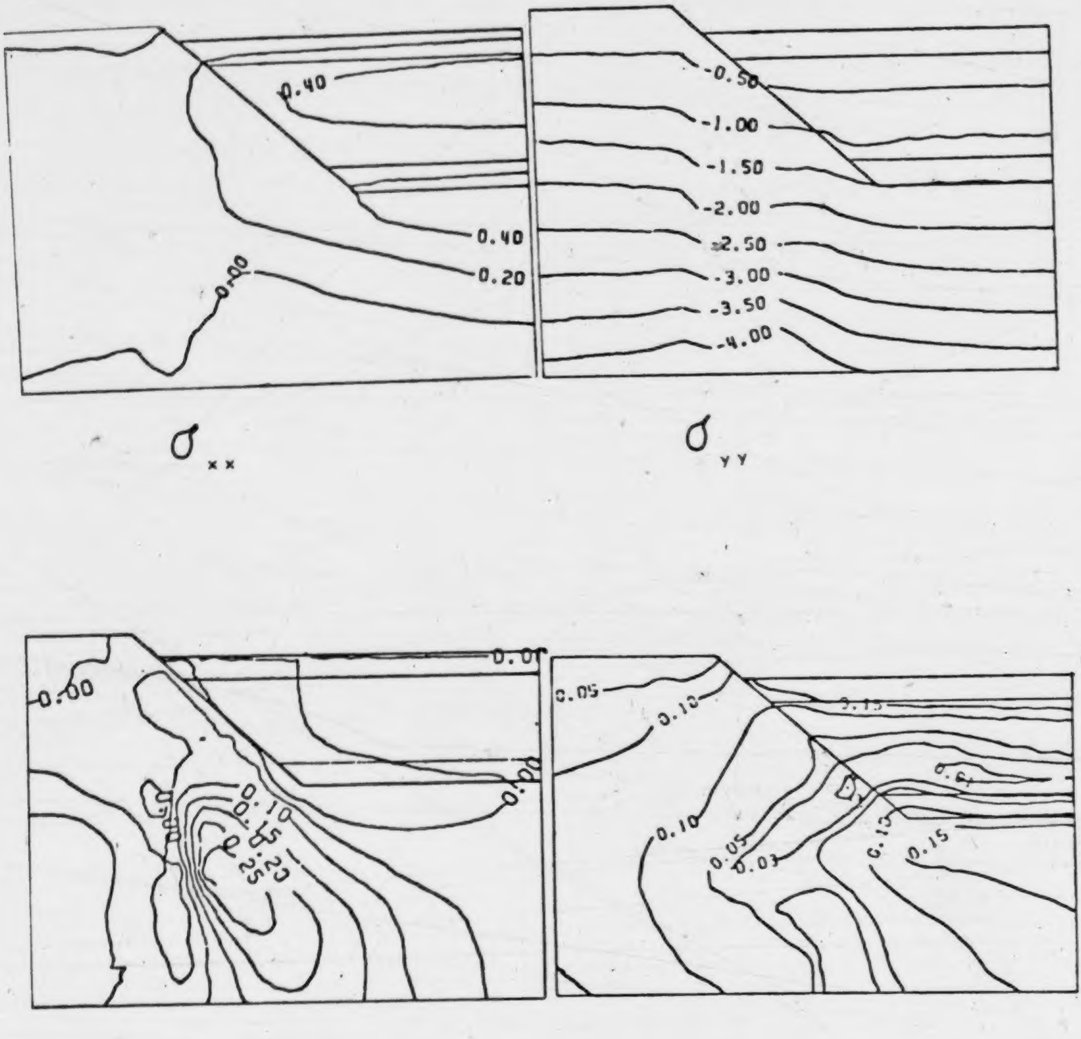

σ_{xx} σ_{yy}

σ_{xy} residual instability

Figure 13c.... Stress components and the corresponding residual instability distribution for a gravitational model of the Valley of Mexico.

element model.

The nature of faulting in this kind of model depends on the relative magnitudes of the principal stresses. Generally in tectonics one is vertical, denoted σ_3. If σ_3 is greater than both horizontal stresses σ_1 and σ_2, the regime is in a normal faulting condition. This is the case for the region of study if the anomalous structure of the valley is not included. If, however, a low density inclusion such as a valley is placed in the model the stress variation induced by gravitation can lead to thrust faulting. This is particularly true if in addition to the gravity the stress field is modified by external agencies such as regional stress fields which can be modelled as boundary conditions on a finite element model.

The contours of equal residual instability in figure 13a show minimum residual stability areas. The displacement of each of the nodes of the model is given by the distortion of the grid of figure 13b. A compression of the material in the zone of low stability has occurred due to the concentration of stress resulting from the density contrast between materials. These displacements have been increased by a factor of 5 in order to make the change visible.

By comparing figure 13a with figure 14 it can be seen that as the slope of the valley wall increases, the zone located beneath the valley becomes more stable. The sediments of the valley behave in a more complex fashion but usually show greater instability for steep sided valleys than for shallow slopes on the valley walls (figure 14).

To incorporate an external stress in a regional sense, it should be recalled that the driving tectonic stress introduced by the movement of the plates is in the range of 200 to 300 bars (Solomon et al, 1980). This can be modelled by increasing the stress by 400 bars in the horizontal direction applied at the left side of the models. No significant change was observed in the location of the unstable zones. Therefore, instability is mostly dependent on the density contrast, that is, on the geometry of the model itself.

It is generally thought that there might be one or several volcanic cones buried beneath the sediments. For this reason a model containing a cone in the bottom of the valley was studied. The resulting instability distribution shown in figure 15a, resembles that of figure 13a with some minor changes: the deeper parts of the valley are slightly more stable, the zone beneath the slope has stabilized somewhat but the zone beneath the valley has become less stable. In order to approach the problem in a more realistic way, the smooth wall of the valley was roughened; its stability distribution is shown in figure 15b. The unstable zones from figures 13a and 15a are somewhat enhanced (figure 15).

Several things can be learned from these simple models. One is that by introducing structures it is possible to change the shape of the instability curves in such a way

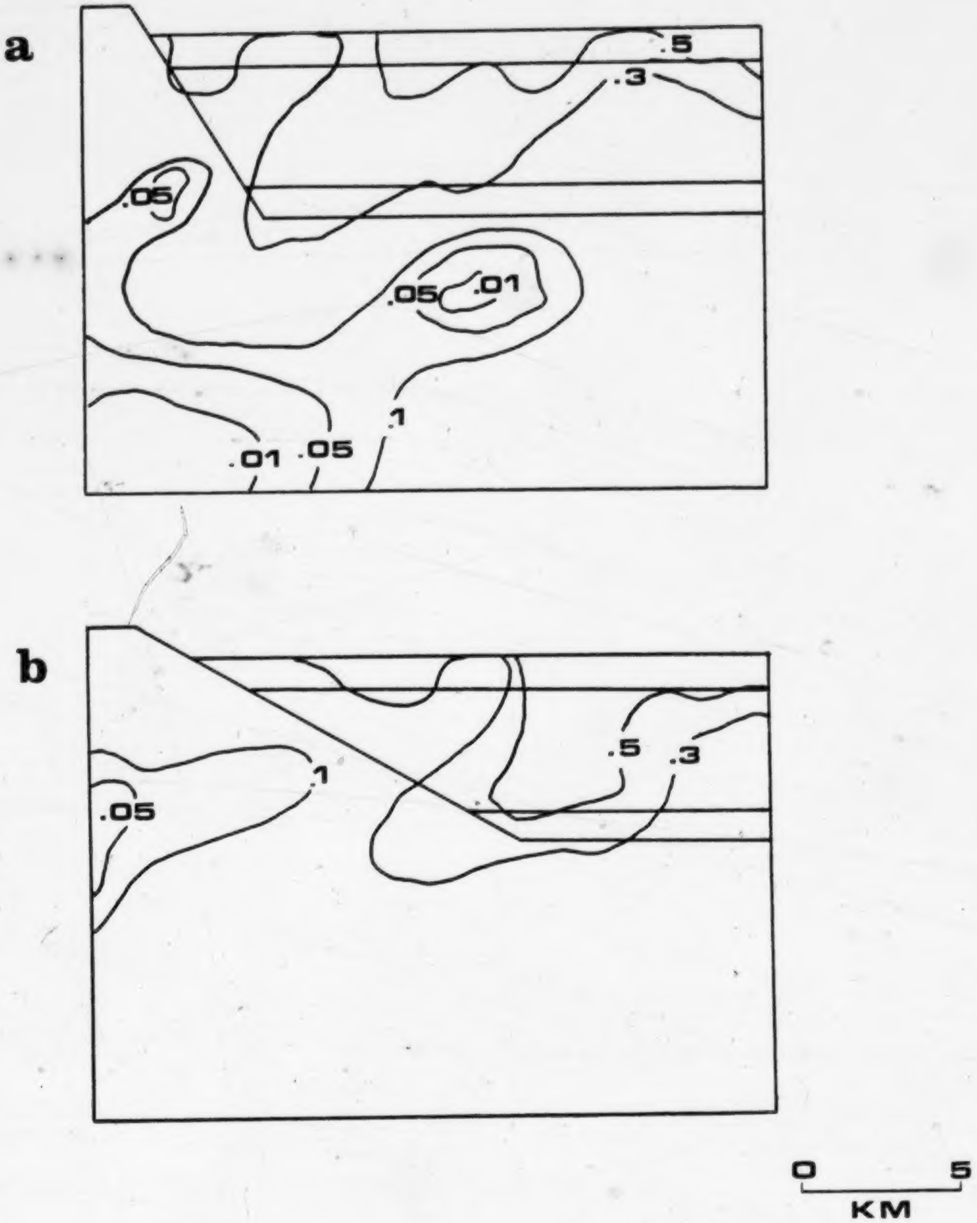

Figure 14.... Shows the residual instability distributions in bars, resulting from varying the slope angle. a) For a slope of 60° and b) For a slope of 30°.

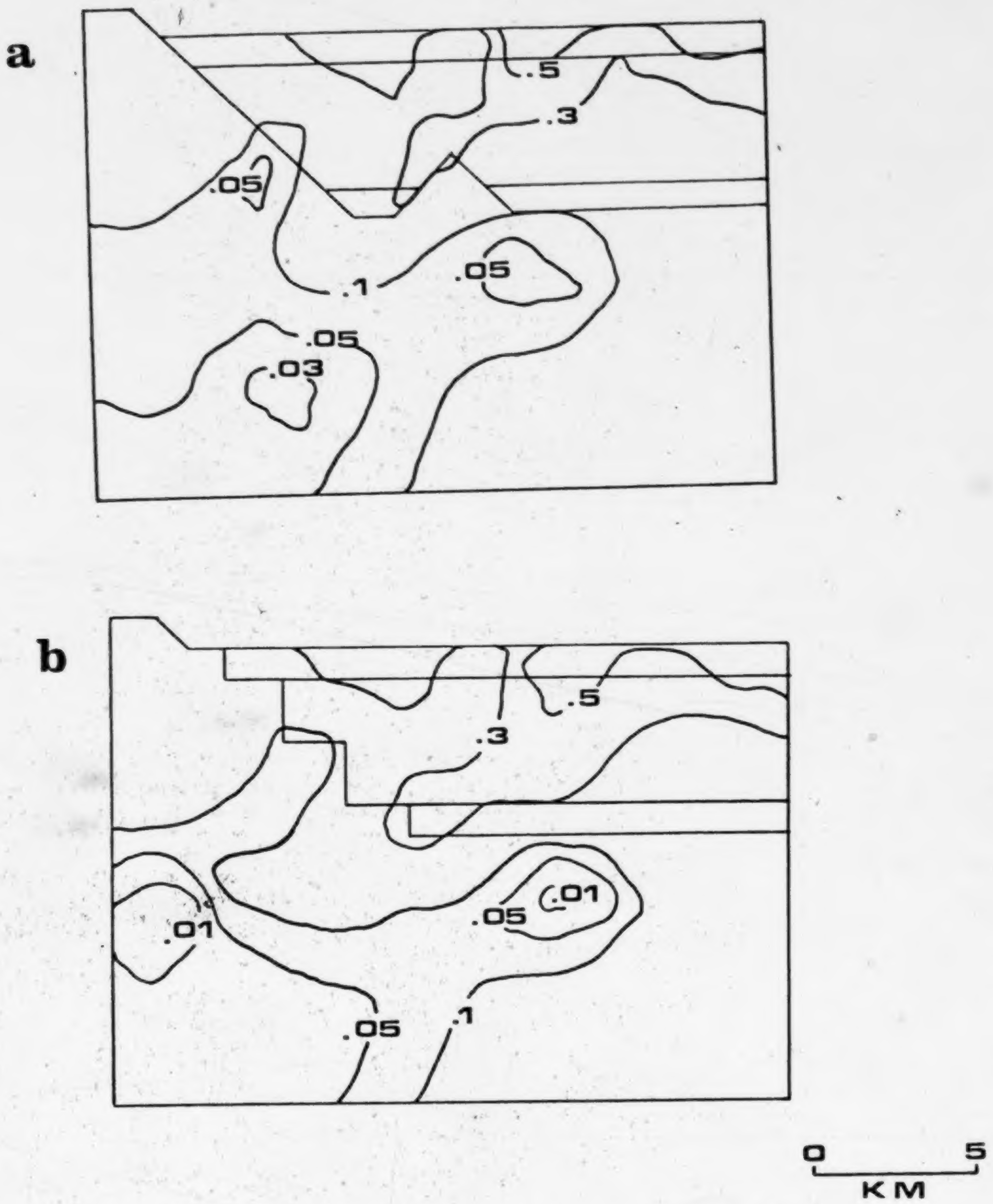

Figure 15.... Shows the residual instability distribution in bars for the following variations: a) a cone has been introduced in the bottom b) the left side of the valley has roughened.

that the maximum values correspond to the areas where earthquakes have been detected. This brings in the danger of exaggerating this procedure in order to force a result in a poor initial model. Clearly, to reduce the inherent nonuniqueness it is necessary to support the conclusions with other information.

In order to improve the model in the upper 3 km of the crust, use was made of the geologic map of the valley (Instituto de Geologia, 1968). Beneath that depth, the Havskov model was adopted for the final model analysed (figure 16). For this analysis the same boundary conditions were used as in the previous models.

Figure 16b shows a stable zone bounded by contours of value .15 at a depth of 3 to 5 km. This stable zone appears to be discontinuous in the stippled area which is a section through the seismically active volume. The stippled area covers the depths at which events occur and is the part of the seismic zone indicated in the plan on figures 17 and 19 which lies under the line AB. Figure 16b also shows an instability area below 6 km which suggests a potential for seismic events at depths below the aquifer.

The results of the preliminary models shown in figures 13 to 16 all show that the zone at the bottom of the sediments at the flank of the basin (lower corner of the valley) introduces a concentration of stresses that results in low stability areas. By considering the valley as a region inside a circle of mountains a low stability ring

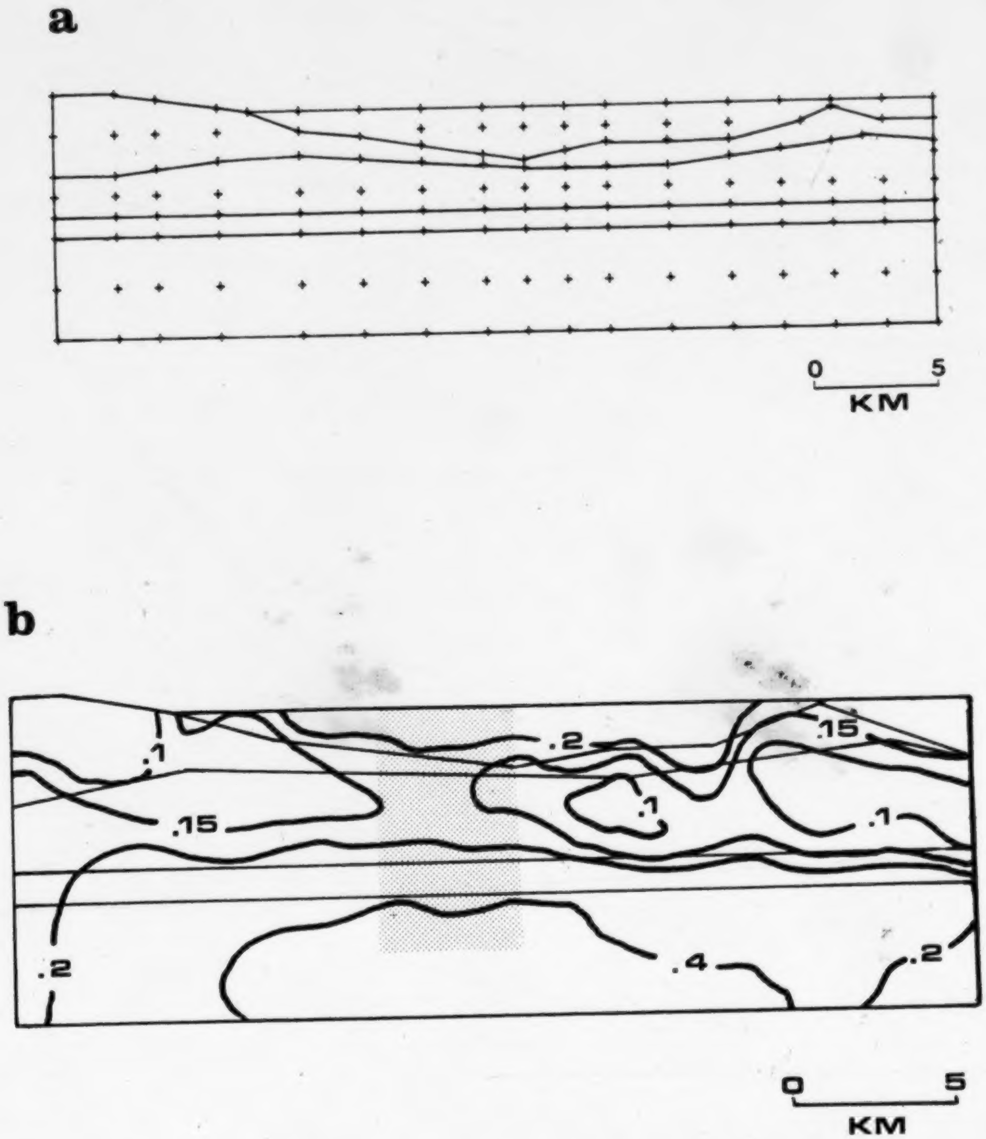

Figure 16.... Shows a) the nodes used, and b)the residual instability distribution for a cross-section on the line AB (figure 17). The shaded area represents the location of observed seismicity.

around the valley is delineated, the ring appearing at different positions at different depths. However, estimates of depths of seismicity are difficult to obtain with the best of seismic networks, and since the data discussed here were obtained with less than ideal observing networks it is considered that the data are not accurate enough to reliably discriminate mechanisms with depth.

Other than the data for the 1981 (Havskov, 1982.b) swarm which is located to ±1 km, supporting data (Figueroa, 1971) rely on historical evidence and damage reports. These are sufficient to isolate the events to the region indicated on figures 17 and 19 but not sufficient to publish more precise locations. Nevertheless the triggering mechanism probably does vary with depth and some of the inconsistencies between the hydrologic behaviour and the model could be explained this way. The ring defined by the depth of the bottom of the valley is considered to be representative. The area where earthquakes have been observed (figure 17) falls entirely within this ring.

3.5 Discussion of Elastic Models

In order to link seismicity and the instability zones indicated by the finite element model calculations it is necessary to propose a mechanism that might trigger events in the anomalous zone of figure 16b only at the location of the observed seismicity. Why events occurred only in a restricted part of the stability low must be explained. Here it is suggested that the triggering mechanism could be related to pumping induced subsidence.

Cruickshank et al.(1979) developed a finite element model of the upper crust of the valley and were able to determine the thickness of the water saturated layer, the thickness of the layer over it, the change of piezometric levels and the rate of sinking of the valley. They stated that there is a direct relationship between the observed sinking and the pumping of water from the water-saturated layer and that the only way of stopping the subsidence would be to stop the pumping. Their model of the valley consisted of a water saturated aquifer overlying the basement and underlying a narrow non-saturated layer. This model is an approximation to the detailed model studied by Marsal and Mazari (1969). Here, the upper layer was treated as perched aquifers separated by thin impermeable strata. Marsal and Mazari pointed out that as a consequence of the exploitation of ground water, a strong alteration of the piezometric levels had occurred. From the nature of equi-pressure drop contours in the area (figures XII-10 and XII-11 from Marsal and Mazari, 1969), they inferred that the effect in the aquifers was more pronounced in the west section of the city. Here they found that not only the gradients are larger, but also maximum pressure drop occurs. Using these facts they proposed that the piezometric level drops are related to the underground recharge and concentration of pumping.

The results of Cruickshank et al. (1979) predict the sinking and the piezometric change in the valley accurately. Therefore for the regional analysis proposed here and due to the reasons explained earlier, the model proposed by Cruickshank et al. will be used in the search for a triggering mechanism. If in fact several aquifers exist, they must be connected by many multiple faults as suspected by Figueroa (1971). The rate of change of the piezometric drop in the upper formations was found to have a high between the observed values of 20 and 30 (Cruickshank et al., 1979) (figure 17). This value represents the piezometric drop, measured as the difference of readings between a piezometer placed in the aquifer and one placed in the water table, and is given in meters. The location of the earthquakes mentioned above coincides with the area where the gradient of this piezometric drop is high. In this area the velocity of flow may be expected to increase.

The zone where the pressure in the pores of the rock has changed the most is where the effective stress has suffered the greatest change. The effective stress that describes the behaviour of porous media is the result of the difference between the normal stress and the pore pressure. It has been shown by several authors e.g. Gough (1978), Simpson and Negmatullaev (1981), Withers and Nyland (1976,1978) and others, that the introduction of a water load can change the state of stress in a given area and can induce some seismic activity depending on the geological

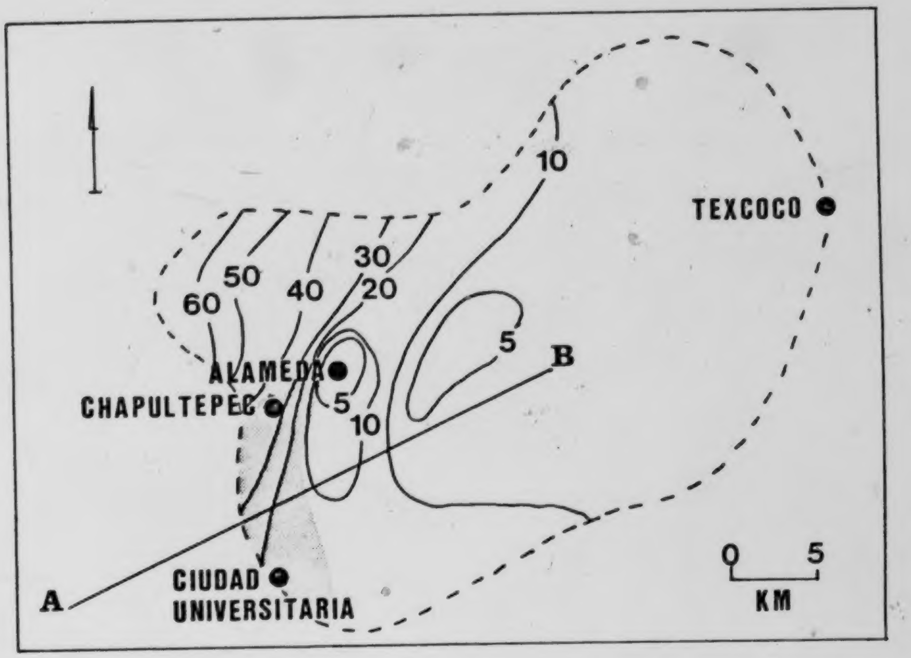

Figure 17.... Observed piezometric drop in the valley given in meters. The shaded area represents the location of observed seismicity.

conditions prevailing in the area. In the case of artificial lakes, the induced activity seems to be concentrated in the upper 10 km of the earth's crust.

Although the general belief is that the increasing water load will decrease the effective stress in such a way that induced seismicity can occur, decreasing a load may also trigger events in an area close to failure (figure 18). This initial effect can be reduced by diffusion of pore pressure if the area is not in a thrust faulting environment. If an increase in water load will increase the risk of seismic activity with normal faulting and tends to stabilize an area prone to thrust faulting (Gough, 1978 and Withers and Nyland, 1978), the decrease of water load will act oppositely in the different stress environments. Figure 18 demonstrates that the reduction of water load IN the aquifer will in fact reduce the value of the stability function in the zone located BENEATH the aquifer. This is so because in this region the major effect of pumping water is a reduction of the normal stress on a less permeable stratum below the aquifer. Since the effect is due to load changes it can be expected to occur rapidly.

Such changes have two effects on the state of stress on the region; one is the increment of the stress due to changes in the mass of the aquifer, the other is the change of the effective stress due to a delayed change of pore pressure at depth (Gough, 1978). These phenomena can be studied with Mohr diagrams which can be plotted for normal

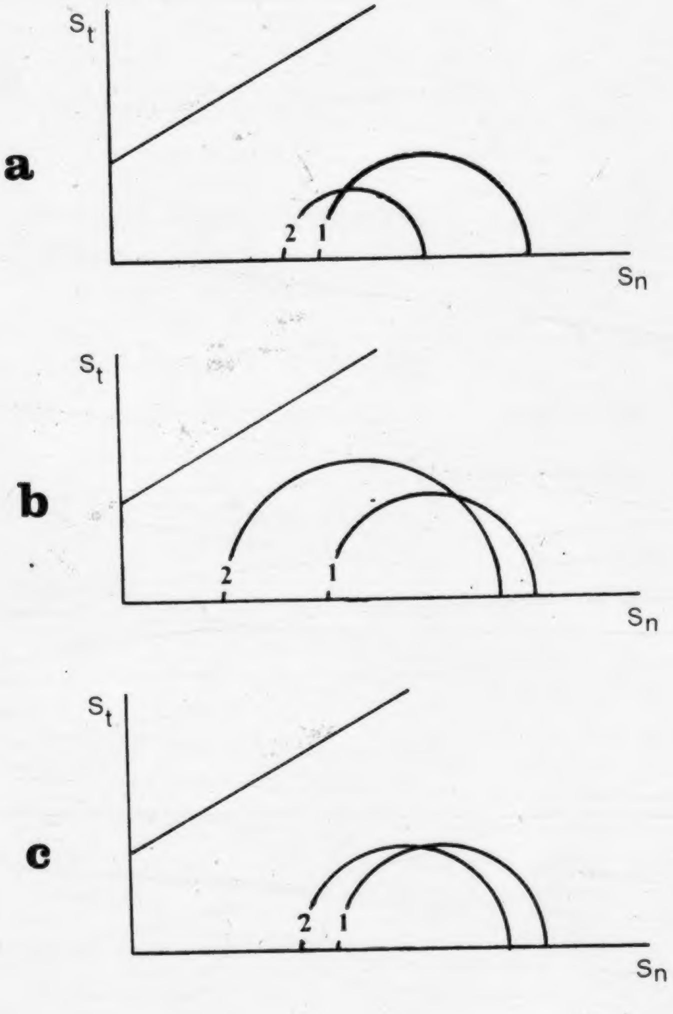

Figure 18.... Stability changes due to the change in the gravitational load for different stress enviroments. a) normal faulting, b) thrust faulting and c) strike-slip faulting enviroment.

faulting regimes (figure 18a), thrust faulting regimes (figure 18b), and strike slip faulting regimes (figure 18c). It should be recognized that in each of these regimes the maximum and minimum principal stresses are oriented differently and as a consequence the application of a fluid load will cause different increments in the Mohr circle.

Circles 1 in figure 18 represent the initial state of stress while circles 2 represent stresses resulting from subtracting the weight of the water above the stress distribution environments. It is clear from these diagrams that unloading decreases stability immediately. Although pore pressure diffusion will tend to stabilize the result the impermeable base of the aquifer may isolate the unstable zone from this phenomenon.

It is likely that the actual sinking is representative of the amount of water removed at the different locations inside the valley, so lines of equal sinking have been overlaid on the area of occurrence of the earthquakes (figure 19). Clearly, subsidence alone is insufficient to explain the presence of events only at one part of the low.

The fact is that pumping of water has been stronger in recent years in the low stability area (Cruickshank, personal communication), which means that the overall sinking reported is not completely consistent with the amount of water retrieved at particular locations. The suggestion that the amount of water pumped out in this zone may be a triggering mechanism is supported by the thrust

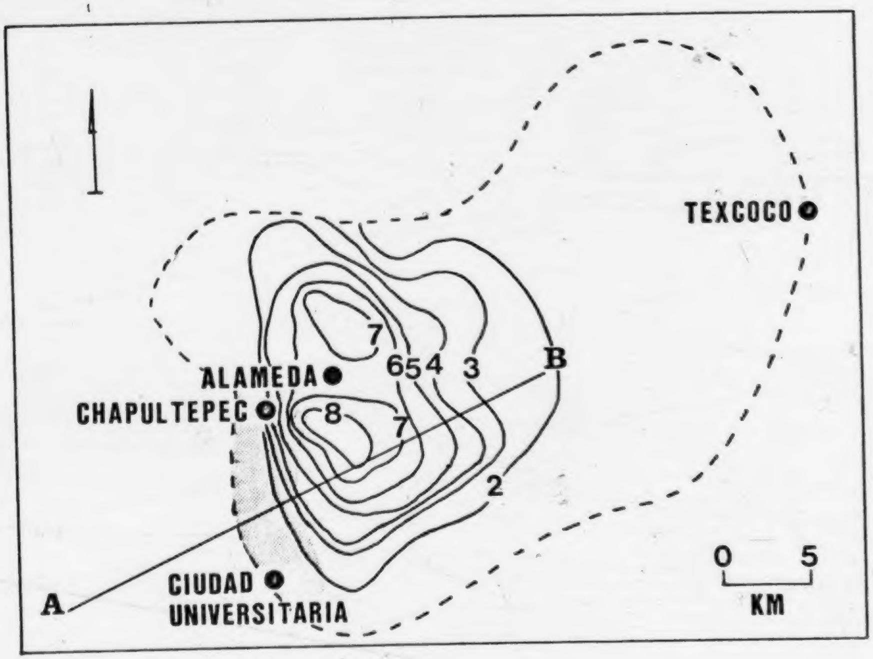

Figure 19.... Shows the observed subsidence of the valley given in meters. The shaded area represents the location of observed seismicity.

mechanisms determined for the 1981 earthquake swarm by Havskov (1982 b). This is so because a reduction in pore pressure can activate a region close to thrust failure.

The results obtained by Cruickshank et al.(1979) suggest that the stability is decreased far more by the change in the effective stress in the area where the zones of low stability and the high rate of piezometric drop intersect (figures 17 and 19). The high velocity of the flow and the high rate of change of the amount of water in the overlying formations affect the effective stresses by introducing load changes in the underlying formations and pore pressure fluctuation in the aquifer.

3.6 Porous media modelling

It has been recognized for a long time that the increase of water content in a geological environment can trigger earthquakes. This is possible if the area is prone to normal or stike-slip faulting mechanisms. This increase in water content could be due to the impounding of an artificial lake or to the direct injection of fluids by boreholes.

The evidence for the second type of induced seismicity comes mostly from the Denver and the Rangely fluid injection studies. Healy et. al. (1968) were able to detect in the Denver experiment a close relationship between the times of injection of waste fluids and the occurrence of seismic activity in the surrounding area. They were able to infer that the activity is delayed approximately one year from when the injection took place. The epicenters determined lay within an elliptic zone of 10 km by 10 km which encloses the disposal well. The events recorded have a strike-slip mechanism which is consistent with the faults observed in the area and have magnitude up to 5. There is no evidence of previous seismic activity in the area. The well was drilled through 3700 m of sedimentary rocks and finished in fractured precambrian granitic gneiss.

At the Rangely, Colorado Oilfield the U. S. Geological Survey carried out an experiment to control the seismic activity of the area (Raleigh et al, 1976). They were able to verify the effects of pore pressure changes on the effective stresses, and relate these stresses determined from field observations to the occurrence of seismic events using a Mohr-Coulomb failure criteria. The oilbearing formation is Weber sandstone which is 350 m thick and at a depth of 1700 m. This overlays other sandstone and limestone formations of Paleozoic age. The basement is found at a depth of 3000 m. The induced events had a strike-slip mechanism which is also in accordance with the observed fault pattern of the area.

In the previous section it has been suggested that if delayed earthquakes with normal mechanisms can be induced by increasing the volume of water involved, it is also possible to induce instantaneous seismic events with thrust mechanisms by decreasing it. This was done by splitting the response of the media into two parts, a rapid reaction due to the weight of the fluid alone and a time delayed effect due to pore pressure relaxation.

Since the models presented to this point did not consider pore pressure changes, the instability values could be overestimated by these calculations. To test this hypothesis a model consisting from porous materials was studied (figure 20). Several assumptions were made:

1. The different materials described in all the other models are now taken to be porous materials, consisting of elastic matrices with the voids saturated with water.
2. Permeabilities were assigned to each of these materials and were chosen in such a way that they were representative of the type of material and, as far as is known, of their geologic characteristics. The material properties assumed in our model are in accordance with the geologic data of the area, and the vertical distribution of seismic velocities observed there.
3. In order to allow for a finite element solution the boundary conditions were taken in such a way that no water can go through the lower boundary of the model. This means that all the water is contained within the upper part of the earth's crust; in our model the impermeable stratum is found at 12 km of depth. This was chosen since the main area of interest here is the behaviour of the top layers of sediments.

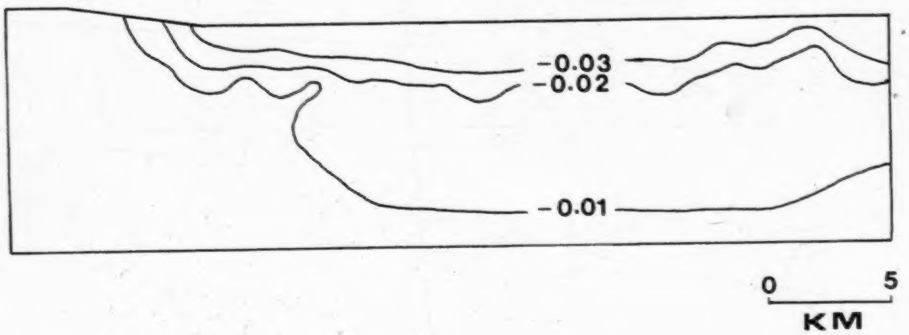

Figure 20.... Shows the change in pore pressure given in bars, calculated due to the pumping of water from the underlying formations of the Valley of Mexico.

The permeabilities assigned are: 30.0, 0.5, 4.0, 2.0, and 0.9 millidarcys for the layers taken from top to bottom of figure 20. The extraction of water is modelled by placing suitable, designed extractors at the surface nodes. The rate at which these "fluid pressure sinks" remove water was adjusted to reproduce the observed subsidence in the Valley of Mexico. There were two phases of constant rate of pumping. The first 60 years accounted for 90% of the total load in the part located to the right of the high risk area of figure 18b and no pumping was done in the high risk area. During the second phase, lasting 5 years, the pumping rate was such that the total load applied during the 65 years was equivalent in volume to the observed subsidence at each location.

The isolines of pore pressure drop that result from this analysis should be interpreted as the long term potential for relaxation of the stresses. They indicate how much the effective stress at a particular location can change due to future pore pressure relaxation. Greater values on figure 20 suggest that the location will become more stable once the pore pressure effect is introduced.

To be able to incorporate this porous media analysis, to the overall instability distributions presented in this chapter, it must be noted that figures 13 to 16 represent the state of stress after the impounding of the water alone. They do not consider any change of stress due to pore pressure variation. With this in mind, the combination of the results presented in figures 16 and 20, will represent a measure of long term instability. The combination of a high residual instability value (figure 16b), with an area of large (positive) change of pore pressure (figure 20) indicates that an unstable area will not recover its stability until after a certain time period unless external stresses are introduced. This shows the potential of these areas to be high risk value zones. One of the possible external sources of stresses are earthquakes.

Comparing figures 16b and 20, it becomes apparent that the shallow seismicity will diminish, if not disappear, after the effect of pore pressure changes is assimilated. This strongly suggests that the events are directly related to the extraction of the water and will disappear some time after the pumping stops. However, the unstable areas below 2 km of depth coincide with the zones at which the pore pressure attains greater values at the same depths. This can be interpreted to mean that if an earthquake occurs at these depths it will be located in these areas.

It is understood that the treatment of the lithosphere as a porous material consisting of an elastic matrix saturated with water is a highly idealized model but it is used here to test if in fact the seismicity of the area could be linked to the change in hydrologic conditions. The use of more complicated models will not affect this result.

It should also be pointed out that although this study and the Denver and Rangely experiments are related to induced seismicity several differences between them exist. At the Valley of Mexico the earthquakes observed have thrust faulting mechanisms, the activity seems to have increased in relation to the higher rate of water EXTRACTION while Denver and Rangely had seismic events with strike-slip mechanisms delayed with respect to the time of fluid INJECTION. In all three cases the earthquake mechanisms are in accordance with the faulting pattern observed in each area.

3.7 Conclusions

The models used for the stability determinations are restricted to elastic materials and do not take into account, except in a qualitative way, diffusion of water through the media. As a result, the curves in the upper layer of figure 16b are only approximate (an alluvial formation). Beneath this depth the results are credible. The general exercise is model dependent however, and the model is far from perfect. Nevertheless, the general features of the stability distribution should be independent of small changes in the model.

These studies have shown that from qualitative geologic knowledge, and some knowledge of induced seismicity due to the change in pore pressure, something can be learned about the nature of the seismicity observed in the valley of Mexico.

The following conclusions have been reached:

1. The concentration of stresses due to the bottom corner

of the valley creates a low stability zone which includes the zone where seismic activity has been observed.

2. There seems to be a relation between the observed events and some parts of the minimum stability zone described in figure 16b.
3. The triggering mechanism in those parts of the minimum where the activity is located might very well be related to the hydrological conditions of the valley.
4. The triggering mechanism of the deeper events may be related to the decrease in water content in the aquifer. There may also be other tectonic processes at these depths, or the aquifer may not be confined and the pore pressure changes might reach greater depths than those predicted by these investigations.
5. Porous media modelling confirms that the shallow activity must be highly related to the pumping of the water.
6. The shallow activity in the Valley of Mexico seems to have no relation to regional stresses that could derive from intraplate processes since the location of unstable areas was not modified by increments in the compressional regional stress.

The results obtained here for the Valley of Mexico are in excellent agreement with the hypothesis that diminishing the amount of fluids in a geologic environment can increase the instability of areas prone to thrust faulting, and may act as a triggering mechanism for earthquakes. Theoretically, this induced activity should appear almost instantaneously after the extraction of fluids takes place, and this seems to be the case in this area.

4. Thermo-elastic Behaviour of the Subducting Lithosphere, and its Relation to Long Range Precursors.

The concept of instability is such that high risk areas will appear along the discontinuities of the models (Chapter 1). A more complex problem in stability studies is the distribution of instability at subducting zones, since at the Middle America trench the Cocos plate subducts beneath the other two plates in this system. Subduction at both sides of the triple junction occurs at different angles.

In this chapter different subduction models are analysed using the probability function described in section 2.6. Earthquakes in the models are simulated as stress drops at the focal location. The analysis of several different models allows the suggestion of a link between the characteristics of the model and the range at which a seismic event can affect the stability of other parts of the model.

Long range precursors have been observed along some parts of the seismic belts of the earth. However, the range at which the anomalous seismicity can affect future activity varies from region to region. The state of stress on the lithosphere also has strong variations through the different geographical locations. Here the possible relationships that exist between the nature of the material that constitutes the lithosphere and the occurrence of long range precursors will be explored.

The probability function defined in section 2.6, is applied to determine the risk of seismic failure in different models of subduction zones, with the intention of determining what consequences the occurrence of a large earthquake has on the overall probability of failure in the model.

The results are similar to the seismicity actually observed in this kind of system. They strongly suggest that the thermally induced stresses, the coupling between the two converging plates and the angle of subsidence may play a very important role in the range at which long range precursors are possible. The range of these seismic patterns will vary widely for different trenches.

4.1 Introduction.

The determination of the state of stress in the earth's lithosphere involves a number of plausible assumptions; One of these is that the deep continental crust is less dense than deep oceanic crust. Another is the notion that the oceanic lithosphere increases its rigidity and its thickness as it moves away from the ridge at which it was generated (Leeds et al.,1974 and Forsyth, 1979). It is also generally assumed that the upper part of the plate behaves elastically and only when its temperature increases with depth does it start to act in a viscoelastic way (Solomon, 1980; Wyss 1977 and others).

This viscoelastic behaviour has been discussed by Savage and Prescott (1978), who pointed out that the short term response of a viscoelastic material will satisfy the requirements for the upper part of the mantle. The short term response to faulting will be elastic. He also concluded that appreciable stress changes may be produced at distances of several times the thickness of the lithosphere away from the source. These stress alterations are relaxed by the material flow, so that the response of the viscoelastic material is an instantaneous pulse followed by a monotone relaxation.

The regularity observed in earthquake recurrence in Japan has lead Shimazaki and Nakata (1980) to the suggestion that the larger an earthquake is the longer the following quiet period. This allowed them to propose several recurrence models for large earthquakes. To do this they assumed a constant accumulation rate of tectonic stress. A similar recurrence pattern has been observed for small earthquakes in California (Bufe, 1977). The constant rate of stress accumulation scheme has been used also by Newman and Knopoff (1982). This is an example of long range interaction in time in an earthquake catalog. Long range interaction in space may also exist.

It has been suggested that earthquakes sometimes affect the seismicity pattern of areas at great distances and that some large earthquakes seem to have been preceded by distant premonitory seismicity clusters. Several of these seismicity patterns for long range precursors have been proposed by Keilis-Borok et al. (1980 a,b,c). These patterns consist of an abnormal clustering of seismic events in time, energy and space. Pattern Bursts of Aftershocks consist of a medium magnitude earthquake with an anomalous sequence of aftershocks. Pattern Swarms consist of a group of moderate events concentrated in space and time. Pattern Sigma roughly consist of an increase of energy released in a sliding time window (Lamoreaux et al.,1983).

These patterns have been applied in algorithm form with some success in the Central Asia, Eastern Mediterranean, Pamir and Assam regions (Keilis-Borok and Malinovskaya, 1964); in Italy (Gasperini et al, 1978); in Anatolia and surrounding regions (Keilis-Borok and Rotvain, 1979); in the Lake Jocassee, South Carolina region (Sauber and Talwani, 1980); in Southern California (Keilis-Borok et al. 1980 b); in Tibet and the Himalayas (Keilis-Borok et al 1980 c); and in the North America-Cocos-Caribbean triple junction region (Lamoreaux et al, 1983).

Premonitory seismicity patterns are regional in nature and they do not indicate the exact location or the time of occurrence of a major earthquake. The results must be interpreted as an increase in the probability within a region inside a time window. Physical explanations for long range precursors are controversial. Barenblatt et al. (1984) suggest that the shear stress in the whole area is large and there exist local areas with higher concentrations. They claim that there is no reason to expect that these concentrations are confined to the vicinity of the earthquakes. It is suggested here that the actual physical properties of the upper part of the lithosphere may very well control the range of the long range precursors.

Newman and Knopoff (1982), on the other hand, pay little attention to the distribution of physical properties and suggest that the presence of long range precursors is linked to a dynamical process. They point out that the fusion of small cracks into larger ones can produce a cascade of events which may culminate in a massive earthquake, due to the nonlinear character of this process. In a later paper they propose that by assuming that the stress accumulates locally at a uniform rate only to be released by a large earthquake, the rate at which little cracks are produced can be related to the tectonic related stress.

The acceptance of these observed seismicity patterns runs into two major difficulties; it is not always possible to detect them and the range at which they might have some influence on the local seismicity of other areas varies greatly. The hypotheses suggested by Barenblatt et al. (1984) and by Newman and Knopoff (1982) deal with the first problem. In this chapter a mechanism that allows a different range for seismic events of the same kind, depending on the regional material properties in the vicinity of their origin will be proposed.

Most large earthquakes along island arcs are thought to be a result of fault motion across the zone of contact between the two lithospheric plates that form the subducting zone. The dimensions of these slip zones vary widely; a rupture zone may extend as much as 1000 km along an arc. Rupture zones of extraordinary length tend to occur along arcs where the two slabs of lithosphere interact across a broad interface. Along those arcs where there appear to be a narrow zone of contact the maximum dimension of rupture is limited to 150 km or less (Kelleher et al., 1974).

Kanamori (1977) suggested that it is almost certain that the degree of mechanical coupling between the two lithospheric slabs varies among different island arcs. An important feature brought up in this study is that the rupture lengths of great earthquakes of nearly identical magnitude vary greatly for different regions. Relationships between the type of interface and the extent of the rupture have also been suggested by Isacks et al. (1968), and for the Circum-Pacific belt by Kanamori (1971).

Kelleher et al. (1974) conclude, that the maximum seismic slip that can occur in a particular trench due to a large earthquake is strongly influenced by the geometry of the interface zone and in particular by the width of the plate interfaces. They analyse observations from several subducting zones and from their study the following remarks are important for the purposes of this chapter.

1. Along the Middle-America subduction zone where the

extent of shallow earthquakes (≤ 70 km) is relatively narrow, the typical observed ruptures are of 70 to 150 km long.

2. Ruptures of extraordinary length have occurred along arc segments where there is evidence of a broad interface between both slabs of lithosphere. For the 1957 Aleutian, the 1964 Alaskan and the 1960 Chilean earthquakes ruptures fault length extended for more than 800 km. For the 1952 Kamchatka and the 1965 Rat Island earthquakes ruptures length extended to more than 400 km.
3. Near each of these large rupture zones along island arcs, the line of volcanoes approaches the surface projection of the contour line for shallow earthquakes (≤ 70 km). By contrast, these two lines are clearly separated along arc segments characterized by moderate rupture zones.

The consistency of these observations suggest that there should be a physical relationship between the geometry of the subducting zone, the location of active volcanoes and the extent of the ruptures due to large shallow earthquakes.

On the basis of multiple seismological observations Kanamori (1977), proposed that a parameter that can be responsible for the difference in rupture lengths might very well be the degree of coupling between the two lithospheric slabs involved in the subduction. He suggested a plate coupling and decoupling model as an attempt to understand the physical mechanisms in the various types of subducting zones (figure 21). This model is an extension of the one proposed by Kanamori (1971).

Figure 21 (Kanamori, 1977; figure 8) shows the different kinds of possible subducting mechanisms that result from coupling considerations. Figure 21a represents a strong coupling between the oceanic and continental lithospheres which results in great earthquakes and break-off of the subducting lithosphere at shallow depths. In 21b partial decoupling leads to smaller earthquakes and continuous subduction while in 21c further decoupling might lead to aseismic events or intraplate tensional events. In 21d the sinking of the plate increases the angle of subduction and results in retreating subduction and the formation of a new thin layer of lithosphere.

4.2 The Method.

The initial state of stress is of great importance in the determination of the risk of reaching failure, therefore the shear stress concentrations that may be present due to faults or other structures are areas with high potential for failure. The stress build-up rate as discussed by Shimazaki and Nakata (1980) and by Newman and Knopoff (1982) justifies the process of modelling a region before and after the occurrence of a stress drop due to an earthquake as a static problem.

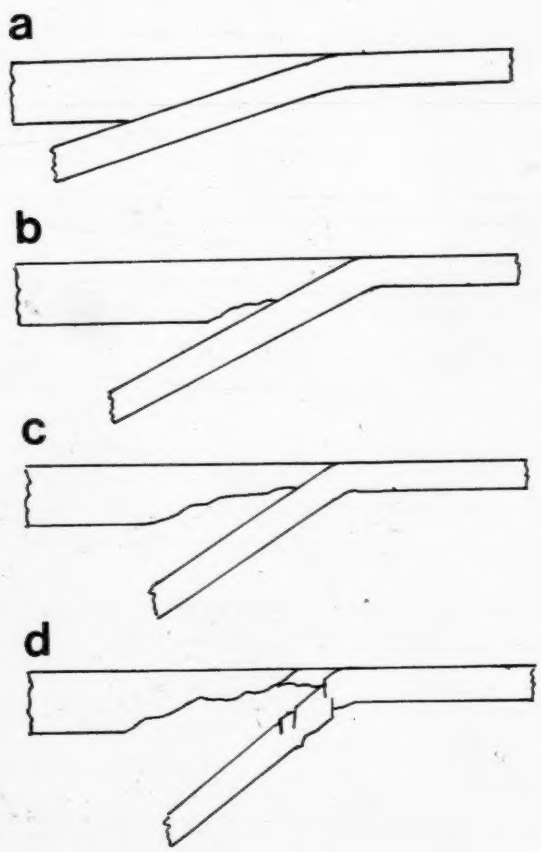

Figure 21.... Different types of subducting zones resulting from plate coupling considerations (modified from Kanamori, 1977).

Such modelling requires computation, almost inevitably by finite element methods. The finite element technique is one of the most closely scrutinized methods in stress calculation, since, as in all quantitative analyses, the theory on which it is based makes approximations and several different approaches can be taken for a particular problem. Also the application of realistic boundary conditions is often a dificult task. Only through experience can the best choice be made. As a result, conclusions derived from numerical techniques are often viewed with reserve. It is obviously desirable to solve the same problem by other methods to serve as an independent check.

The temperature distribution used for both of the plates involved in the subducting mechanism here is in accordance with that suggested by McKenzie (1969). Where the temperatures inside the subducting slab are calculated from

$$\frac{\partial^2 T'}{\partial x'^2} - 2R\frac{\partial T'}{\partial x'} + \frac{\partial^2 T'}{\partial z'^2} = 0 \tag{4.1}$$

where $T=T_1T'$, $x=lx'$ and $z=lz'$. The solution of this equation is of the form

$$T'=1+2\Sigma_n(-1)^n\cdot\exp\{R-(R^2+n^2\pi^2)^{1/2}\}x'\sin n\pi z'/n\pi \tag{4.2}$$

In this formulation R, the Reynolds number, does not have y dependence because the slab is assumed a two dimensional structure.

The values taken for the parameters in this chapter are:

Specific heat C_0=0.25 cal $g^{-1}{}^{\circ}C^{-1}$

Thermal expansion coefficient $\alpha=4\times10^{-5}{}^{\circ}C^{-1}$,

Temperature T_1=800°C

Thermal conductivity k=.001 cal $cm^{-1}{}^{\circ}C^{-1}sec^{-1}$

Width of the slab l=40 km.

The resulting temperature distribution is similar to that of McKenzie (1969, figure 2). Note that this kind of formulation can be applied if the thermal effects due to thermo-elastic stresses are included in the calculation. The finite element program used herein allows this effect in the calculation of the principal stress components of each of the nodes of the model.

It is important to start the analysis with an elastic model in order to obtain a general idea of how the stability changes as the model becomes more complicated. This kind of modelling has been proven useful in several geophysical problems (i.e. Solomon, 1980; Hanks and Raleigh, 1980) and in particular in seismic stability studies (Uribe-Carvajal and Nyland, 1983 a,b). Nevertheless elastic models can only be representative of the upper few tens of kilometers of the earth's crust, where the temperature of the lithospheric material is beneath 300°C. Below this temperature the thermally induced stress is small and the tectonics is describable by elastic stresses (Turcotte, 1974).

The lithosphere can be thought of as an elastic layer over a high viscosity layer. Beneath the lithosphere there exists a 'low strength' zone known as the asthenosphere, which by definition is not capable of resisting great loads for a very long period of time. This means that at a given depth, above the asthenosphere, the stress due to permanent vertical loads cannot produce vertical displacements after a certain relaxation time. It is unlikely that the boundary between the lithosphere and the asthenosphere is sharp; the lower part of the lithosphere should have similar physical properties to those of the upper part of the asthenosphere. The material in the upper layer of the plate should become gradually less viscous as depth decreases.

Since oceanic lithosphere cools as it moves away from the ridges (Forsyth, 1979) its strength and density increases. Strength and density are the main difference between continental and oceanic plates which is primarly due to the physical characteristics of their materials. Strength is the maximum differential stress ($\sigma_{mx}-\sigma_{min}$) that can be applied to the material without reaching failure; it increases with increasing confining pressure. It has been assumed here that the oceanic lithosphere has basaltic physical properties, while continental plates have rhyolitic.

The most important force acting in a boundary zone between two plates with converging relative velocities is the gravitational pull of the downgoing slab (Chapple and Tullis, 1977). This force has been proposed as the probable driving mechanism of plate tectonics (e.g. Press, 1972; McKenzie, 1972; Richter 1977). The frictional forces acting on plate boundaries are very small compared with the gravitational pull, the viscous drag of the mantle, and the ridge push force (Chapple and Tullis, 1977). However, it is of great importance to include these frictional forces in stability studies, since it has been proven in our previous studies (Uribe-Carvajal and Nyland, 1982,1983) that small shear stress changes can affect the overall stability distribution. The shear acting at the boundaries of all our models is in accordance with the one determined by McKenzie (1969).

The other force that must be included in any subduction zone model is the viscous drag of the mantle; it is the only one with the capability of balancing the action of the slab-pull (Richardson, 1978), so that plate velocities are restricted to few centimeters per year. Such velocities are indicated by Chase (1972), Minster et al. (1974), Sacks (1983) and others, for all the plates.

The resistive forces that oppose the movement of the plates are due to differential movements at the edges of the plates and viscous counter flow of the asthenosphere. The resistive forces at the interplate boundaries are difficult to estimate. However, earthquakes clearly show that these forces are not sufficient to stop the movement of the plates. This has been recognized by Jacoby (1970), Richardson (1978) and many others.

The assumption that there is an elastic lithosphere drifting over a viscous asthenosphere implies the existence of a drag force opposing this movement. In order to model this force it is necessary to assume a velocity distribution in the asthenosphere that depends on its flow. If the elastic plate is drifting over a passive viscous layer it is dragged over a base which is at rest.

The drag stress per unit length (Richardson, 1978) is

$$\tau=\eta V/h \qquad (4.3)$$

where V is the velocity of the plate, η and h the viscocity and the thickness of the asthenosphere. The term asthenosphere applies to the viscous layer that underlies the elastic plate, at the bottom of this plate no displacement is possible, and the drag force is then a function of its thickness (h). Following Richardson (1978), we take a velocity $V=10\text{cm/year}$, $h=3\times10^7\text{cm}$ and $\eta=10^{20}$ poise, to obtain $\tau=1\text{bar}$.

The integration of this force over the bottom surface of a plate gives values that can equlibrate the stresses due to the slab pull and the ridge push. The frictional forces due to the plate boundaries and transform faults are much smaller and represent a secondary contribution to the overall quasi-equilibrium of the plates. All these forces have been calculated for all the major plates by Chapple and Tullis (1977). They demonstrate that only a few forces are responsible for the observed velocities of the plates. These are the ones that have been taken into account in our model calculations.

In this chapter a geodynamical study of a subduction zone is presented. This is done using the ADINA finite element program (Bathe, 1978). The use of models is only justified to the extent that the model is a reasonable facsimile to reality, and in order to be able to model stresses in a subduction zone several assumptions have to be made. The stress-strain relationships that accurately represent the stresses at depth are uncertain. Nevertheless, for the use of stability functions it is sufficient to have an approximate model since they are affected only locally by small variations to the model (Uribe-Carvajal and Nyland, 1982,1983).

In the present case a continuum in which material property changes can be modelled by finite elements is dealt with, and the boundary conditions can be specified at the required locations. Therefore, the internal properties of the model can be varied and the variations of stability (derived from the stresses determined by ADINA) that result can be interpreted. Finite element models of subducting zones have been studied previously by others. Bird (1978), applies the technique to calculate the shear stress distribution within a subduction system involving a slab dipping at 45°. The greatest difference between Bird's model and the one shown here is the boundary condition at the upper part of the model; he considers the plates to be fixed at the surface, that is, the model does not allow for gravitational deformation of the plates.

The present model assumes that the system is not *hanging* from the surface, but *supported* by a surface at its bottom. The same kind of boundary condition was used in the analysis of the Valley of Mexico in chapter 3 of this Thesis.

The model presented here consists of an oceanic layer of 40 km of thickness underthrusting a 80 km thick continental layer. In the lower part of these plates the temperatures are well above the 300°C value (i.e. McKenzie, 1969; Griggs, 1972; Minear and Toksoz 1970), accepted as the limit for elastic behaviour. The thermal dependence of the stresses plays an increasingly important role in the overall state of stress as depth becomes greater. This can be modelled using the ADINA option for thermo-elastic modelling. In essence, the variation with temperature of the elastic parameters is specified.

The thermal dependence of the Young's modulus (E) is taken to be

$$E=E_{min}+E_0e^{-x} \qquad (4.4)$$

where E_0=E at the surface of the earth minus E_{min}, $x=T^2/C$, T is the temperature and C=600. This equation describes the exponential non-linear temperature versus depth behaviour of the upper mantle suggested by Kirby (1977) and others. It should be noted that as depth increases the temperature of the material is also increasing. At small temperatures E remains virtually unchanged up to a given temperature T_1, where the material starts to increase its viscous behaviour rapidly until a temperature T_2 is reached. Then the value of E becomes asymptotically equal to a lower limit value E_{min}. It is our claim that this E_{min} is that one representative of the value of viscosity of the upper asthenosphere stated earlier as η.

The exponential decay of E with temperature has been suggested previously in geophysics. Vening Meinesz (1964) pointed out that at a certain temperature the elastic limit indeed diminishes and that for some substances like Mg_2SiO_4, which is assumed to be an important constituent of the mantle at a given temperature, this elastic limit does not continue to decay.

Theoretically, Poisson ratio ν has an upper limit of 0.5, and for most crustal rocks ν is around 0.25 and it is a common assumption in geophysical modelling to use this 0.25 value. Therefore, I have adopted this value for surface rocks and have interpolated to ν=0.3 for the rocks at the bottom of the plate. The value of the thermal conductivity, a, has been taken to be constant (McKenzie, 1970) throughout the whole exercise. The values of the parameters have been varied (table 1) to simulate the dependence of temperature variations on the materials modelled.

There is an apparent contradiction between the values in table 1 and the general notion that seismic velocities increase as depth increases (Stacey, 1977, figure 6.18), and the increasing Young's modulus E with depth used by Turcotte (1974). This work focusses on the behaviour of the lower part of the plate from a quasi-static or isothermal point of view. We are not dealing with the dynamical or adiabatic properties of the material. Then as depth increases E should become smaller because the material is becoming more ductile as temperature increases, even if the moduli are not explicitly temperature dependent.

The difference between the adiabatic (dynamic) and isothermal (static) parameters comes from allowing temperature changes within the model of the earth. The relation between them can be found directly from

$$E_d=E/(1-ET\alpha^2/9C_0)$$

$$\nu_d=(\nu+ET\alpha^2/9C_0)/(1-ET\alpha^2/9C_0) \qquad (4.8)$$

where C_0 is the specific heat per unit volume at constant pressure. E_d and ν_d are the dynamic Young's modulus and Poisson's ratio (Landau and Lifshitz, 1970). Nevertheless, this kind of differentiation between dynamic and static

SUBDUCTING PLATE

DENSITY 3.

TEMP.	20	100	200	400	600	800	1000	1250
YOUNG	.7E12	.68E12	.63E12	.46E12	.1E12	.7E11	.57E11	.3E11
POISSON	.25	.25	.26	.265	.27	.28	.29	.3
ALPHA	4.E-5	4.E-5	4.E-5	4.E-5	4.E-5	4.E-5	4.E-5	4.E-5

UPPER PLATE

DENSITY 2.7

TEMP.	20	100	200	400	600	800	1000	1250
YOUNG	.6E+12	.58E12	.54E12	.40E12	.24E12	.12E12	.49E11	.2E11
POISSON	.25	.25	.26	.265	.27	.28	.29	.3
ALPHA	4.E-5	4.E-5	4.E-5	4.E-5	4.E-5	4.E-5	4.E-5	4.E-5

Table 1.... Shows the dependence of the material properties on temperature of the thermo-elastic models studied. Density is given in g/cm^3, Young modulus in $dyne/cm^2$, Temperature in °C, and α in $°C^{-1}$

parameters only makes their values vary by a small percentage. An additional statement is made however, by attempting to include *softening* due to increasing temperature.

All the forces involved in the models are placed at the node nearest to the actual point of application, as is done in other geophysical finite element modelling exercises (Richardson, 1978; Richardson, Solomon and Sleep, 1979); The occurrence of an earthquake is modelled by introducing a sudden displacement or stress drop in the model at the location of the hypocenter. This kind of earthquake simulation is usual in finite element analysis (Richardson, 1974). The stress drop due to an intermediate depth intraplate earthquake with focus in a subduction zone is of the order of 100 to 200 bars (Chinnery, 1964). Recently this value is now believed to be arround 40 bars.

4.3 The subduction zone models.

Several types of island arcs have been discussed and and summarized in figure 21. Geometrical changes in the model and the variation of the forces involved in the model should generate changes in the overall distribution of seismic instability. If the seismic behaviour of the different types of subduction zones depends mostly on these parameters, it is then necessary to study how these changes are reflected in the probability distribution.

This kind of geometrical dependence of any risk function must result from the analysis of several models. The models considered here will include

1. Material property changes, from elastic to thermo-elastic stress-strain relationships.
2. Changes in the angle of subduction and the value of the frictional forces. This will account for the coupling and partial uncoupling effects (Kanamori, 1977).
3. The length of the subducting slab has also been changed in order to model slabs of different ages, which also involves changes of the gravitational pull exerted by the downgoing slab.

The element distribution (figure 22) used for the model studies shown in figures 23, 24 and 25 is the same. However, the ratio between the horizontal and vertical total lengths varies to model slabs subducting at different angles.

The initial model is one plate underthrusting a second plate at an angle of 45° (figure 23). A linear elastic model of this kind of subduction zone and the boundary conditions and restrictions mentioned produce the probability distribution given in figure 23a. The higher risk of failure seems to be concentrated in specific locations, at which the analysis will be focused.

The high risk area is located in the intraplate boundary from a depth of about 50 km. This area has a probability of failure of more than 0.75 with respect to the other parts of the model. The highest probability of failure

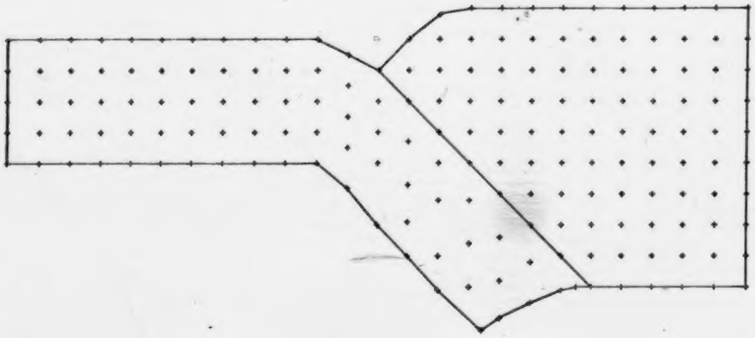

Figure 22.... Nodal distribution used in the initial models

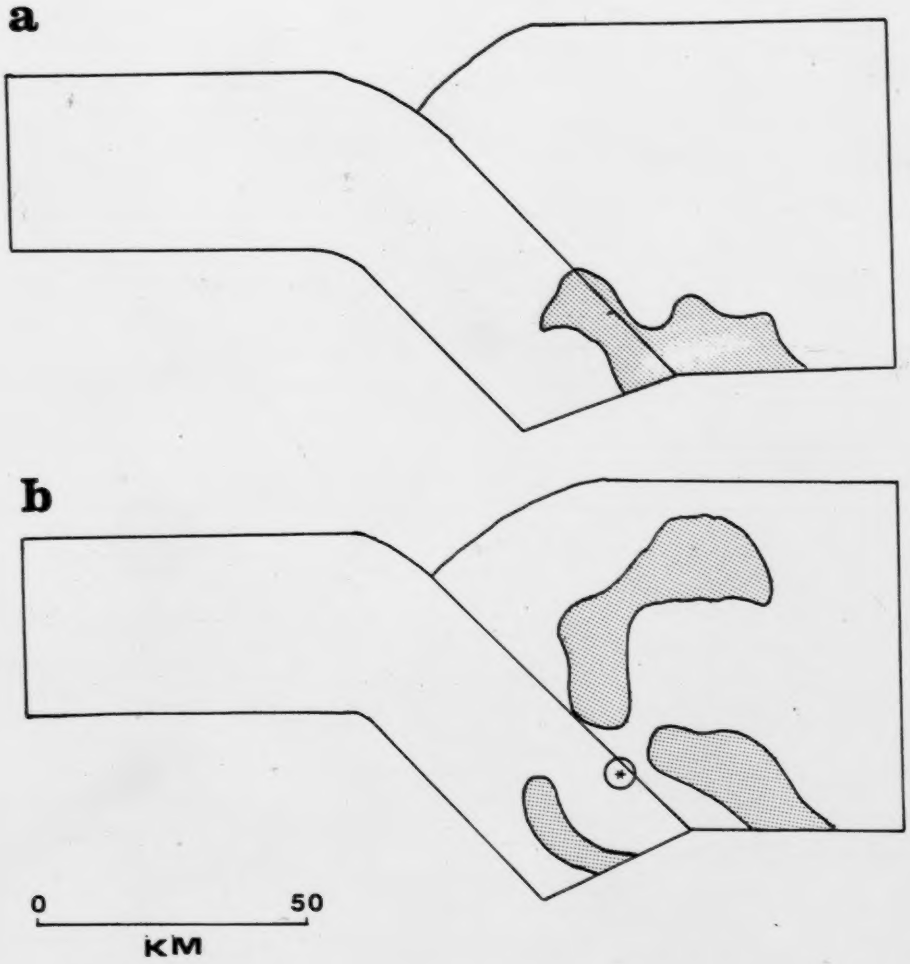

Figure 23.... Elastic modelling of a subducting zone. a, b are the probability distributions before and after the occurrence of an earthquake at *.

occurs at the location * on this figure. It seems from this simple model that there tends to be a band of instability at depth along the boundary, which strongly suggests that the band should be present for models containing longer (older) subducting slabs.

Figures 23a and 23b represent the same model and the only difference is that in figure 23b a seismic event has been introduced in the location * which is inside the high risk valued zone of figure 23a. The seismic event has been simulated by introducing a stress drop of 100 bars at the desired point of the model. This value corresponds to that calculated for intraplate earthquakes of magnitude 7 , with $\mu=3\text{x}10^{12}$ dynes/cm^2, $\eta=.75$, $D=5$ m, and $w=100$ km, using the Kanamori and Anderson (1975) formula for a strike-slip mechanism:

$$\Delta\sigma=2\mu D/w\pi \tag{4.9}$$

where $\Delta\sigma$ is the stress drop due to the earthquake, μ is the rigidity of the material, D is the average offset and w is the rupture width.

The probability distribution throughout the model has been changed. After the simulation of the earthquake the area of the hypocenter has become more stable since stress has been released there. The high valued zone seems to have been broken apart and expanded in a radial direction. The two lower high valued zones might correspond to a double

Benioff zone similar to that observed in Japan (Uyeda, 1977), and in the Central Aleutian Arc (Engdahl and Scholz, 1977). The minimum stability zone has moved nearer to the inside of the slab. This result implies that the occurrence of an earthquake in this kind of model indicates, by changing the whole probability distribution, where the next failure is likely to take place. It is a comparative scheme and shows that the introduction of stress changes may not directly affect particular stress components in the distant zones significantly, but it can produce changes in the probability of failure with respect to the model as a whole.

The overall stability of a region is changed by the occurrence of a large earthquake; stress accumulates constantly and earthquakes are required to release this stress. Therefore, changes in the probability function may very well represent new states of quasi-equilibrium for the whole system, since it is defined as the probability of failure of a given location with respect to the whole model.

A smaller stress drop was tried to see how far the changes due to such a seismic event can be seen. A stress drop of 30 bars was then modelled and the general results were the same - a general reduction in probability throughout the model and a small migration of the high valued area towards the inside of the slab.

From the discussion in the introductory part it can be seen that the elastic model of the whole plate is unrealistic. An improvement is the analysis of a thermo-elastic model (figure 24) where the same approach as in the elastic case was taken. Figure 24a shows the probability function distribution for a simple thermo-elastic model and figure 24b shows the same model including a stress drop of 100 bars at the location shown.

Figure 24a shows that in the plane part of the underthrusting plate there is a high probability of failure. This pattern remains for the upper part of the plate until depths at which the material has almost reached its plastic state. High valued zones also appear in the same region as that in the elastic model and in a narrow zone which runs inside the subducting slab approximately parallel to its dip. In this figure again the double Benioff zone seems to be present, and the area with major probability is located in the intraplate boundary at approximately 60 km deep. As in the elastic model after an explosion of 100 bars, the general features of the probabilistic distribution have been altered; the probability in the elastic part of the slab has suffered the greatest change and the stability in the viscous parts remains greater than in the elastic layers of the plates. The viscous parts have not been affected at all except in the immediate neighbourhood where the explosion took place. Another similarity observed between this and the previous model is the presence of some kind of ring of high risk areas surrounding the stress drop and that aftershocks on both plates are likely to occur.

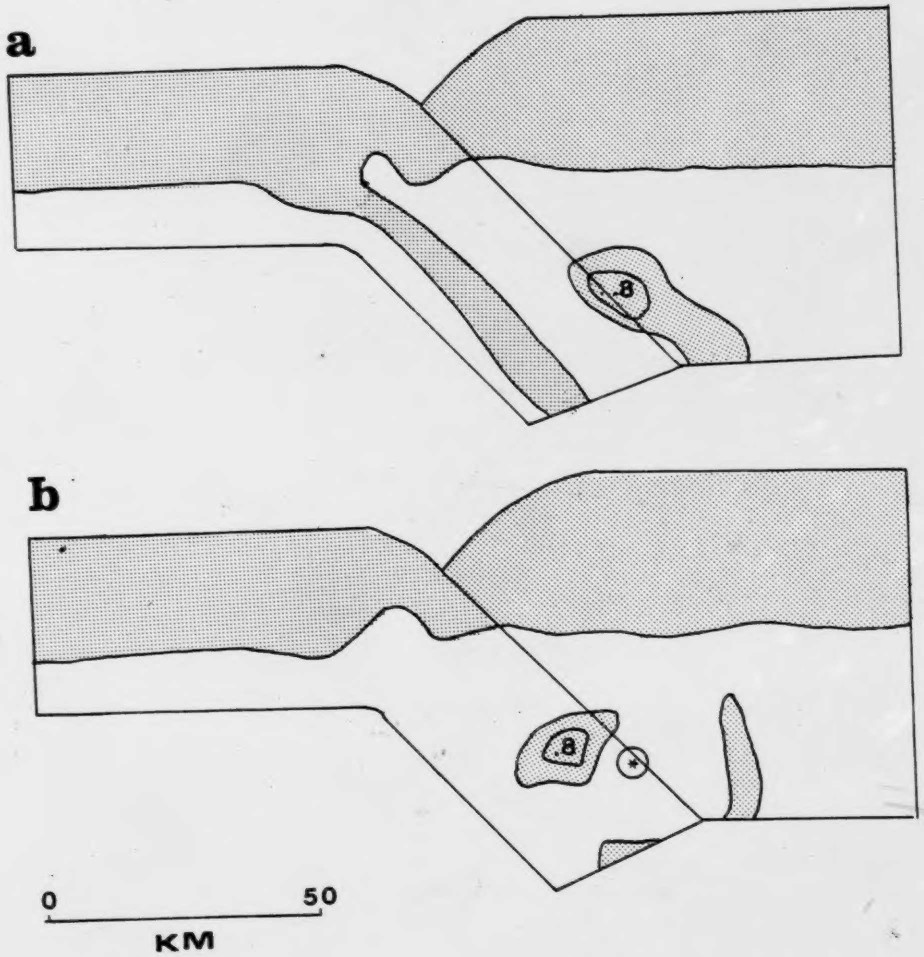

Figure 24.... Thermo-elastic model of a subducting zone at 45°. a and b the same as in figure 23.

From this comparison it can be seen that the upper part of both plates becomes relatively more unstable in the thermal analysis. This indicates that the viscous part has actually become more stable than in the elastic case, since the parameters of the elastic parts remain the same. After the occurrence of the stress drop the "instability ring" seems to have propagated further away from the focus in the elastic case. This implies that in the viscous material stress propagation will have a larger attenuation.

This result is for a plate model consisting of an elastic layer overlying a material which is gradually becoming viscous with a thermal dependence for Young's modulus given by equation (4.4). It strongly suggests that the effect that a given stress change has on the probability distribution is greatly dependent on the material properties assumed. It presents the possibility that changes in this function can be observed at distant locations from the source if the stress change can be transmitted to them through elastic materials, i.e. viscous materials should act as highly attenuate the shear stress and shear energy transmission within the kind of static that are dealt with here.

The next step is to determe the effects on the probability function distribution of the variation of the angle of subsidence. As in the case of the Valley of Mexico (chapter 3), this is necessary to create a general idea of how geometry affects instability, and to investigate why the different kinds of trench-arc systems described in figure 21 have different observed seismic behaviour.

Probability distributions were calculated for two models using the same kinds of boundary conditions used for figure 24, the temperature dependence of the material properties and the temperature distribution of the models being maintained the same.

The angle at which the slab subducts was changed to 10° (figure 25), and the intraplate frictional forces were made 3/2 of that used in the previous model. This is an effort to model the high coupling which is expected in low angle subduction (Kanamori, 1977). Figures 25a and 25b represent the probability distribution before and after the modelling of a 100 bar stress drop at location *. The high instability zone (valued at 0.6 for illustration purposes) shows a more continuous distribution than that of figure 24a, and the highest valued area (0.8) seems to be locally concentrated. Again, most of the unstable area coincides with the elastic material in the upper part of the lithosphere and the elastic part of the subducting slab. However, when the earthquake has been introduced, the instability seems to have moved to the viscous parts. The exception to this general result is the zone above the hypocenter which may correspond to the upper part of the instability ring observed in figure 24b .

The next model (figure 26) is the result of changing the angle of subduction of the downgoing slab to 60° and the

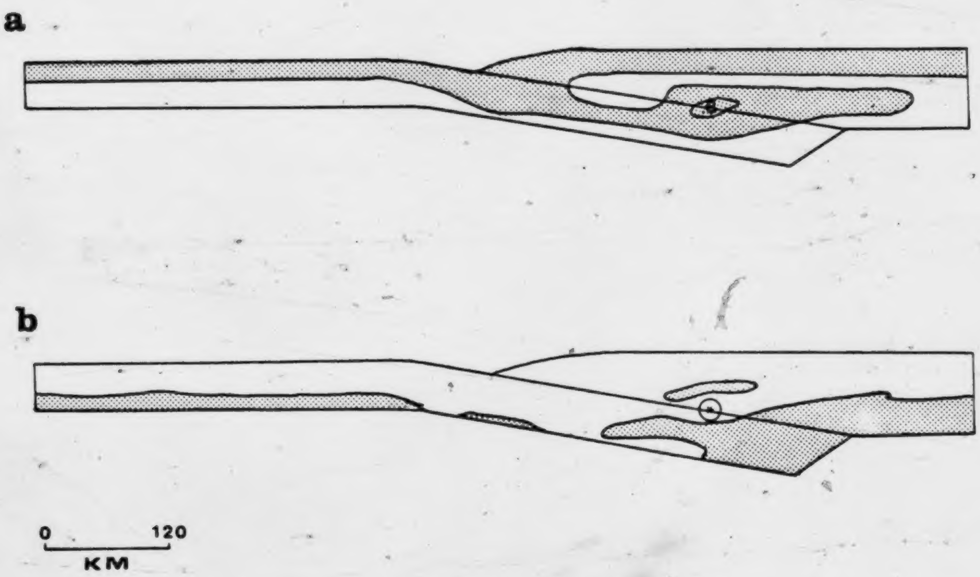

Figure 25.... Probability distributions for a trench with a slab subducting at 10°. a and b as before.

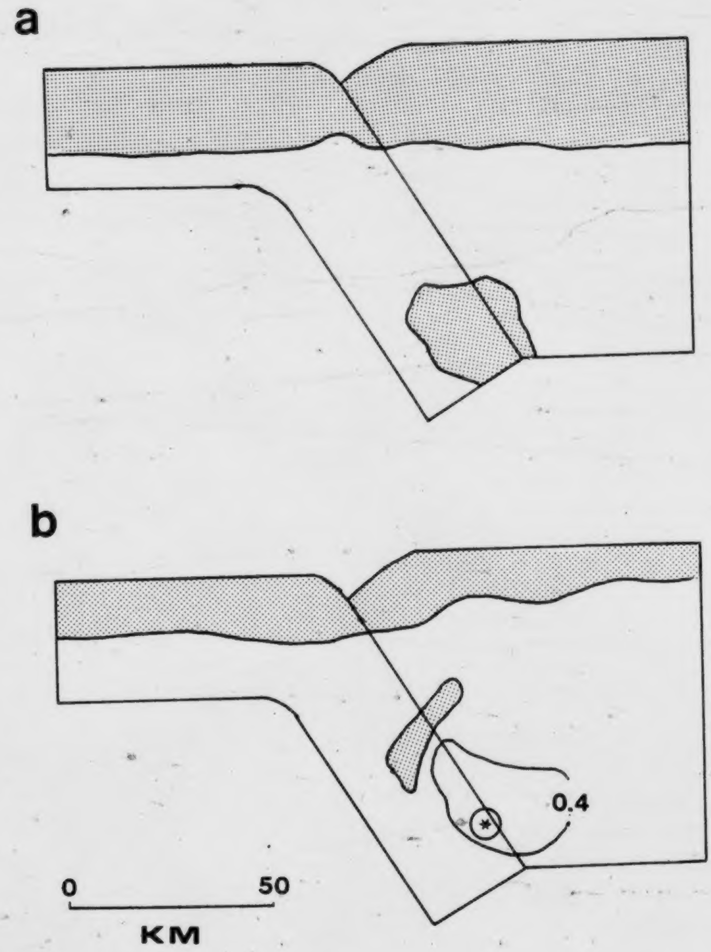

Figure 26.... Probability distributions for a trench with a slab subducting at 60°. a and b as before.

frictional intraplate force to 1/2 of that of figure 25. This last modification is made to simulate the partial uncoupling between the two plates, described earlier for this kind of model. Figure 26a (before the earthquake) shows similar characteristics to figure 24a, the elastic layer of the lithosphere and a region in the intraplate boundary having the highest probability of reaching failure. The simulation of the earthquake (figure 26b) shows that although the area surrounding the focus has become the most stable, this effect seems to be highly localized. The upper part of both plates remains approximately at the same probability as in figure 26a . The lower high seems to have been pushed upwards.

Older slabs can be modelled by applying the same kind of reasoning to larger models. The results of using a model with a slab dipping at 45° (figure 27), and one with the slab at 60° (figure 28) are presented. Again a and b represent the probability distribution before and after the occurrence of a large event at location * which is the location with maximum probability. The general results are similar to those of figures 25 and 26, but the presence of this kind of high probability at these depths requires more discussion since at these depths the earthquake mechanisms are not easily visualized as sudden failures due to applied stresses but rather to volume increases due to phase changes suffered by the subducting material.

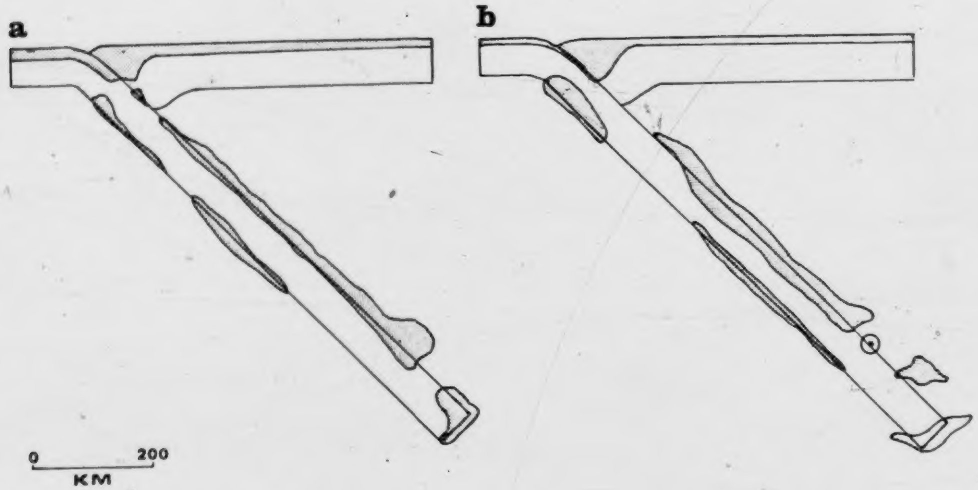

Figure 27.... Probability distributions for a trench with a long slab subducting at 45°. a and b as before.

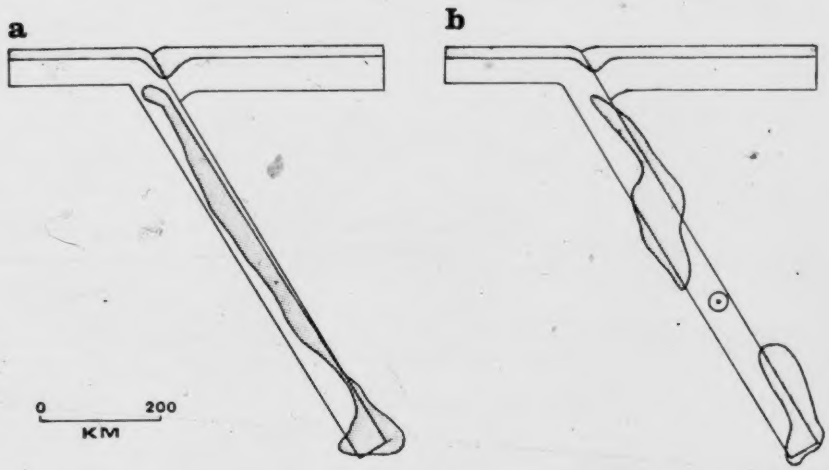

Figure 28.... Probability distributions for a trench with a long slab subducting at 60°. a and b as before.

4.4 Discussion of results.

A change in the overall distribution of the probability function values does not mean that the stresses in a particular location have changed substantially, but rather that its probability of reaching failure has been modified. The degree to which a point is affected depends on the physical properties of the material in which it is located and the state of stress in which it was previously.

If in fact the shear energy is trapped in the elastic part of the plate then there exists the possibility that the thickness of this elastic layer (H) will determine the range at which the effects of a stress drop (like the earthquake) should affect the probability of failure. Then it is possible that the reason for the existence of the so-called long range precursors is linked directly to H. It is possible that the stress drop due to an earthquake produces changes at greater distances than those predicted by simple theory.

To test this hypothesis it is necessary to calculate the solution to the Boussinesq's problem for the case of an elastic layer over a viscoelastic half-space. Solutions to this problem have been known since the begining of the century (Michell, 1900).

The shear energy is (Landau and Lifshitz, 1970, p11)

$$F=\mu(\epsilon_{ij}-1/3\ \delta_{ij}\epsilon_{kk})^2 \tag{4.10}$$

where ϵ_{ij} are the components of the strain tensor. This exercise gives the result that for all H (within reasonable limits) the total shear energy in the elastic plate is more than 0.9 of the total shear energy of the whole model. This is expected from our finite element models.

The result that most of the shear energy tends to remain within the elastic part of the plate can be useful to test our stability results obtained by finite element calculations. Both problems are similar and can be solved by making the same assumptions, using the same boundary conditions and same kind of material elements. A finite element calculation of the same Boussinesq's problem has been prepared by assuming a two layered material. The elastic constants chosen are $E_1=7x10^{12}$, $E_2=7x10^{10}$, $\nu_1=.25$ and $\nu_2=.3$. These correspond to temperatures of 20°C and 800°C on our thermo-elastic subduction model. The upper layer has a thickness of 40 km and the bottom one 90 km. The shear energy in the upper layer is again more than 90% of the total shear energy of the model. This result adds credibility to the previous stability calculations.

The concentration of shear energy in the elastic layer is a common feature of both of the solutions to the Boussinesq's problem. It is therefore possible without losing generality to approach this problem using the continuum mechanics thin plate theory as described by Love (1924), Landau and Lifshitz (1970) and many other textbooks.

The specific problem to solve is: For a thin plate determine the effects of an applied force at a given distance r; then, by changing H, the distance r_1 at which the same effect calculated previously can be determined in such a way that the variation between H and the range at which a fixed observation occurs can be stated.

The deflection of a circular plate with clamped edges due to the application of a force f in its center is given by

$$\zeta=3f(1-\nu^2)/2\pi Eh^3\ [1/2\ (R^2-r^2)\ln(R/r)] \tag{4.11}$$

where h=H/2 and R is the radius of the plate.

It can easily be demonstrated that if ζ is to remain constant as H decreases, r must increase. The following parameters were given in order to record the variation of r with respect to H. R=2000 km, ν=.25, E=7×10^{12}, f=100 bars, ζ=0.12 E-8 cm, (table 2).

This table clearly shows the role that H plays in the range at which effects due to a particular stress drop can be observed.

The double Benioff zone which seems to be present in figures 23b, 24a and 27 could be justified by some observations in some island arcs (Engdahl and Scholz, 1977 and Uyeda, 1977). The presence of this kind of weakness pattern would indicate that in this subduction zone the downgoing slab has an angle of about 45°. However, the lack

THICKNESS OF THE ELASTIC PLATE (H IN KM)	RANGE OF THE OBSERVATION (r IN KM)
20	1876
30	1770
40	1641
50	1490
60	1318
70	1118
80	888
90	610
100	200

Table 2.... Shows the effect of the thickness of an elastic plate on the distance from an applied force at which a displacement z takes place.

of this pattern in figure 24b makes the last remark weak in the sense that earthquakes in any of the Benioff zones should have aftershocks in both of these zones due to the proximity between them.

To interpret figure 25 two assumptions made should be recalled. First, the shear energy due to the presence of the source stays almost entirely in the elastic part of the model and secondly, that the stability distribution does not necessarily represent a large change in the state of stress of particular locations, but rather a stability estimate with respect to the rest of the model at a given time. With this in mind figure 25b shows that after the earthquake the stability of the elastic part has decreased to values smaller than those of the inelastic part which is supposed to be in the same stress state as in figure 25a. That is, the stable part of figure 25a remains the same but the unstable part has become more stable.

The long range stabilization of figure 25 and the very localized one shown in figure 26b are in accordance with the observations that at shallow angles of subduction the effects of earthquakes are felt at longer distances than those at slabs with bigger angles (Kanamori, 1977 and Kelleher, 1974). This means that the distribution of probability function changes due to external forces is greatly dependent on the geometry of the subduction model and on the magnitude of the frictional forces or coupling between the two plates. For a bigger coupling or a smaller subduction angle there is a larger effect range.

The common feature in all the after-earthquake figures is the presence of an instability ring around the hypocenter. This represents the immediate aftershock area due to the large event. This ring is somewhat vague in some cases, as in figure 28b where only an arc above the focus can be seen. However, since the earthquakes are simulated as stress drops in a particular location, this stress relaxation should stabilize its immediate neighbourhood for large earthquakes.

The concentration of seismic activity in the surroundings of the focus of a recent large earthquake is in accordance with the secondary stage of the doughnut pattern (Mogi, 1969), which states that with the occurrence of the great earthquake the observed seismic pattern of a region disappears and the activity is concentrated near the focal region. This kind of nearby aftershock area is also suggested by other seismic activation patterns observed (Keilis-Borok et al., 1980.a).

The deep high probability areas shown in figures 27 and 28 are due to the nature of the approach. A quasi-static approach of the problem has been taken here. First, the model is taken at equilibrium and at a given time the forces are set free to act in the model, from that the final distributions of probability presented were calculated. This kind of analysis shows for a viscous material its probability of yield. It does not assume a particular mode of yielding.

Although the mechanism of deep and intermediate earthquakes is stricly unknown this kind of analysis will only be valid if a rapid form of yielding of the material is possible.

Several probable causes have been proposed for intermediate and deep earthquakes. Isacks and Molnar (1971), suggested that if the slab cannot penetrate beyond 650 km, then this involves an upward transmission of compressional stress that could cause deep earthquakes. Griggs (1972), has shown that this kind of resistance would result in some kind of buckling of the subducting plate, for which there is little evidence.

The most widely accepted theory is that due to Ringwood (1975) which suggests that intermediate and deep events are caused by phase transformations of the material that is being subducted, which result in sudden volume changes in the slab that might create instabilities. However, it is not very well understood how phase changes could occur fast enough to produce earthquakes.

Spanos (1977), suggested that intermediate and deep earthquakes could be due to a shear heating instability in the fluid layer between the slab and the mantle outside the upper boundary of the subducting slab. He demonstrated that if the earthquake occurs within this layer it will reproduce the observed focal mechanism for deep earthquakes. That is, the principal stresses are developed within the downdipping slab and in the direction of motion of the plate(Isacks and Molnar, 1971). Sharp changes in material properties have not been included in this calculation. This has resulted in smooth probability curves such as those shown in chapter 3. In this particular case the high probability zones on the downgoing slabs of the large models appear without gaps. It is not the purpose here to find a mechanism that accounts for the presence of deep earthquakes, but rather to see the effects of a sudden stress release on the distribution of probability of the models, and how these distributions change with the geometry of the model and the magnitude of the applied forces.

However, the sudden displacements at great depths in the form of earthquakes is controlled by the amount of heating required for melting and by how well defined is the melting point (Spanos, 1977). If the temperature of the slab is far from the melting point the fluid layer will be narrow while if the melting point is well defined the portion of the slab that reaches this temperature will have significantly less viscosity than the rest of the slab. In any of these two cases the material will yield almost its entire deformation suddenly, causing total melt and a complete stress relief. This kind of mechanism generalizes our results to the ductile regime.

4.5 Conclusions.

The thickness of the elastic part of the lithosphere influences the range at which long range precursors can be observed. This is because the shear energy tends to remain within this elastic layer, that is the viscous material acts as a barrier and rather than dissipate this energy it just does not permit its propagation. Rupture size could be linked to how localized an anomalous high probabilty is. Longer areas may be broken in more high probability valued areas.

Probability values are relative within a model calculation, therefore the actual value is just an indicator of where failure is more likely to occur for a set of given conditions. It is more reasonable to focus this kind of analysis on the study of the distribution of high and low valued areas rather than on the values themselves. High probability values do not mean that an earthquake will necessarily take place, but just that at a particular location failure is more likely than at other parts of the same model.

The decrease of probability in the upper tens of kilometers observed in figures 25b and 26b indicates that the whole model becomes more stable at these depths after the occurrence of a large earthquake and that aftershocks in the high valued zones of this figure are the most likely kind of activity to occur in this case.

The result that after an earthquake has been modelled, zones of high risk are created in the continental plate presents the possibility that, if this plate is fractured and partial melting occurs at depth, then this molten magma can more easily reach the surface.

No difference can be seen in the range of effect of the deep earthquakes modelled in figures 27 and 28. This is so because they are both originated outside the elastic parts of the plates.

The assumption that the lithosphere can be modelled as an elastic layer over an inelastic one seems to be a plausible one and the solution to Boussinesq's problem and the thin plate approach shown in the discussion of results add credibility to this kind of model.

I believe that Barenblatt is correct by suggesting that local concentrations of stresses are responsible for the presence of seismic patterns in some areas, and that this can be modelled by adopting Newman and Knopoff's ideas of crack populations or by just considering the presence of geological discontinuities in the lithosphere. However, the range of effect that these seismic patterns might have is strongly linked to the regional characteristics of the material in which these concentrations take place. That is, it is controlled by the thickness of the elastic part of the lithosphere.

5. Earthquake risk studies for the problem of induced seismicity on water reservoirs applied to the Itzantun site.

This chapter is an application of the instability function described in section 2.4 to a site located in the mountain belt associated with the Middle America trench south of the Tehuantepec ridge, the Cocos-Caribbean subduction zone. It will provide some insight into the role of this system in the local seismicity observed in the Itzantun area. This part of the thesis deals with the use of time dependent instability curves to make estimates of the time at which a particular location becomes more unstable. Here the changes of the stress components are calculated analytically by means of the formulation described in appendix B.

The Itzantun site is located approximately 100 km inland of the boundary between the North-American and the Cocos plates. It is located a few tens of kilometers North-West of the portion of the Motagua Fault that serves as boundary between the North-American and the Caribbean plates. This fault is the westward continuation of the tectonic feature known as the Cayman Trough. As mentioned earlier, in chapter 1, one of the features of plate tectonics is the relation between the mountain belts and the plate limits.

In the portion of the Middle America Arc near the Itzantun area seismic activity occurs often. It is interesting to see how the stability distribution behaves in this particular case since the area is located in the Sierra Madre del Sur. This is the mountain belt associated with the Middle America Subduction Zone.

Consolidation theory and concepts of rock failure can be used to evaluate the probable risk of induced seismicity as a result of filling of reservoirs. The evaluation of seismic instability distribution due to the water load superimposed by the filling of a reservoir is treated in this chapter. As an example of a particular application, the procedure that will be described is applied to a particular reservoir. This evaluation has the potential to indicate the safest way to fill a reservoir, and depends only on the geometry of the load, the rate of filling and the geological structures in the area. The stability functions as discussed in chapter 2 can actually be a measure of the risk of having failure, with time, for a particular loading history in respect to a plane of weakness.

5.1 Evaluation of the risk of induced seismicity.

Drawdowns can increase the risk of triggering earthquakes in this area, which is prone to thrust faulting. It is possible to estimate the stresses after a period during which the water level is maintained and a decrease in stresses with the depth of the observation point.

The estimates of the probable induced seismicity are limited as the residual stress in the area prior to the impounding is unknown. With a measure of the residual tectonic stress it will be possible to determine an optimal filling rate to reduce the probability of induced seismicity.

The relationship between mountain belts, continental limits and earthquakes has been recognized for more than 40 years. Gunnn (1947) suggests that the parallel distributions of mountains, ocean deeps and volcanoes follow naturally from the properties of the lithosphere, if it is assumed to be strong, elastic and supported by an underlying weak asthenosphere. He proposed that the generation of ocean deeps were possible if the following conditions occur (figure 29):

1. Down-folding produced by horizontal compression accompanied by a thickness of the sedimentary layers.
2. Down-folding derived from downward convective circulation of the underlying magma.
3. Overthrusting and Underthrusting at shear faults in the lithosphere.

Gunn (1947) gives some ideas that have become fundamental for plate tectonics. He shows that in order to describe the gravity anomalies near mountains, deeps and continental boundaries, the lithosphere cannot be weak even if moderate stresses are applied to it for long time. He suggests that the continental lithosphere must be at a higher state of stress and at a different flexural rigidity than the oceanic one. He notes that most earthquakes in these boundaries represent shear fractures and that their

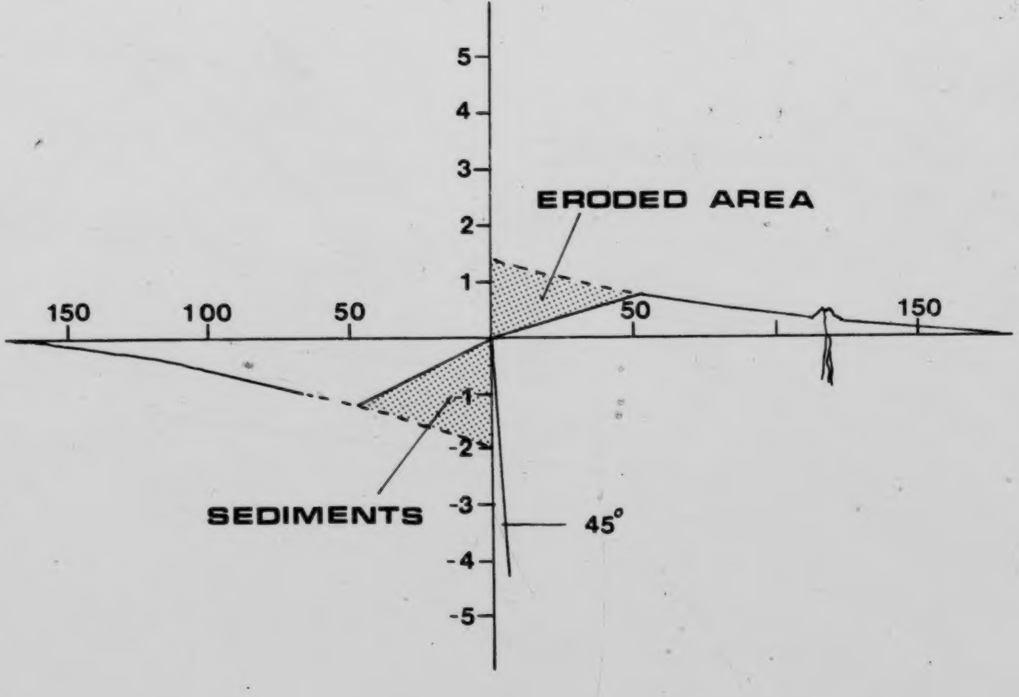

Figure 29.... Calculated deformation of a shear fractured lithosphere subjected to a horizontal compressive stress of 10^9 dynes/cm^2 (modified from Gunn, 1947).

spatial distribution in depth suggests a great shear fracture extending throughout the surface layers.

5.2 General concepts on induced seismicity

During the last twenty years, it has been observed that large engineering projects may change the characteristics of the seismic events in the surrounding region. These changes are induced by changes in stress that are a result of man's activities. Among the activities and events that cause induced seismicity are fluid injection, fluid extraction, mining, underground detonations, flooding, and reservoir impoundment (Packer et al. 1977). Here we will deal only with reservoir impoundment.

There are many examples of where the filling of reservoirs has changed the characteristics of events in an area. These changes range from the inducement of large magnitude events to changes in micro-earthquake activity. The filling of large reservoirs, however has not always resulted in induced seismicity. Attempts to relate induced seismicity to size or depth of a reservoir have had little success. The changes in seismic activity do not follow a simple pattern (Gough, 1978). Excellent reviews of the observed changes have been prepared by Simpson (1976), and Gupta and Rastogi (1976).

Induced seismicity is difficult to prove. An increase in seismic activity in areas that were already active is difficult to attribute entirely to the filling of the reservoir. In other areas the pattern of seismic events changes radically, and there seems to be an obvious association with the filling of the reservoir. In some areas, there appears to be an increase of seismic activity during the initial filling, whereas in others, the increase occurs some years after filling. There appears to be a correlation between the water depth and the number of earthquakes at some reservoirs (Withers and Nyland, 1978). And there also appears to be a relation to the rate of filling (Simpson and Negmatullaev, 1981).

The amount of data on reservoir induced seismicity is limited. Up to 1977, there had been 55 reported cases of reservoir induced seismicity (Packer et al, 1977). Of these, Packer classifies 16 as clear cases, 35 as questionable and four as probably not reservoir related. Packer et al. reach the following conclusions regarding induced seismicity due to reservoir loading:

1. The initial state of stress in the ground is of prime importance.
2. Failure of unfractured material as a result of reservoir filling is unlikely, but failure is likely to occur along pre-existing faults in fractured material.
3. "Instantaneous" stresses generated by rapid reservoir filling lead to shear stress along faults without increasing the effective stress.
4. Instability along faults could occur at great depths as shown by the curvature of the failure envelope. The

shearing resistance of the material is reduced as the confining pressures increase.

There is by no means unanimous agreement about the existence of reservoir induced seismicity. Other authorities claim only 3 clear cases of reservoir induced seismicity exist. The difficulty is to provide a viable mechanism for failure caused by reservoirs and to use a convincing stress-strain relation for crustal rock. The evidence from other reservoirs indicates convincingly that failure can be caused by relatively small external influences (i.e. Gough, 1978; Wetmiller, 1981; Raleigh et al., 1976; Pomeroy et al., 1976; Cook, 1976). The fact that statistically rigorous observations do not exist for reservoirs does not imply that reservoirs can not induce seismicity, it merely means that seismic evidence by itself, from reservoirs alone, is not sufficient to resolve the matter.

A consideration, however, of the existence of faults on which seismicity is known to occur, the fact that stimulated seismicity has been observed for other kinds of processes, and the fact that a reasonable physical mechanism for reservoir induced seismicity can be postulated, justifies modelling studies of this problem to determine the range of risk.

Any prediction of seismicity involves assumptions about the stress-strain relations of crustal rock and the conditions under which faults will fail. The largest stress increment due to large reservoirs is of the order of 10 bars. Under incremental loads of 10 bars most crustal rocks deform elastically. Of course the incremental response of a rock confined under 10^3 bars at 10 km depth may be different from that of a rock at the surface, but its elastic nature remains due to the small size of the stress increment. Therefore, the assumption of elastic behaviour is plausible.

The variation of elastic behaviour can be deduced from seismic data. Young's modulus deduced from seismic data for depths from 0 to 25 km varies from 6×10^5 to 8×10^5 kg/cm^2. This variation is small compared with its magnitude. Hence, the assumption that the elastic properties are constant is reasonable albeit not entirely satisfactory. Other authorities (i.e. Kirby, 1977; Turcotte, 1974) have considered the upper 25 kilometers of the lithosphere to be elastic.

Obviously water pressure plays a crucial role in the dynamics near a reservoir. The simplest extension of elasticity theory that takes into account the presence of water is the Biot consolidation theory. It is normally applied to soils and is justified here only by the fact that it is a simple tractable extension which can deal with the presence of pore fluids in a plausible way. It may not be correct, but at these relatively low pressures it is a reasonable first approximation.

The general conclusion from the observation of induced seismicity is that reservoir volume is not always a reliable indicator of the risk of induced seismicity. The larger the volume, the greater the probable risk, but there is always the potential for suprises such as was encountered at Hydro-Quebec in Canada (Leblanc, 1978). Manicouagan 3 on the Canadian Shield caused seismicity changes while the nearby Manicouagan 5, twice as deep and with a considerably larger volume, has not induced any seismicity. Manicouagan 3 has a height of 108 meters, its volume is 1.04×10^{10} m^3.

In only a few cases have the depths of these seismic events been determined accurately. Local observations and the teleseismic data all indicate that the hypocentres are shallow. Gupta et al. (1972) have determined the depths and positions from the events at Koyna from a local array, and found that the majority of the events occurred at a depth of less than 10 km, but some occurred as deep as 30 km.

Migration of seismic events has also been observed in some reservoirs. Simpson (1976), Simpson and Negmatullaev (1981) and Soboleva and Mamadaliev (1976) indicate that the events at Nurek are migrating toward the reservoir.

The focal mechanisms (Bufe et al., 1976. Gough and Gough, 1976 and others), observed at different reservoirs are consistent with the types of pre-existing faults in the neighbourhood. At Kariba, Kremasta and Oroville, dip-slip faulting was observed, while at Koyna, Hsinfengkiang and Hoover, the mechanism was strike-slip faulting. At Nurek the induced seismicity is occurring along a series of thrust faults connected by short segments that show strike slip motion, (Simpson and Negmatullaev, 1981). Simpson (1976), Bell and Nur (1978) and Withers and Nyland (1976), suggest that rapid lowering and raising of the water level may be an important factor in inducing seismicity in regions of thrust faulting.

The magnitudes of the main shocks near reservoirs have been as high as 6.5 at Koyna (Gupta et al., 1972), 6.3 at Kremasta (Comninakis et al, 1968), 6.1 at Hsenfengkiang (Wang et al., 1976). It is not possible to give an upper limit for the magnitude of induced earthquakes, as the filling of reservoirs acts only as a trigger of the pre-existing stress.

5.3 The Itzantun site

The Itzantun site is in the state of Chiapas in the southern part of Mexico 120 km NE of the city of Tuxtla Gutierrez (figure 30) It is in a region with several rivers, the most important of which are the Tlacotalpa, the San Pedro and the Huitupan. The Tlacotalpa flows in the Itzantun gorge, and at this location the flow is $2x10^{6}$ m^{3} of water per year. The geologic formations in the area are chiefly thick assemblages of mudstones and massive limestones.

The foundation of the Itzantun dam will be sandstone, mudstone, and limestone which appears reasonably homogeneous, at least at the surface. Many fractures in the formations near the dam have been filled with calcite but some are open and show evidence of recent movement of the order of centimeters.

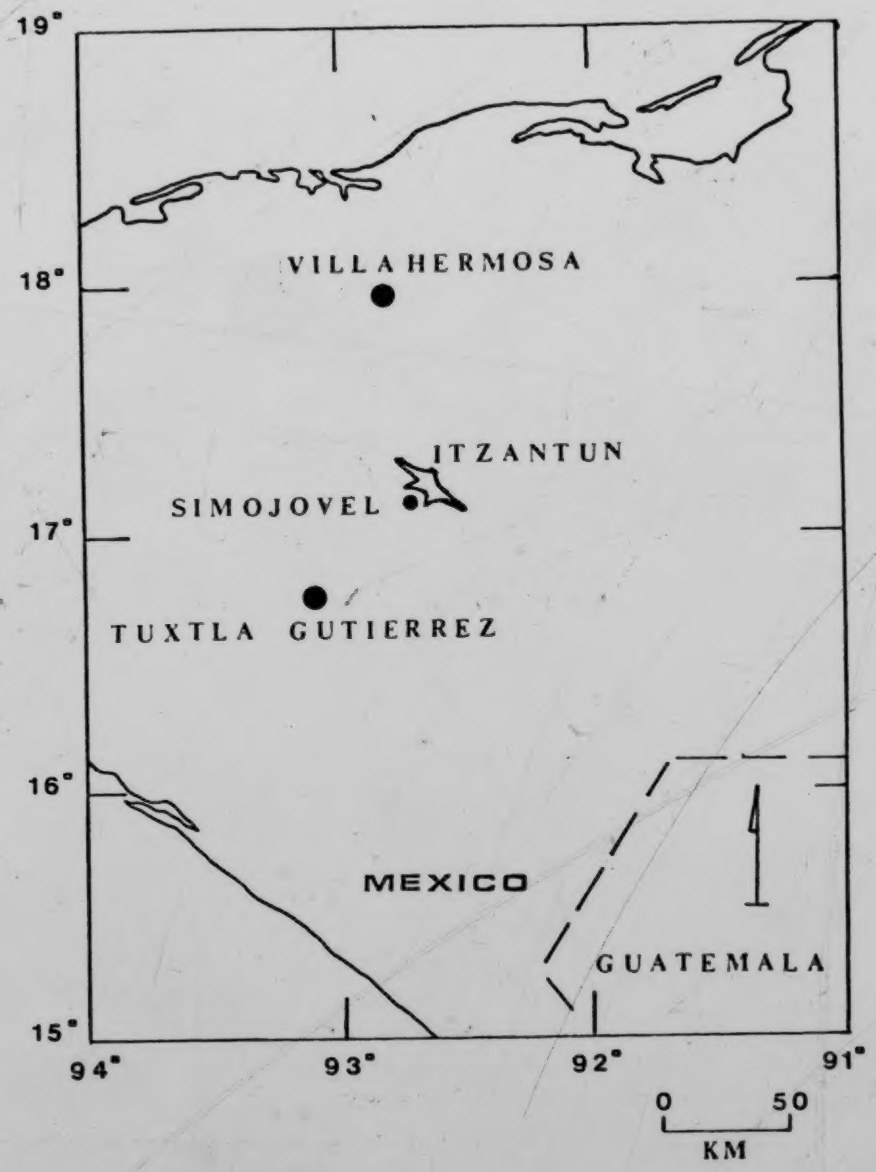

Figure 30.... Location map of the study area.

The Itzantun fault crosses the reservoir just upstream from the dam and is clearly the significant structural feature in the analysis of the risk of induced seismicity (figure 31). The gorge itself was not developed along a fault zone. The irregular directional changes of the river, and the fact that no fault breccia was found in a borehole slanted to go under the gorge, indicate that the river has eroded along minor fractures and joints. Nevertheless the strike of the river is along a potential failure plane (the known faults in the area are approximately at right angles to the strike of the river).

5.4 Natural seismicity levels

Historically the region in which Itzantun is located has been the origin of several earthquakes. Molnar and Sykes (1969) studied 21 earthquakes in the portion of the Middle America Arc that lies north-west of the intersection of the arc with the Motagua fault, and in general found that the depth of the events increases as their epicenters move inland. The maximum depth determined is of about 133 km; most of which had thrust mechanisms. Of these earthquakes the majority are located within a 250 km radius of Itzantun. Although no events are reported by Molnar and Sykes in the continental part of the North American-Cocos plate boundary the 1976 Motagua earthquake of magnitude 7.5 had its focus there.

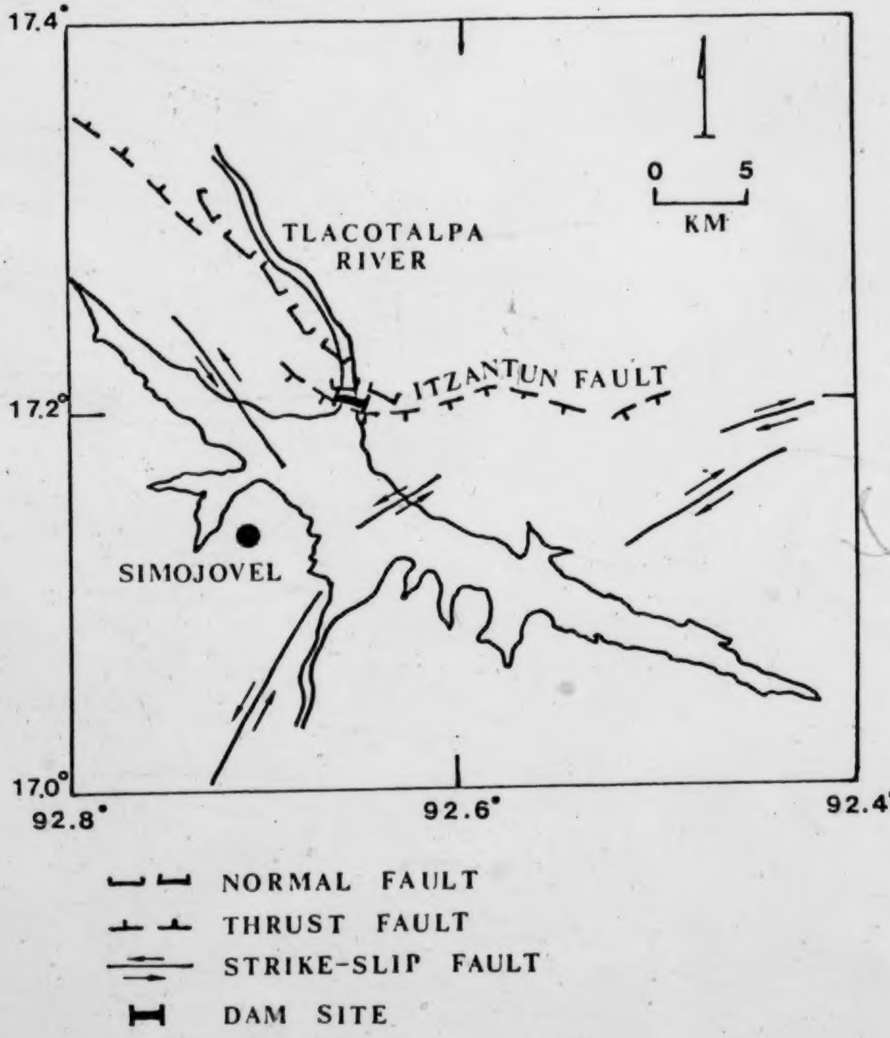

Figure 31.... Major geologic features of the area of Itzantun.

These tectonic characteristics made it necessary that the project of building a deep hydroelectric reservoir needed an assesment of the natural seismic level of the area. In order to accomplish this a nine months' microearthquake survey was carried out in 1979 in the area by the Institute of Engineering of The National University of Mexico. Six portable seismomenters MQ-800 of record in smoked paper were set in the area (figure 32). More than 70 shallow events with a depth ≤ 30 km were detected in the area, all of them with a magnitude < 2.2. With the information obtained in this first period of recording it is not possible to determine if any of the faults in the area is active. However, the majority of the events are located in the north of the intended site, which is the part where more faults are present.

The local network described was able to record during the same time 120 deep earthquakes with a magnitude range from 3.0 to 5.0 (figure 33). In the analysis of these deep events the records from the seismological stations Comitan (COM), Chicoasen (CSN) and Oaxaca (VOH) were also used. The locations of these earthquakes (Novelo, 1978) suggest, that the events are aligned in narrow equal-depth bands perpendicular to the Tehuantepec ridge and that the depth of the earthquakes increases with the distance from the trench, which is in accordance with Wilson's (1963) proposal that the direction of subduduction may be determined by the aseismic ridges. The hypocentral locations shown in figure

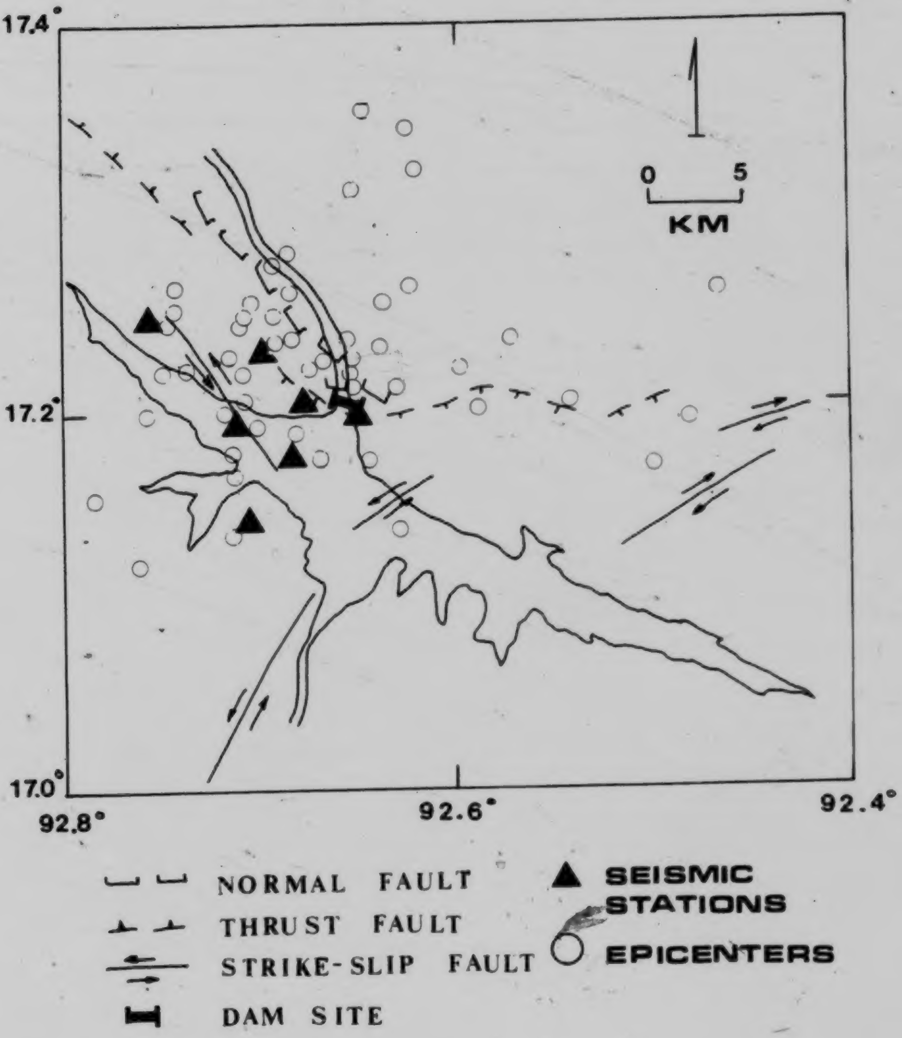

Figure 32.... Seismic stations and epicentral determinations.

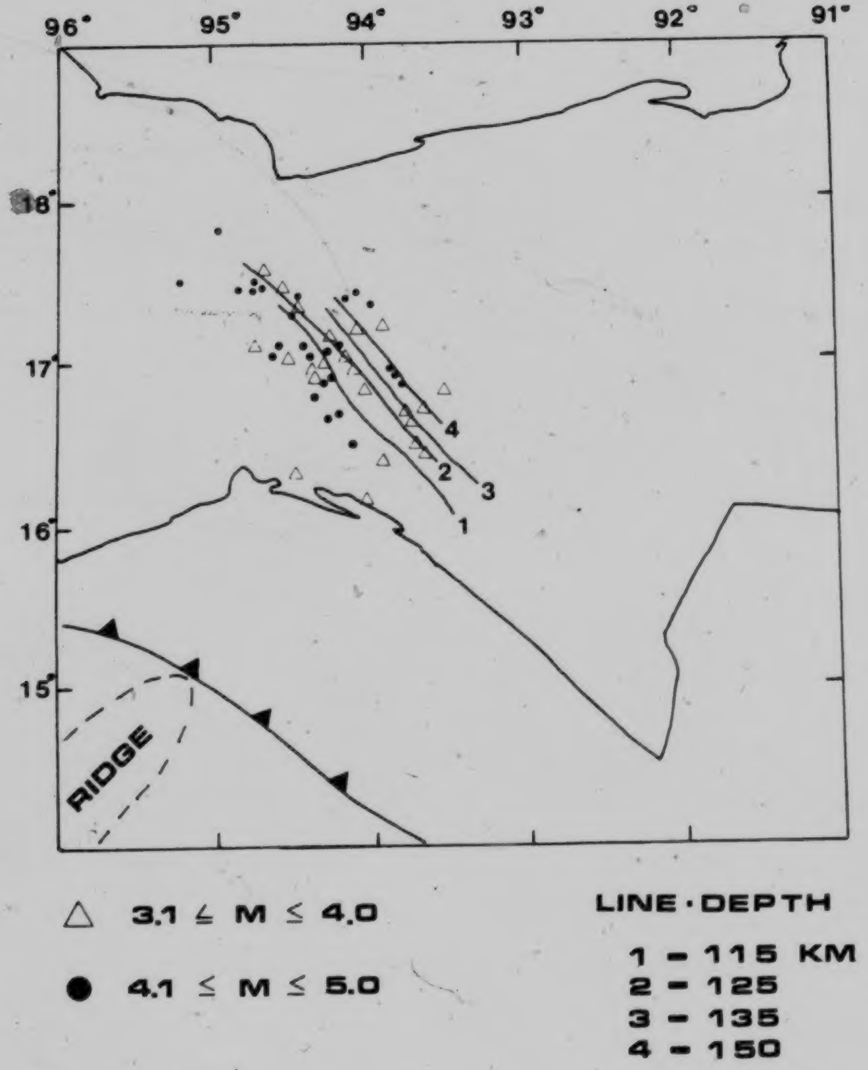

Figure 33.... Deep events located by the Itzantun network.

33 can be confined to a certain distance from the trench (figure 34). This exercise enables one to fit by least squares an angle of subduction of 45° at the Cocos Cocos-North American plate boundary.

5.5 Model studies

As a first approximation it is possible to model the problem as consolidation of a water logged half-space. Our computer programs for 2 and 3 dimensional analysis treat the modelling problem by considering the earth to be a uniform, isotropic half-space consisting of an elastic matrix affected by fluid under pressure. This material is characterized by a single permeability, a relative fluid matrix compressibility, a coupling factor (or hydraulic transmissibility) for the bottom of the reservoir, and two elastic moduli. The reservoir load can be approximated as a "long" 2 dimensional load or within limits treated as 3 dimensional.

The major deficiency of this approach is that effects on the strength of faults must be judged qualitatively. Interpretive examples are given in Withers and Nyland (1978). They point out that the incremental stresses due to a reservoir are rarely large enough to cause failure by themselves. The potential for failure must exist and may be triggered by the reservoir.

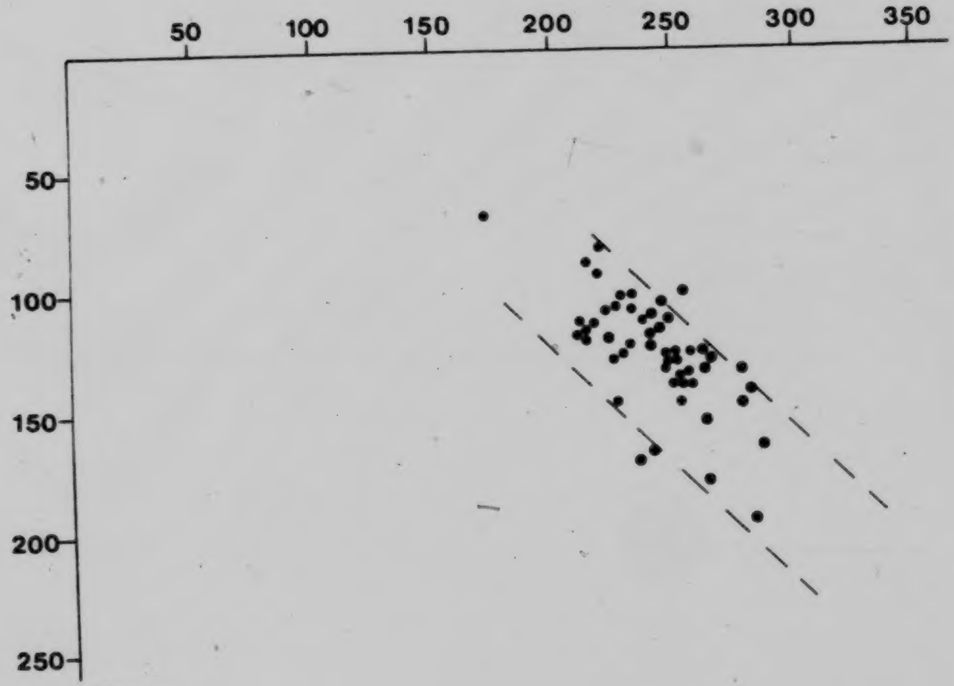

Figure 34.... Shows the deep events from figure 33 in a depth vs their distance to the Middle America trench diagram.

5.6 The approach

The definition of stresses in porous media meets with certain difficulties, but some heuristic theory has been developed to deal with these stresses. Terzaghi(1951) proposed that stresses in porous media are a 'neutral stress', the stress in the fluid and an 'effective stress', the difference between the total stress prevailing in the fluid-filled media and the neutral stress. It is the effective stress that causes deformation (Scheidegger,1974).

Biot (1941) suggested that the compaction of soils is caused by a phenomenom called 'soil consolidation'. This means that the settlement is caused by the gradual adaptation of the soil to a load variation. Biot made the following assumptions: 1) Isotropy of the material, 2) linear stress-strain relations, 3) the strains in the media are small, 4) the water contained in the pores is incompressible but may contain air bubbles, and 5) the water flows through the porous skeleton acording to Darcy's law.

With these assumptions, Biot developed the theory for the consolidation of porous media, the basic relations that describe the phenomenom are given by Biot in a series of papers published since 1941. Little has changed in this theory since then (Rice and Cleary, 1976).

In order to approach the consolidation problem outlined earlier, we have followed the technique described by Withers and Nyland in their series of papers (1976, 1977, 1978). In order to solve the consolidation equations, use is made of the displacement functions of McNamee and Gibson(1960). This implies the development of a procedure to allow us to determine the double Fourier and Laplace transforms of the water load. The Fourier transforms are done by using the Advanced Mathematical Library of the array processor (AP-190L), which allows the whole computation to be overlapped with data access time. This permits us to deal with the two dimensional transforms of the load at a given time as a vector and determine the change of the stresses up to that time.

Once the values of the transforms of the stresses at the desired location (corresponding to each of the times of the known load history) are known, there is adequate information to construct a curve for which inverse Laplace transform will give the behaviour of one of the components of stress at any time is available. From these components, a failure criterion and an assumption about the orientation of a plane of weakness, we calculate estimates of stability of a point in the formation. The inclusion of several segments in the loading history curve is done applying the superposition principle. Thus after the inverse Fourier transform is performed in the AP for a given component of stress, the resulting values at some X, Y, Z, are the Laplace transform in discrete form of the change in time of one component of stress. The result is a function of time, which defines the way a point in the formation moves toward, or away from, failure.

Instability distributions can then easily be determined by using the procedure described in section 2.4 of this thesis. The primary assumption is that at the time of impounding the reservoir all the parts of the porous halfspace beneath the reservoir were stable. That is, the instability values are derived from the incremental stresses due to the reservoir and the geology of the area, and they will represent how instability values of particular locations are changing.

5.7 Discussion of Results

I attempt here to evaluate the risk of induced seismicity in a qualitative way. In order to do this I have made and justified as far as possible a number of assumptions.

1. In the upper 25 km of the earth incremental stress changes cause elastic response and failure occurs according to a Mohr-Coulomb failure criterion.
2. The in-situ stresses are such that small increments on them can cause failure.
3. The effect of water can be modelled by Biot Consolidation theory.
4. A uniform halfspace is a reasonable approximation to reality.
5. The geologic estimates of fault orientation define the location and direction of expected failure. Intact rock will not fail under reservoir induced loads.

Based on these assumptions the results shown in figures 35 to 38 were obtained. The stability function for two loading histories consisting of monotone increasing loads, to a constant load were calculated. The total loading times were 2 years (figure 35) and 16 years (figure 36) Both have been calculated for a point beneath the deepest part of the reservoir at a depth of 1 km. and show the relation of the resulting stress to the rate of filling. For the curve where the complete load is reached 16 years after the beginning of the impoundment, the increase in stress is much smaller than when the total load is reached after 2 years.

Figure 35 also illustrates that when the load is kept constant for a certain time period, the stresses begin to decrease to a limiting value. This means that the effect of the anomalous stress produces changes that lead to an equilibrium state that does not necessarily have to be the initial state of stress in the area. This can be thought of as related to the existence of residual stresses.

The risk function has a non-linear dependence on the rate of filling (table 3). This table shows the value of the stability function 20 years after impounding began and maximum value attained during that period. This is done for a location at 1 km beneath the deepest part of the Itzantun reservoir. The loading histories used to obtain this table are as follows, where T is the time at which the lake was first completely filled, and D is the maximum depth of the reservoir. After .25 T the reservoir had water up to .45 D.

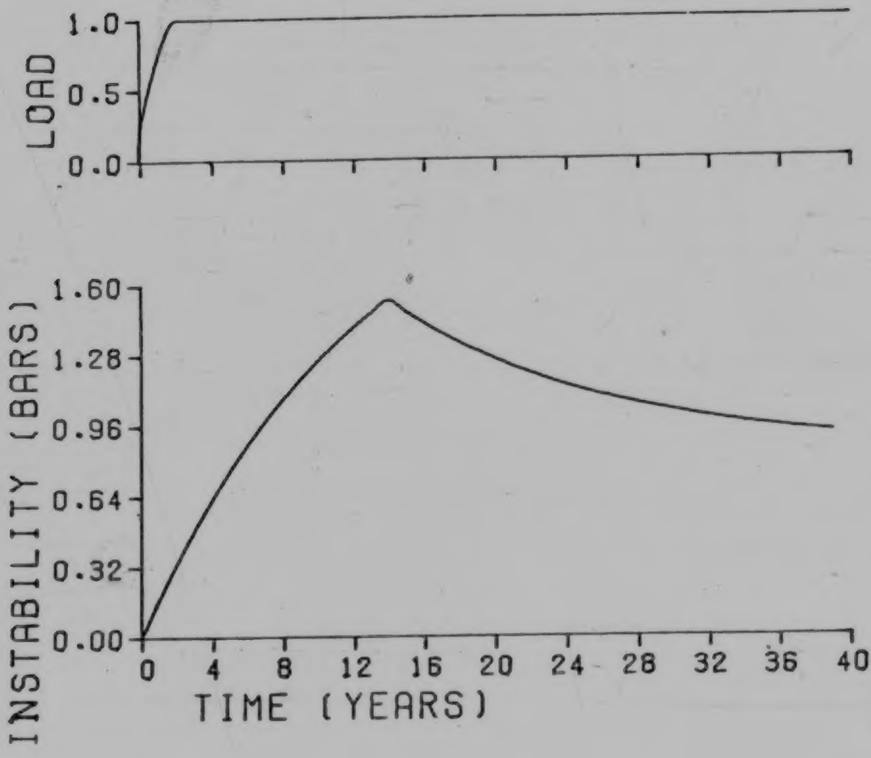

Figure 35.... The upper graph shows a loading history, where the total load is reached after 2 years of loading. The bottom graph shows the instability at 1 km depth.

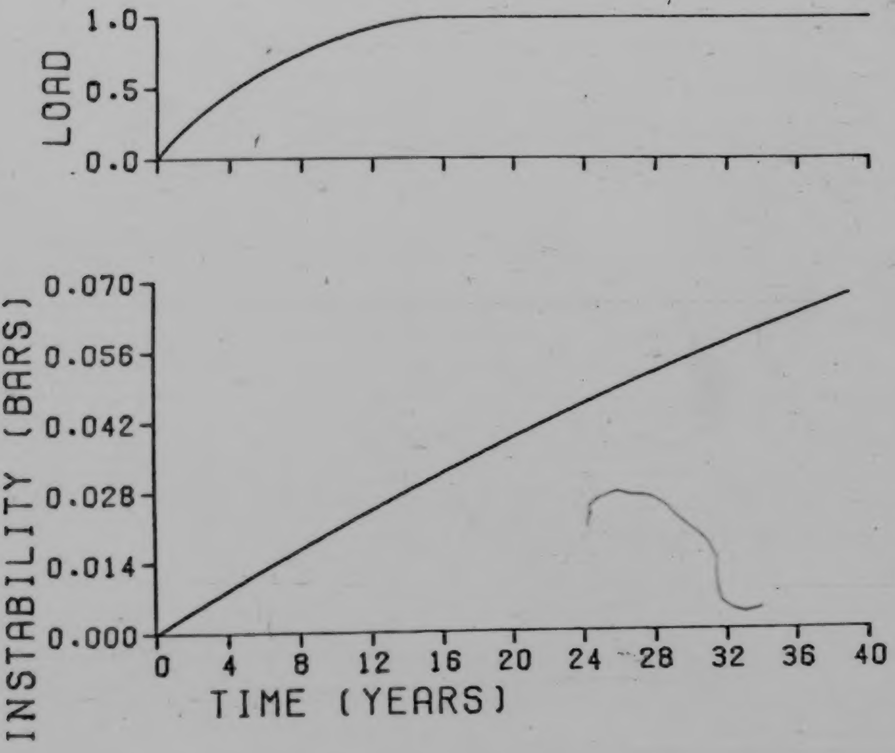

Figure 36.... The upper graph shows a loading history, where the total load is reached after 16 years of loading. The bottom graph shows the instability at 1 km depth.

DURATION OF LOADING IN YEARS	STABILITY FUNCTION IN BARS	
	MAX. VALUE ATTAINED / TIME	VALUE AFTER 20 YEARS
2	1.54 / 15 yrs.	1.21
3	0.95 / 20 yrs.	0.95
4	0.51 / 20 yrs.	0.51
8	0.15 / 20 yrs.	0.15
16	0.04 / 20 yrs.	0.04

Table 3.... Variation of the stability function for different rates of filling of the reservoir.

After .5 T it had .75 D. At .75 T it was .9 D full. From the time T the reservoir remains filled. It is obvious that a peak in the stability function has been reached during this 20 year interval only for the first case in table 1. With a faster rate of filling the risk of reaching failure is higher, for the first case the risk increases sharply, it reaches its maximum value 2 years from the beginning of the filling of the reservoir and then it decreases to a value of about .9 bars and remains constant.

The rate of filling of the reservoir is not the only way in which artificial lakes could change the seismic activity of an area. Some changes have been observed after filling and draining the reservoir, as in the case of Oroville CA, where an event of magnitude 5.9 occurred after this kind of loading history (Withers, 1977).

In order to see the effect of draining of a reservoir on the instability function we applied this kind of loading history (figure 37). This example shows that the instability function for unloading tends to have a second minimum, in this case after 13 years. The effect of a fast decrease in the value of the stability function must generate sudden changes in the stresses that might trigger seismic events.

Other histories involving reduction of loads show that if lowering the water level is done rapidly, the negative slope of the stability function moves toward a horizontal positon. This reduces the risk over a thrust fault but increases it for a normal fault, as the values in the latter

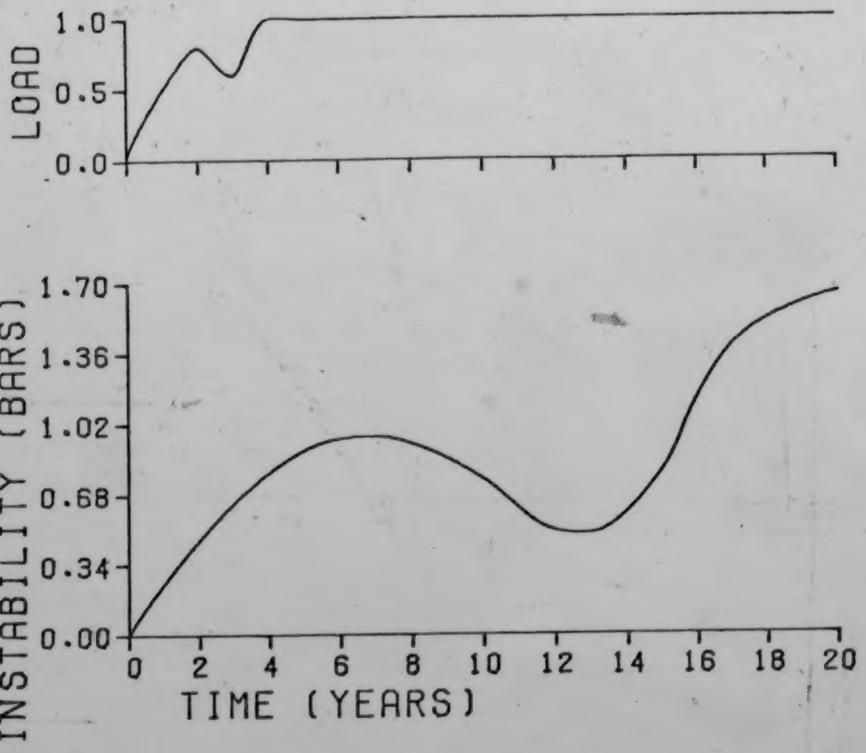

Figure 37.... The upper graph shows a loading history in which an unload takes place before the total load is attained. The bottom graph shows the instability at 1 km depth.

part of the stability curve are much bigger.

Decrease in loads in the loading history result in a stability decrease that attenuates rapidly with the depth of the observation point. For a depth of 4 Km the effect is not observed at all (figure 38).

5.8 Conclusions about instability at Itzantun.

Why the filling of some reservoirs causes seismic events is poorly understood. We give no firm predictions for Itzantun. Studies indicate residual stresses, differences in permeability, and differences in physical properties of the formations under the reservoir may determine whether there is induced seismicity risk or not. None of these factors is known with precision at Itzantun.

The changes in stability around a water reservoir due to the presence of the water can be predicted in a qualitative way by assuming: a) a model of a porous halfspace consisting of an elastic matrix saturated with water, b) that brittle failure can occur in the upper ten kilometers of the lithosphere if small stress changes are made, and c) that the effect of water in rocks can be approximated with Biot's consolidation theory.

To diminish the risk of induced seismicity at Itzantun, the filling of the reservoir should be as slow as economics permits, with intervals when the water level is held constant.

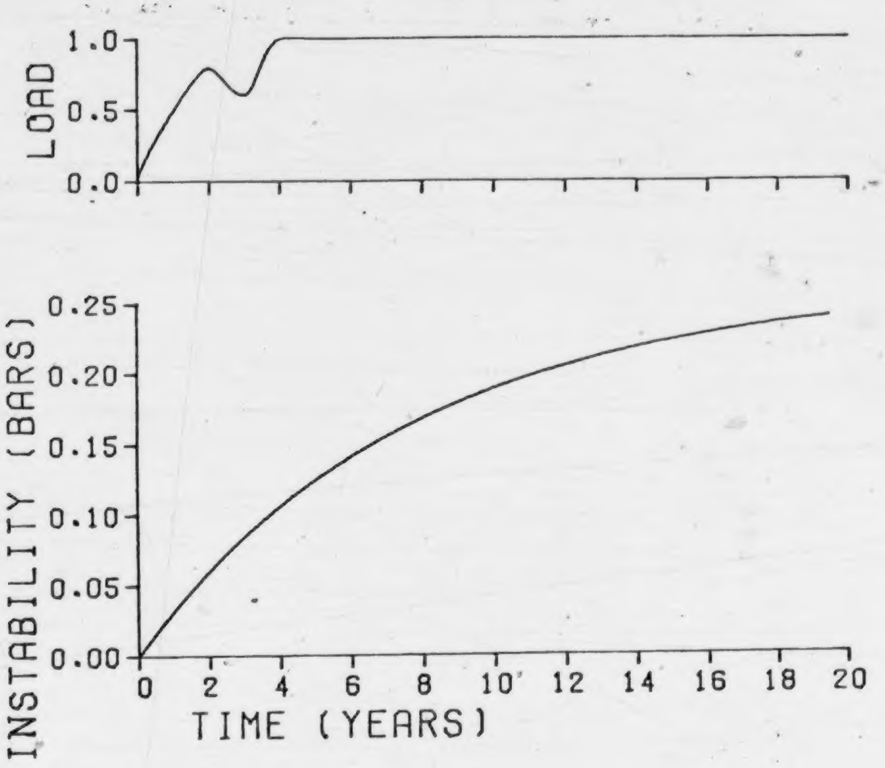

Figure 38.... The upper graph shows the same loading history as that of figure 37. The bottom graph shows the instability at 4 km depth.

It is unlikely that the shallow seismic activity detected in the Itzantun area could be somehow artificially induced. These two areas are also different because of the presence of deep seismicity near Itzantun, which seems to occur at depth on planes parallel to the Middle America trench. The distribution of the deep seismic observed events along the trench is in accordance with this result.

South of the Tehuantepec ridge the observed relative velocity of the plates is less than in the northern part. The angle of subduction in the southern branch of the Middle America trench is 45°. This is less than than the 30° angle deduced for the northern part. Therefore, the deep seismicity observed in the Itzantun area must be related to the Cocos-Caribbean subduction mechanism. This 45° angle implies that the shallow activity observed in the region is not related with deep stress drops or due to the lower coupling between these two plates. Probable causes for it could be upgoing magmas and more likely the shallow events could be related to the presence of the Motagua fault in the vicinity of the area.

6. Discussion of results and further studies proposed

In the preceding chapters of this thesis I have developed the suggestion of treating tectonic problems with stability measures. The concepts are very general but once they are understood they can be explored by making changes in the parameters involved. These changes can be in the definition of the failure envelope, the value of the shear angle used, and the interdependence of the material properties of the models. Changes that are physically reasonable do not usually affect the nature of the instability. In some cases they might enhance the distributions. For this reason it is important to justify as much as possible the use of a particular set of parameters. The choices taken throughout this thesis are not necessarily optimal ones for each case, they are in some cases simplistic to illustrate the method. In general they are representative of what is known about the materials involved in each model. These particular choices have been made for the reasons outlined in the text of the chapters where they were applied.

Following the same procedure many other studies are possible. One of the most interesting ones is that of a triple junction, for which three dimensional analysis is required. Another could be the study of seismic active zones with complicated geology in order to refine the initial model in the relation to the observed seismicity. Geothermal zones might also benefit from this kind of treatment, by following in general, the procedure outlined in chapter IV.

6.1 The Cocos-North America-Caribbean triple junction.

The Middle America trench is the arc where the Cocos plate subducts beneath the North American and the Caribbean plates. The boundary between these last two near the trench is the Motagua fault, which is the continuation of the Cayman trough. These three plates meet in an unstable triple junction (figure 39). The area surrounding this triple junction is the object of this study.

Along the trench several small seismic gaps exist that correlate with the topographic highs of the ocean floor, which are associated with the fracture zones and the aseismic ridges. The Tehuantepec ridge is in the area of interest for this work. It is probable that at this location slip occurs aseismically or that seismic slip takes place in large events rare in time or perhaps the subduction process has been severely modified (McNally and Minster,1981).

The seismic characteristics of the area have been summarized in figure 39. The shallow activity (depth< 70 km, figure 39a), occurs in bands parallel to the plate boundaries. Taking the Middle America trench as divided by the triple junction (at approximately longitude 95° W), no significant difference can be observed between the North-West and the South-East parts of the trench. However, figure 39b shows that the distribution of deep earthquakes (depth > 140 km) is completely one-sided. Deep seismic

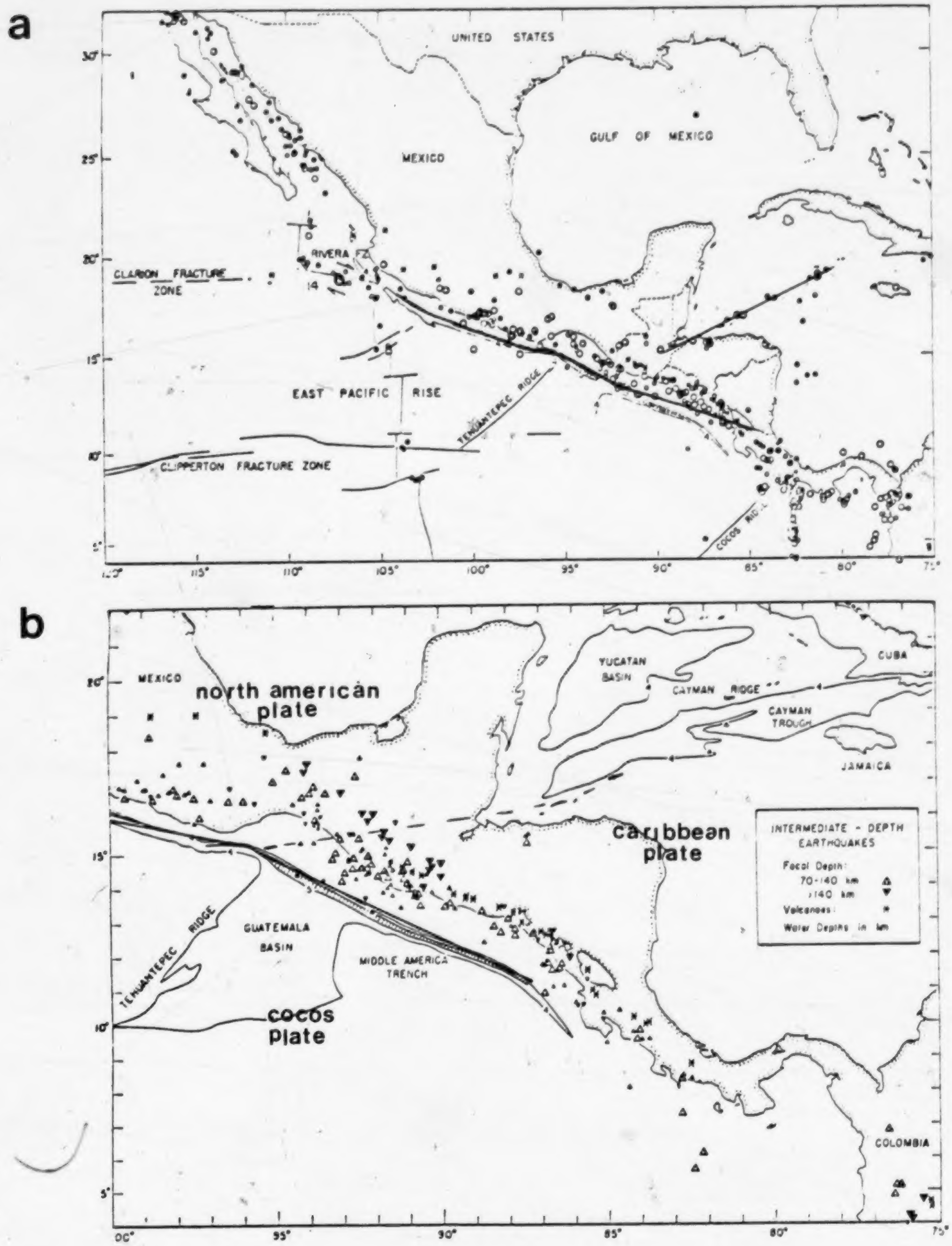

Figure 39.... Tectonic features and epicentral locations recorded in the triple junction area. a) Shows the shallow earthquakes (depth ≤ 70 km) and b) the intermediate and deep events (modified from Molnar and Sykes, 1969)

activity is concentrated mainly in a narrow band on the continental side of the South-East branch of the trench. Deep earthquakes occur where the Cocos plate subducts beneath the Caribbean more frequently than in the Cocos-North American subduction system.

In order to make a first approach to this problem a two dimensional elastic model in the plan of the area was prepared (figure 40). In this simplistic model the Cocos plate pushes the North American and the Caribbean plates in normal directions to the boundaries between them and the Cocos plate. The Caribbean plate is taken as fixed. The velocities of subduction assumed for the Cocos plate are 4.0 cm/year for Mexico and 2.3 cm/year for Central America (after McNally and Minster, 1981). This model also takes into account the shear stress developed between the Caribbean and North American plates along the Cayman trough. Figure 40a shows this model in which all the plates are taken as 50 km thick. Due to the nature of the model it does not permit the modelling of any kind of three dimensional structures such as subduction zones. Although it is highly idealized the earthquake risk distribution (figure 40b) resulting from the use of the instability function as described in section 2.6 shows the following interesting features.

1. It predicts a banded zone of high risk that runs parallel to the boundaries between the Cocos and the other two plates involved in the system.

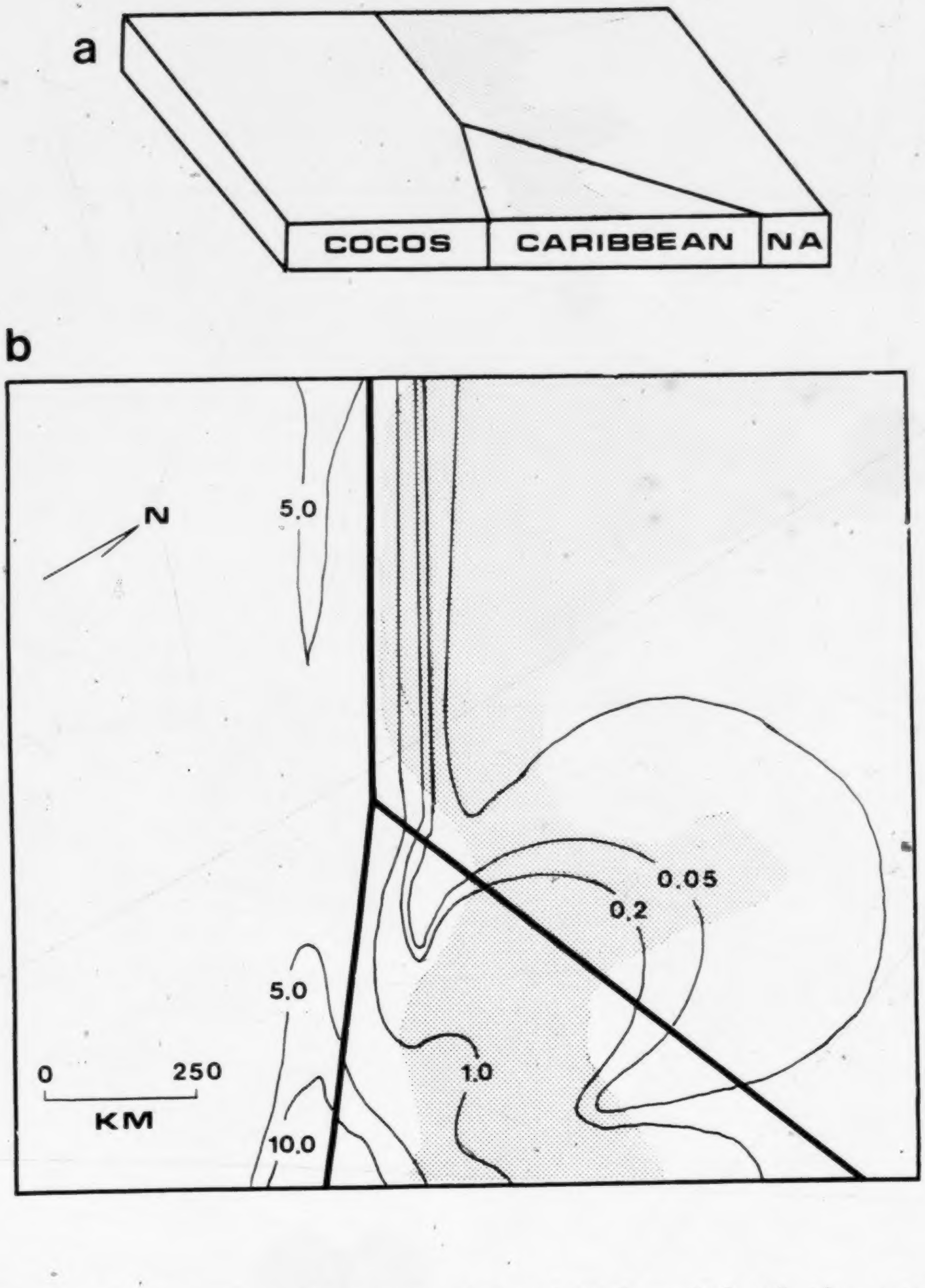

Figure 40.... Shows the two dimensional model of the area in the upper diagram, and the resulting instability function for this model in the bottom one.

2. This risk band is discontinuous in the triple junction area.
3. The instability varies along the Cayman trough creating concentrated areas of high risk along it.

It is remarkable that this simple model delineates some of the high seismicity areas that have has been observed. It also predicts the non-uniform seismic behaviour of the Motagua fault in which events have been rare and localized. However, the most important feature that this model predicts is the presence of the Tehuantepec gap, which is a feature that has been the object of many investigations.

The agreement between the results of this model with the seismic behavior observed for the region suggests the use of instability functions for more complicated models. This will allow a better understanding of the tectonics of the area.

The three dimensional modelling exercise can be approached with the help of the ADINA program. This finite element model is representative of the geodynamical processes that are thought to occur in the area. For its understanding the discussion of the results presented throughout this thesis is of primary importance, since this model involves most of the situations that have been treated in the different parts of this work. The characteristics of the model shown in figure 41 are:

1. The materials of the upper 25 km of the lithosphere are treated as elastic.

2. Visco-elasticity is assumed beneath this depth. The material properties, their inter-dependence and their distribution as a function of depth is taken to be the same as in the models of the different slabs on chapter IV.
3. The coupling force between the plates varies with the angle of subduction as described in section 4.1.
4. At the North-Western part of the Middle America trench, the Cocos plate subducts beneath the North America plate at an angle of 30°, in N37°E direction (McNally and Mister, 1981).
5. At the South-Eastern branch of the triple junction the Cocos plate moves beneath the Caribbean plate at a subduction angle of 45° in a N26°E direction (McNally and Mister, 1981).
6. The model consists of 550 nodes and 405 parallelopiped elements (figure 41).
7. Only vertical displacement is allowed for the nodes located in the vertical outer walls of the model.
8. The model represents an area of 2.75×10^5 km^2, and a depth range from 0 to 200 km.

For the instability study of this model the probabilty function described in section 2.6 was used. To do this, first the stress components for each of the nodes of the model were determined in the same way as in chapter IV. The resulting distribution of probability of seismic failure for this model is shown in figures 42 and 43. Horizontal cross

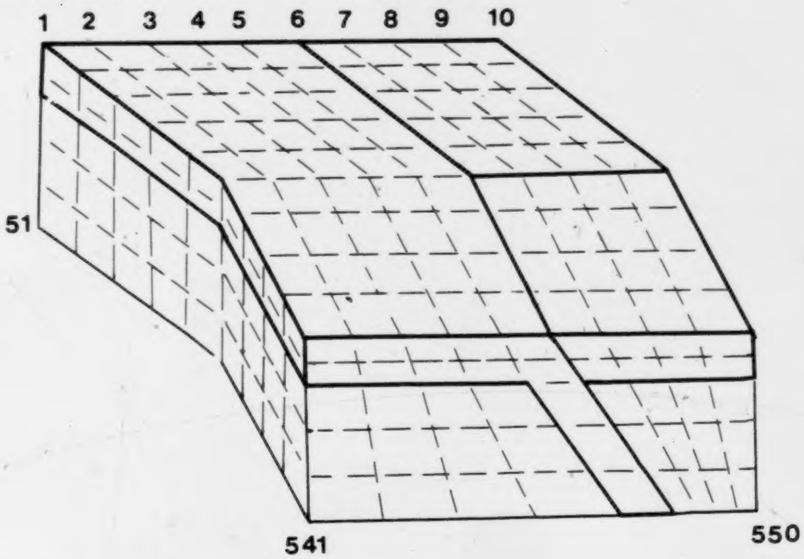

Figure 41.... Shows the element distribution used for the three dimensinal model

sections of this distribution are shown at a depth of 25 , 50, 100, and 150 km (figure 42). The other cross section represents the probability of failure along the plane of the boundary between the plates (figure 43) that is, along the upper surface of the subducting slab.

Figures 42 show the variation of the distribution of this function as a function of depth. In these figures the broken dotted line between points A and B represents the upper surface of the subducting slab. The other dotted line represents the vertical projection of the Cayman trough at depth.

At a depth of 25 km (figure 42a) the high probabilty area is a wide band that seems to follow the boundaries between the Cocos and the other two plates. The interesting part is that the band becomes narrower in the area of the Tehuantepec gap. This high probability band seems to reduce its width with depth, as it appears as a narrow band in figure 42b which corresponds to the 50 km cross section. However, it remains located at the intraplate boundary.

Figure 42c shows that at a depth of 100 kilometers the high probability area has vanished completely. This figure also shows two highly localized areas where the probability function attains values of less than 0.2, one of them intersects the Cayman trough projection and the other is by the North-Western part of the Cocos-North America plate boundary.

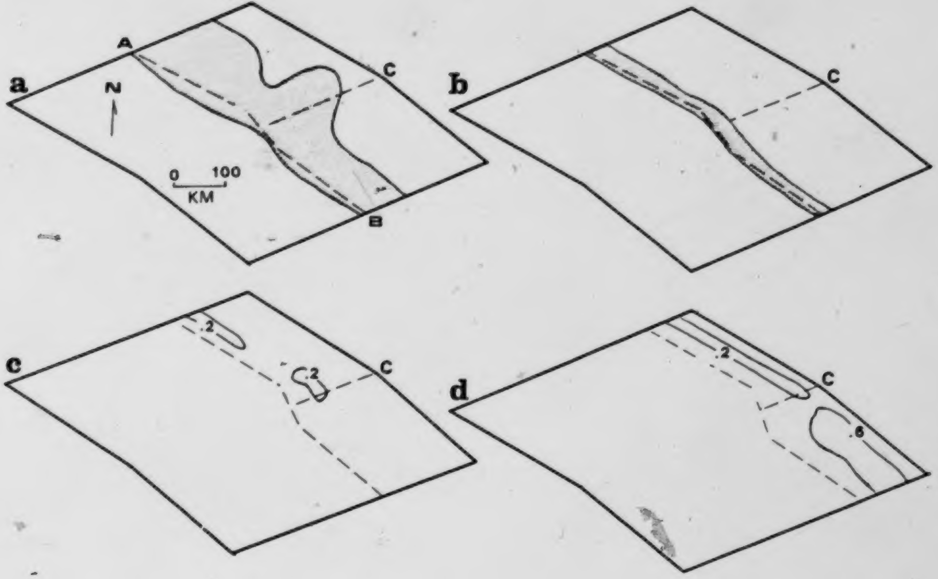

Figure 42.... Shows the probability function distributions for horizontal cross-sections at depths of a) 25, b) 50, c) 100 and d) 150 km.

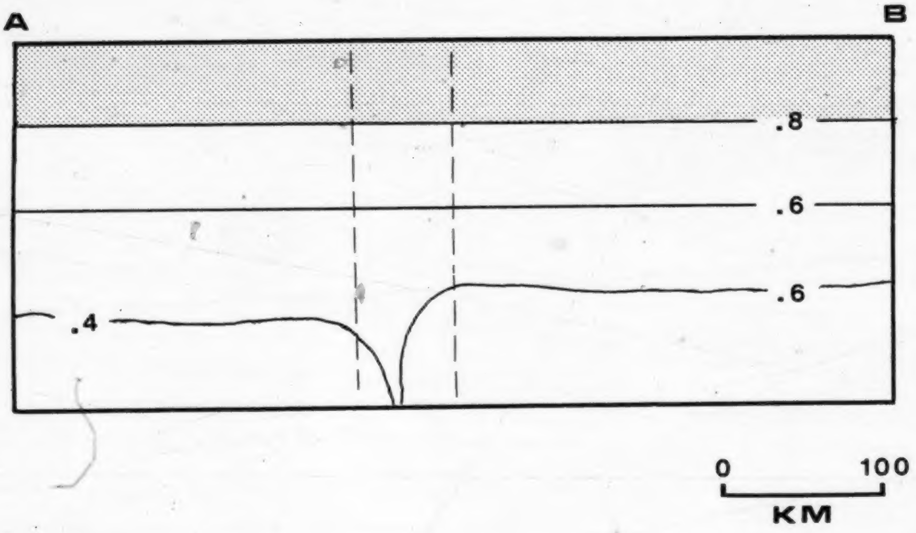

Figure 43.... Shows the probability distribution at the upper surface of the slab with depth

This low probability zone seems to be expanding with depth as shown in figure 42d, in which the other important feature is the significantly different value attained by the probability function at both sides of the Cayman trough at depth. An area of probability values higher than .6 is present inland of the South-Eastern branch of the Middle America trench. All these can be interpreted as follows: if deep events are to occur they should be focussed to the south-east of the triple junction. This is in accordance with the deep events described in chapter V.

The other point to be made from figure 42 is that although the probability along the Cayman trough is by no means uniform with depth, little can be said that relates to the localized activity observed here. It seems to behave like the upper part of the North-Western branch of the triple junction. Its results seem anomalous mostly because both areas are separated by the Tehuantepec gap area.

Figure 43 shows that the distribution of the probability function is discontinuous across the zone located just North of the triple junction. This is where the Tehuantepec gap is located. It confirms the increase of stability with depths inferred from figure 42, and also shows a big difference in the distribution of probability at depth between both sides of the Caribbean-North America boundary. This figure indicates little about the behaviour at shallow depths probably because of the size of the elements of the model.

6.2 Stress determination on seismic active areas.

In regions in which the general structure of the upper crust has been determined to some extent, and in which seismic events are present, instability studies can be used to determine the state of stress of the area and help to refine the understanding of the geologic processes which are still shaping it.

For instance, consider a thick uniform sedimentary layer in which an igneous body is intruding (figure 44). This represents the instability distribution from a two dimensional model of this problem, using the function described in section 2.3. Figure 44a shows the case in which the intrusive mechanism is considered no longer active. That is, the model is in equilibrium. Figure 44b, on the other hand, considers that the intrussive igneous body is being pushed toward the surface by a vertical force.

From the comparison of both distributions of figure 44, it is apparent that the introduction of buoyancy forces changes the distribution of risk, in such a way that the probability for the occurrence of events in a depth range of 12 to 24 km increases. This is useful in two ways. One is that if events have been observed at particular depths the actual buoyant force can be determined, and the other is the opposite. If the state of stress can be determined from other sources then the probable depth of the activity of the area can be estimated.

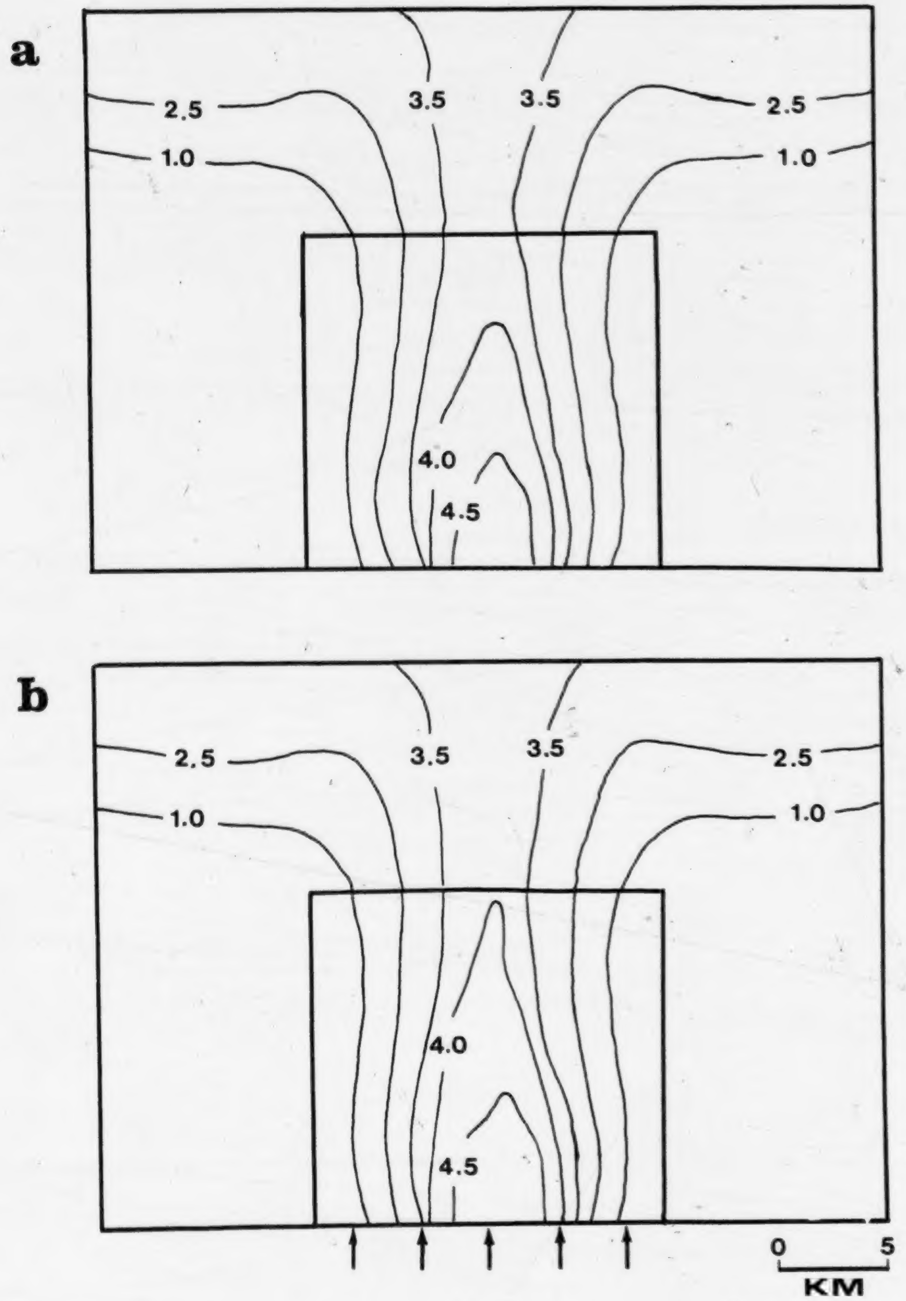

Figure 44.... Shows the instability of a model of a magmatic intrusion. a) no buoyancy forces are applied. b)Buoyancy forces are applied at the bottom of the intruding body.

The same kind of approach can be applied to problems involving other kinds of geological structures as faults, folds, horsts or grabens.

6.3 Concluding remarks.

Instability functions are useful in the interpretation of the geodynamical processes that take place in the lithosphere. The results are highly dependent on the accuracy of the model used to calculate the stresses. This restricts the instability distributions to be representative only in a regional sense. Local high resolution studies can be done if a detailed model is available.

The results obtained here for the Middle America region are in accordance with the overall knowledge about the tectonics of the area. The observed deep seismicity at Itzantun and the probability distributions for the three dimensional model coincide with the observed seismicity. Shallow events ($\leq$ 70 km deep), are more likely to occur and deep events must occur more often south of the Tehuantepec ridge. On the Motagua fault the probability distribution indicates that events should occur rarely.

The stress drops due to seismic activity to the north of the Tehuantepec ridge are associated with a shallower subduction angle than those occurring in the southern branch of the trench. Therefore, the range at which they may have any effect on local seismicity of other areas should be greater.

The three dimensional probability calculation is not able to predict the Tehuantepec gap in a satisfactory way This could be because the size of the elements used to model the elastic plates is too big, or because the model is inaccurate for this part. The subducting plate is modelled to simulate the Cocos plate bending from a angle of 45° in the south to one of 30° in the northern branch of the trench across the Tehuantepec ridge. One way to decrease the probability and create the gap is to assume that the plate is uncoupled between both subduction mechanisms, which is one of the proposed theories for the existence of the gap.

References.

Aki, K. and Richards, P. (1980). *Quantitative Seismology* , W. H. Freeman and Company, San Francisco. 557p.

Allen, C. R. (1975). Geological Criteria for evaluating seismicity ; *Bull. Geol. Soc. Amer.* **55**, 1041-1057.

Barenblatt, G. I.; Keilis-Borok V. I. and Vishik, M. M. (1983). A model of the clustering of earthquakes ; *Geophys. J. R. Astron. Soc.* (in press).

Bathe, Klaus-Jurden (1978). ADINA: a finite element program for automatic dynamic incremental nonlinear analysis; *Massachusetts Institute of Technology* , 82448-1.

Bathe, Klaus-Jurden (1981). ADINAT: a finite element program for automatic dynamic incremental nonlinear analysis of Temperatures; *Massachusetts Institute of Technology* , AE 81-2.

Bell, J. S. and Gough, D. I. (1981). Northeast-Southwest compressive stress in Alberta: Evidence from oil wells; *Earth and Planetary Science Letters* **45**, 475-482.

Bell, M. L. and Nur, A. (1978). Strength changes due reservoir pore pressure and stress and application to lake Oroville; *J. Geophys. Res.* **83**, 4469-4483.

Biot, M. A. (1941). General theory for three dimensional consolidation ; *Journal of Applied Physics* **12**, 578-581.

Bird, P. (1978). Finite element modelling of lithosphere deformation: The Zagros collision orogeny; *Tectonophysics* **50**, 307-336.

Brown, C. B. and King, I. P. (1966). Automatic embankment analysis: equilibrium and instability conditions; *Geotechnique* **16**, 209-219.

Bufe, C. G.; Lester, F. W.; Lahr, K. M.; Lahr, J. C.;Seekins, L. S. and Hanks, T. C. (1976). Oroville earthquakes: Normal faulting in the Sierra Nevada foothills ; *Science* **192**, 72-74.

Bullard, E. C.; Everett, J. E. and Smith, A. G. (1965). Fit of Continents Around the Atlantic , in *A Symposium on Continental Drift*, Roy. Soc. London Phil. Trans. 258, London 41-75.

Byerlee, J. D. and Brace, W. F. (1969). High-pressure mechanical instability in rocks ; *Science* **164**, 713-715.

Cazenave, A.; Lago, B.; Dominh, K. and Lambeck K. (1980). On the response of ocean lithosphere to sea-mount loads from GEOS 3 satellite radar altimeter observations ; *Geophys. J. Roy. Astron. Soc.* **63**, 233-253.

Chase, C. G. (1972). The N plate problem of plate tectonics ; *Geophys. J. R. Astron. Soc.* **29**, 117-122.

Chapple W. M. and Tullis T. E. (1977). Evaluation of the Forces that Drive the Plates ; *J. Geophys. Res.* **82**, 1967-1984.

Chinnery, M. A. (1964). The strength of the earth's crust under horizontal shear stress ; *J. Geophys. Res.* **69**, 2085-2089.

Comninakis P. ; Drakopolus J. ; Moumoulidis, G. and Papazachos, B. C. (1968). Foreshock sequences at the Kremasta earthquake and their relation to water loading of the Kremasta artificial lake ; *Annali di Geofisica (Rome)* **21**, 39-71.

Cook, N. G. W. (1976). Seismicity associated with mining ; *Engineering Geology* **10**, 99-122.

Cox A. (1973). *Plate Tectonics and Geomagnetic reversals* , W. H. Freeman and Co., San Francisco. 690p.

Cruickshank, C.; Herrera I.; Yates R.; Hennart, J. P.; Baladerezo, D. and Magana, R. (1979). Modelo de prediccion del hundimiento del subsuelo del Valle de Mexico; Report 9138 from the Instituto de Ingenieria; *UNAM* , 1-51.

Engdahl, E. R. and Scholz, C. H. (1977). A double Benioff zone beneath the Central Aleutians: an unbending of the lithosphere; *Geophys. Res. Lett.* 10, 473-476.

Evinson, F. F. (1977). The precursory earthquake swarm ; *Phys. Earth Planet. Interiors* 15, 19-23.

Figueroa, J. (1971). Sismicidad en la Cuenca del Valle de Mexico; *Instituto de Ingenieria, UNAM* 289, 237-248.

Forsyth, D. W. (1979). Lithospheric Flexure ; *Rev. of Geophys. and Space Phys.* 17, 1109-1114.

Gasperini, P.; Caputo, M.; Keilis-Borok, V. I.; Marcelli, G. and Rotvain, I. M. (1978). A swarm of weak tremors as precursors of strong earthquakes in Italy; *Vichislitelnaya Seismol. (Computational Seismology* 11, 3-13.

Gough, D. I. (1978). Induced seismicity , in *The Assesment of Mitigation of Earthquake Risk*, UNESCO, 341.

Gough, D. I. and Bell, J. S. (1981). Stress orientations from oil wells in Alberta and Texas ; *Can. J. Earth Sci.* 18, 638-645.

Gough, D. I. and Gough, W. I. (1970). Stresses and deflection in the lithosphere near lake Kariba-I ; *Geophys. J. Roy. Astron. Soc.* 21, 65-78.

Gough, D. I. and Gough, W. I. (1970.b). Load induced earthquakes at lake Kariba-II ; *Geophys. J. Roy. Astron. Soc.* 21, 79-101.

Gough, D. I. and Gough, W. I. (1976). Incremantal stresses near the Cabora Bassa Gorges ; *Engineering Geology* 10, 211-218.

Gradshteyn, I. S. and Ryzhik, I. M. (1965). *Table of*

Integrals, Series, and Products , Academic Press, New York. 1086p.

Griggs, D. T. (1972). The sinking lithosphere and the focal mechanism of deep earthquakes , in *The nature of solid earth*, Robertson E.C., Mcgrall Hill, 361-384.

Gunn, R. (1947). Quantitative aspects of juxtaposed Ocean Deeps, Mountain Chains and Volcanic Ranges ; *Geophysics* 12, 238-255.

Gupta, H. K. and Rastogi, B. K. (1976). *Dams and Earthquakes* , Elsevier, Amsterdam. 229p.

Gupta, H. K.; Rastogi, B. K. and Narain (1972). Common features of the reservoir associated seismic activities ; *Bull. Seismol. Soc. Amer.* 62, 481-492.

Gutenberg, T. J. T. (1949). *Internal Constitution of the Earth* , Dover, U.S.A.. 439p.

Haimson, B. (1978). The hydrofracturing stress measuring method and recent field results; *International Joun. of Rock Mechanics and Mining Soc.* 15, 167-178.

Haimson, B. and Fairhurst, C. (1970). In situ stress determination at great depths by means of hydraulic fracturing, in *Proc. 11th Symp. on Rock Mechanics*, American Inst. of Mech. Eng., U.S.A. 559-584.

Hanks, T. C. and Raleigh, C. B. (1980). The conference on magnitude of deviatoric stress in the Earth crust and uppermost mantle; *J. Geophys. Res.* 85, 6083-6085.

Hast, N. (1958). The measurement of rock pressure in mines ; *Abs. Geol. Unders.* 52, 3.

Havskov, J. (1982a). Preliminary report on the 19 February, 1980 Mexico City earthquake: Foreshocks, Mainshock and Aftershocks; *Geofisica Internacional* (in press).

Havskov, J. (1982b). The 1981 earthquake swarm in Mexico

City ; *Geofisica Internacional* (in press).

Havskov, J. and Singh, S. K. (1978). Shallow crustal studies below Mexico City ; *Geofisica Internacional* 17, 223-229.

Healy, J. H.; Rubey, W. W.; Griggs, D. T. and Raleigh, C. B. (1968). The Denver earthquakes ; *Science* 161, 1301-1310.

Hess, H. H. (1962). History of ocean basisns , in *Petrologic Studies*, Geo. Soc. of America, U.S.A. 599-620.

Hoek, E. and Brown, E. T. (1981). Empirical strength criterion fro rock masses ; *ASCE Geotech. Engng. Division* 106, 1013-1035.

Hubert, M. K. and Willis, D. G. (1957). Mechanics of hydraulic fracturing ; *Joun. Petrol. Technol.* 9, 153-168.

Instituto de Geologia (1968). *Carta Geologica de Mexico, Hoja Mexico 14Q H*, Universidad Nacional Autonoma de Mexico, Mexico. 5p.

Isacks, B. and Molnar, P. (1971). Distribution of stress in the descending lithosphere from a global survey of focal mechanism solutions of mantle earthquakes; *Rev. Geophys. Space Phys.* 9, 103-174.

Isacks, B.; Oliver, J. and Sykes, L. R. (1968). Seismicity and the new global tectonics ; *J. Geophys. Res.* 73, 5855-5899.

Jacoby, W. R. (1970). Instability in the upper mantle and global plate movements; *J. Geophys. Res.* 75, 5671-5680.

Jaeger, J. C. and Cook, N. G. W. (1979). *Fundamentals of Rock Mechanics* , Wiley, New York. 593p.

Kanamori, H. (1971). Great earthquakes at island arcs and the Lithosphere ; *Tectonophysics* 12, 187-198.

Kanamori, H. (1977). Seismic and aseismic slip along subduction zones and their tectonic implications, in *Island Arcs, Deep-Sea Trenches and Back-Arc Basins, Maurice Ewing Series I, A.G.U.*, M. Talwani and W. C. Pitmann III, Washinton D.C. 163-174.

Kanamori, H. and Anderson, D. L. (1975). Theoretical basis of some empirical relations in seismology; *Bull. Seismol. Soc. Amer.* **65**, 1073-1095.

Keilis-Borok, V. I.; Knopoff, L. and Rotvain, I. M. (1980a). Bursts of aftershocks, long-term precursors of strong earthquakes; *Nature* **283**, 259-263.

Keilis-Borok, V. I.; Knopoff, L.; Rotvain, I. M. and Sidorenko, T. M. (1980b). Bursts of seismicity as long-term precursors of strong earthquakes; *J. Geophys. Res.* **85**, 803-811.

Keilis-Borok, V. I.; Knopoff, L. and Allen, C. R. (1980c). Long-term premonitory seismicity patterns in Tibet and the Himalayas; *J. Geophys. Res.* **85**, 813-820.

Keilis-Borok, V. I. and Malinovskaya, L. N. (1964). One regularity in the occurrence of strong earthquakes; *J. Geophys. Res.* **69**, 3019-3024.

Keilis-Borok, V. I. and Rotvain, I. M. (1979). Two long range precursors of strong earthquakes ; *Vichislitelnaya Seismol. (Computational Seismology)* **12**, 18-27.

Kelleher, J.; Savino, J.; Rowlett, H. and McCann, W. (1974). Why and where great earthquakes occur along Island Arcs; *J. Geophys. Res.* 79, 4889-4899.

Kirby, S. H. (1977). State of Stress in the Lithosphere: Inferences from Flow Laws of Olivine; *Pure and Appl. Geophys.* **115**, 245-258.

Knopoff, L. (1971). A stochastic model for the occurrence of main-sequence earthquakes; *Rev. Geophys. Space Phys.* **9**, 175-188.

Lambeck, K. (1980). Estimates of stress differences in the crust from Isostatic considerations; *J. Geophys. Res.* **85**, 6397-6402.

Lamoreaux, R. (1982). *Cluster Patterns in Seismicity* , Ph. D. Thesis, University of Alberta, Edmonton. 199p.

Lamoreaux, R.; Uribe, A. and Nyland, E. (1983). Bursts of seismicity near the Cocos-North American triple junction; *Tectonophysics* **91**, 1-13.

Landau, L. D. and Lifshitz, E. M. (1970). *Theory of Elasticity* , Pergamon Press, Oxford, England. 165p.

Leblanc, G. and Anglin, F. (1978). Induced seismicity at the Manic 3 reservoir, Quebec ; *Bull. Seismol. Soc. Amer.* **68**, 1469-1485.

Leeds, A. R.; Knopoff, L. and Kausel, E. G. (1974). Variations of the upper mantle structure under the Pacific Ocean; *Science* **186**, 141-143.

LePichon, X. Francheteau, J. and Bonnin, J. (1973). *Plate Tectonics* , Elsevier Scientific Publishing Co., Amsterdam. 300p.

Lomnitz, C. (1966). Statistical prediction of earthquakes ; *Rev. Geophys.* **4**, 377-393.

Love, A. E. H. (1924). *A Treatise on the Mathematical Theory of Elasticity* , Dover, New York. 643p.

Marsal, R. J. and Mazari, M. (1969). *The Subsoil of Mexico City* , Universidad Nacional Autonoma de Mexico, School of Engineering, Mexico. 377p.

Mathews, J. and Walker R. L. (1964). *Mathematical Methods of Physics* , Benjamin/Cummings Publishing Co., U.S.A.. 501p.

McGarr, A. (1980). Some constraints on level of shear stress in the crust from observations and theory; *J. Geophys. Res.* **85**, 6231-6238.

Mckenzie, D. P. (1969). Speculations on the consequences and causes of plate motions; *Geophys. J. R. Astron. Soc.* 18, 18-32.

McKenzie, D. P. (1972). Plate tectonics , in *The nature of solid earth*, Robertson E.C., Mcgrall Hill, 323-360.

McKenzie, D. P.and Morgan, W. J. (1969). The evolution of triple junctions ; *Nature* **224**, 125-133.

McNally, K. C. (1977). Patterns of earthquake clustering preceding moderate earthquakes, central and southern California, abstract; *EOS* **54**, 1195.

McNally, K. C. and Minster, J. B. (1981). Nonuniform seismic slip rates along the Middle America trench; *J. Geophys. Res.* **86**, 4949-4959.

McNamee, J. and Gibson, R. E. (1960). Displacement functions and linear transforms applied to diffusion through porous media ; *Quart. Jour. Mech. App. Math.* **13**, 98-111.

McNutt, M. (1980). Implications of regional gravity for state of stress in the earth's crust and upper mantle; *J. Geophys. Res.* **95**, 6377-6396.

Michell, J. H. (1900). The stress in an aelotropic elastic solid with an infinite plane boundary; *London Math. Soc. Proceedings* **32**, 247-258.

Minear, J. W. and Toksoz, M. N. (1970). Thermal regime of a downgoing slab and the new global tectonics; *J. Geophys. Res.* **75**, 1397-1419.

Minster, J. B.; Jordan, T. H.; Molnar P. and Haines, E. (1974). Numerical modeling of instantaneous plate tectonics ; *Geophys. J. R. Astron. Soc.* **36**, 541-576.

Molnar, P. and Sykes, L. R. (1969). Tectonics of the Caribbean and Middle America regions from focal mechanisms and seismicity; *Geo. Soc. of America Bull.* **80**, 1643-1684.

Mogi, K. (1969). Some features of recent seismic activity in and near Japan, 2 . Activity before and after great earthquakes; *Bull. Earthquake Res. Inst. Tokio* **47**, 395-417.

Newman, W. I. and Knopoff, L. (1982). Crack fusion dynamics: a model for large earthquakes ; *Geophys. Res. Letters* **9**, 735-738.

Newman, W. I. and Knopoff, L. (1984). A model for repetitive cycles of large earthquakes ; *J. Geophys. Res.* (in press).

Novelo, D. C. (1980). *Sismicidad Profunda en el Sur de Mexico* , Tesis Profesional, UNAM, Mexico. 76p.

Nyland, E. and Withers, R. J. (1976). A fast method for computing load induced stresses in the earth ; *Geophys. J. Roy. Astron. Soc.* **44**, 689-698.

Obert, L.; Merril, R. H. and Morgan, T. A. (1962). Borehole deformation gauge for determining the stress in mine rock; *U.S. Bureau of Mines* **5978**, 11.

Ohtake, M. T. (1976). Search for precursors of the 1974 Izu-Hanto-Oki earthquake, Japan; *Pure and Appl. Geophys.* **114**, 1083-1093.

Oviedo, A. (1967). Estudio geologico del subsuelo, basado en los datos del pozo profundo Texcoco No. 1; *Instituto Mexicano del Petroleo* , 1-14.

O'Neill, M. E. and Healy, J. H. (1973). Determination of source paramenters of small earthquakes from P-wave rise time; *Bull. Seismol. Soc. Amer.* **63**, 559-614.

Packer, D. R.; Lovegreen, J. R. and Born, J. L. (1977). *Reservoir Induced Seismicity. Vol 6* , Woodword-Clyde Consultants, San Francisco. 124p.

Parsons, B. and Sclater, J. G. (1977). An analysis of the variation of ocean floor bathymetry and heat flow with age; *J. Geophys. Res.* **82**, 803-827.

Pomeroy, P. W.; Simpson, D. W. and Sbar, M. L. (1976). Earthquakes triggered by surface quarrying - Wappingers Falls, New York sequence of June, 1974; *Bull. Seismol. Soc. Amer.* **66**, .

Press, F. (1972). The earth's interior inferred from a family of models , in *The nature of the solid earth*, E. C. Robertson editor, McGrall Hill, New York 147-171.

Raleigh, C. B.; Healy, J. H. and Bredehoeft, J. D. (1976). An experiment in earthquake control at Rangely, Colorado ; *Science* **191**, 1230-1237.

Reed-Hill, R. (1973). *Physical Metallurgy Principles* , D. Van Nostran, . 920p.

Reichl, L. E. (1980). *A Modern Course in Statistical Physics* , University of Texas Press, U.S.A.. 710p.

Richardson, R. M. (1978). Finite element modelling of stress in the Nasca plate: driving forces and plate boundary earthquakes; *Tectonophysics* **50**, 223-248.

Richardson, R. M.; Solomon, S. C. and Sleep, N. H. (1979). Tectonic stress in the plates ; *Rev. of Geophys and Spa. Phys.* 17, 981-1019.

Richter, C. F. (1958). *Elementary Seismology* , W. H. Freeman, San Francisco. 768p.

Richter, F. M. (1977). On the driving mechanism of plate tectonics ; *Tectonophysics* **38**, 61-88.

Rice, J. R. and Cleary, M. P. (1976). Some basic stress diffusion solutions for fluid-saturated elastic porous media with compressible constituents ; *Rev. Geophys. Space Phys.* **14**, 227-241.

Rikitake, T. (1977). *Earthquake Prediction* , Elsevier, Amsterdam. 357p.

Ringwood, A. E. (1975). *Composition and Petrology of the*

Earth's Mantle , McGrall-Hill, New York. 618p.

Rothe, J. P. (1973). Summary: geophysical report , in *Man made lakes: their problems and enviromental effects*, Washington, Amer. Geophys. Union (Geophysical monograph 17), 441-454.

Sacks, I. S. (1983). The subduction of young lithosphere ; *Geophys. Res. Letters* 88, 3355-3366.

Sauber, J. and Talwani, P. (1980). Application of Keilis-Borok and McNally algorithms to earthquakes in the Lake Jocasse area, South Carolina; *Phys. Earth Planet. Inter.* 21, 267-281.

Savage, J. C. and Prescott, W. H. (1978). Comment on "Nonlinear stress propagation in the earth upper mantle by H. J. Melosh"; *J. Geophys. Res.* 83, 5005-5010.

Scheidegger, A. E. (1974). *The Physics of Flow Through Porous Media* , University of Toronto Press, Toronto. 353p.

Scholz, C. H. (1968). The frequency-magnitude relation of microfracturing in rock and its relation to earthquakes; *Bull. Seismol. Soc. Amer.* 58, 399-415.

Scholz, C. H. (1977). A discussion of the state of stress on faults in rock and its relation to earthquakes, in *Proceedings of the conference on experimental studies of friction with applications to earthquake predictions*, U.S. Geological Survey, Reston, Va. .

Shimazaki, K. and Nakata, T. (1980). Time predictable recurrence model for large earthquakes; *Geophys. Res. Letters* 7, 279-282.

Simpson, D. W. (1976). Seismicity changes associated with reservoir loading ; *Engineering Geology* 10, 123-150.

Simpson, D.W. and Negmatullaev, S.K. (1981). Induced seismicity at Nurek reservoir Tadjikistan, USSR ; *Bull. Seismol. Soc. Amer.* 71, 1561-1586.

Singh, S. K.; Astis, L. and Havskov, J. (1981). Seismic gaps and recurrence periods of large earthquakes along the mexican subduction zone: a reexamination; *Bull. Seismol. Soc. Amer.* 71, 827-843.

Singh, S. K.; Espindola, J. M.; Yamamoto, J. and Havscov, J. (1983). Seismic potential of the Acapulco-Sn Marcos region along the mexican subduction zone ; *Geofisica Internacinal* (in press).

Soboleva, O. V. and Mamadaliev, U. A. (1976). The influence of the Nurek reservoir on local earthquake activity ; *Engineering Geology* 10, 293-306.

Solomon, S. C.; Richardson, R. M. and Bergman, E. A. (1980). Tectonic stress: models and magnitudes; *J. Geophys. Res.* 85, 6086-6092.

Solomon, S. C. and Sleep, N. H. (1974). Some physical models for absolute plate motions ; *J. Geophys. Res.* 79, 2557-2567.

Spanos, T. J. T. (1977). *A Stability Analysis of Thermo-Mechanical Flow in the Earth's Mantle*, Ph. D. Thesis. University of Alberta, Edmonton. 120p.

Stacey, F. D. (1977). *Physics of the Earth* , John Wiley and Sons Co., New York. 414p.

Stagg, K. S. and Zienkiewicz, O. C. (1968). *Rock Mechanics in Engineering Practice* , Wiley, New York. 442p.

Stuart, W. D. (1979). Quasi-static earthquake Mechanics ; *Rev. Geophys. Space Phys.* 17, 1115-1120.

Sykes, L. R. and Quittmeyer, R. C. (1981). Repeat times of great earthquakes along plate boundaries, in *Third Maurice Ewing Symposium-Earthquake prediction*, D. Simpson and P. Richards, Washington, D. C.

Thatcher, W.; Matsuda, T.; Kato, T.and Rundle, J. B. (1980). Lithospheric loading of the 1896 Riku-u earthquake, Northen Japan: Implications for plate flexure and asthenopheric rheology; *J. Geophys. Res.* 85, 6429-6435.

Terzaghi, K. Van (1951). *Theoretical Soil Mechanics* , Wiley, New York. 777p.

Turcotte, D. L. (1974). Are transform faults thermal contraction cracks? ; *J. Geophys. Res.* 79, 2573-2577.

Turcotte, D. L.; Tag, P. H. and Cooper, R. F. (1980). A steady model for the distribution of stress and temperature on the San Andreas fault; *J. Geophys. Res.* 85, 6223-6230.

Uribe-Carvajal, A. (1979). *Determinacion de Epicentros y Magnitudes para Sismos Locales en el Area de Itzantun, Chiapas.* , Tesis Profesional, UNAM, Mexico. 79p.

Uribe-Carvajal, A. and Nyland, E. (1982). Elastic models of seismic failure in the Valley of Mexico; *Pure and Appl. Geophys.* 120, -13.

Uribe-Carvajal, A. and Nyland, E. (1983). Evaluation of the risk of induced seismicity at the Itzantun hydroelectric site. Chiapas, Mexico; *Engineering Geology* 19, 247-259.

Uyeda, S. (1977). Some basic problems in the trench-arc-back arc system, in *Island Arcs, Deep-Sea Trenches and Back-Arc Basins, Maurice Ewing Series I, A.G.U.*, M. Talwani and W. C. Pitmann III, Washinton D.C. 1-14.

Vening Meinesz, F. A. (1964). *The Earth's Crust and Mantle* , Elsevier P. Co., Amsterdam. 124p.

Wang, M.; Hu, Y.; Chen, Y.; Yang, M.; Li, T.; Chin, Y. and Feng, J. (1976). Mechanism of the reservoir impounding earthquakes at Hsinfengkiang and a preliminary endeavour to discuss the case; *Engineering Geology* 10, 331-351.

Wetmiller, R. J. (1981). Microseismicity in the Rocky Mountain House seismogenic zone, Western Canada;

Abstract G.A.C./C.G.U. Meeting, Calgary , A-61.

Wilson, J. T. (1965). Submarine fracture zones, aseismic ridges and the international council scientific unions line: proposed western margin of the East Pacific ridge; *Nature* 207, 907-911.

Withers, R. J. (1977). *Seismicity and Stress determination at Man-made Lakes Ph.D. Thesis*, The University of Alberta, Edmonton. 241p.

Withers, R. J. and Nyland, E. (1976). Theory for the rapid subsidence near reservoirs on layered and porous media ; *Engineering Geology* 10, 169-185.

Withers, R. J. and Nyland, E. (1978). Time evolution under artificial lakes and its implication for induced seismicity ; *Can. J. Earth Sciences* 15, 1526-1534.

Wyss, M. (1977). *Stress in the Earth* , Birhauser Verlag, Basel. 458p.

Appendix A. Introduction to Finite Elements.

This appendix has been included to enable the reader to follow the mathematical procedure followed for the determination of the components of stress in chapters 3, 4, and 6. It shows the development of the finite element technique for its most simple application to continuous elastic materials (Zienkiewicz, 1971). The extension to other kinds of materials is done by changing the stress-strain relationship that describes the behaviour of the material, as described in chapters 1 and 4 for visco-elastic materials.

Elastic properties.

For a three dimensional anisotropic material the six stress components and the strain components in a Cartesian coordinate system are related by

$$\begin{bmatrix} \epsilon_x \\ \epsilon_y \\ \epsilon_z \\ \gamma_{xy} \\ \gamma_{yz} \\ \gamma_{zx} \end{bmatrix} = \begin{bmatrix} a_{11} & a_{12} & a_{13} & a_{14} & a_{15} & a_{16} \\ a_{21} & a_{22} & a_{23} & a_{24} & a_{25} & a_{26} \\ a_{31} & a_{32} & a_{33} & a_{34} & a_{35} & a_{36} \\ a_{41} & a_{42} & a_{43} & a_{44} & a_{45} & a_{46} \\ a_{51} & a_{52} & a_{53} & a_{54} & a_{55} & a_{56} \\ a_{61} & a_{62} & a_{63} & a_{64} & a_{65} & a_{66} \end{bmatrix} \begin{bmatrix} \sigma_x \\ \sigma_y \\ \sigma_z \\ \tau_{xy} \\ \tau_{yz} \\ \tau_{zx} \end{bmatrix} \qquad (A.1)$$

where it is easy to show by the conservation of energy principle that the coeficients of the above matrix must be symmetrical and that constants are sufficient to describe the behaviour of the material.

In geodynamical applications generally and in particular in rock mechanics, we often look at layered or stratified materials. In such materials symmetry in behaviour is obtained about any axis perpendicular to the plane of stratification. The properties in this plane are independent of the orientation of the axis in the plane.

The elastic independent constants remaining in the stress-strain relation are:

$$\begin{bmatrix} \epsilon_x \\ \epsilon_y \\ \epsilon_z \\ \gamma_{xy} \\ \gamma_{yz} \\ \gamma_{zx} \end{bmatrix} = \begin{bmatrix} a_{11} & a_{12} & a_{12} & 0 & 0 & 0 \\ & a_{22} & a_{23} & 0 & 0 & 0 \\ & & a_{22} & 0 & 0 & 0 \\ & & & a_{44} & 0 & 0 \\ & & & & 2(a_{22}-a_{23}) & 0 \\ & & & & & a_{44} \end{bmatrix} \begin{bmatrix} \sigma_x \\ \sigma_y \\ \sigma_z \\ \tau_{xy} \\ \tau_{yz} \\ \tau_{zx} \end{bmatrix} \tag{A.2}$$

By analogy with the isotropic case this can be written as

$$\epsilon_x=(1/E_1)\sigma_x-(\nu_1/E_1)\sigma_y-(\nu_1/E_1)\sigma_z$$

$$\epsilon_y=(\nu_1/E_1)\sigma_x+(1/E_2)\sigma_y-(\nu_2/E_2)\sigma_z$$

$$\epsilon_z=-(\nu_1/E_1)\sigma_x-(\nu_2/E_2)\sigma_y+(1/E_2)\sigma_z$$

$$\gamma_{xy}=(1/G_1)\tau_{xy}$$

$$\gamma_{yz}=(1/G_2)\tau_{yz}=\{2(1+\nu_2)/E_2\}\tau_{xy}$$
$$\gamma_{zx}=(1/G_1)\tau_{xz}$$

(A.3)

if we limit ourselves to the solution of two dimensional, plane strain problems. Considering plane strains parallel to the xy plane we have

$$\epsilon_z=\gamma_{yz}=\gamma_{xz}=0$$

(A.4)

Substituting this into the above we get

$$\sigma_z=\nu_1(E_2/E_1)\sigma_x+\nu_2\sigma_y$$

(A.5)

which results in the following stress strain relations in the xy plane:

$$\epsilon_x=(1/E_1)(1-\nu_1{}^2E_2/E_1)\sigma_x-(\nu_1/E_1)(1+\nu_2)\sigma_y$$
$$\epsilon_y=-(\nu_1/E_1)(1+\nu_2)\sigma_x+(1/E_2)(1-\nu_2{}^2)\sigma_y$$
$$\gamma_{xy}=(1/G_1)\tau_{xy}$$

(A.6)

In the solution by stiffness methods it is more convenient to express the stresses in terms of strains. Writing $E_2/E_1=\eta$, we have

$$\sigma_x=E_1(1+\nu_2)^{-1}(1-\nu_2-2\eta\nu_1{}^2)^{-1}\{(1-\nu_2{}^2)\epsilon_x+\eta\nu_1(1+\nu_2)\epsilon_y\}$$
$$\sigma_y=E_1(1+\nu_2)^{-1}(1-\nu_2-2\eta\nu_1{}^2)^{-1}\{\eta\nu_1(1+\nu_2)\epsilon_x+\eta(1-\eta\nu_1{}^2)\epsilon_y\}$$
$$\tau_{xy}=G_1\gamma_{xy}$$

(A.7)

Or in matrix form

$$\{\sigma\}=\begin{bmatrix}\sigma_x\\ \sigma_y\\ \tau_{xy}\end{bmatrix}=[D]\begin{bmatrix}\epsilon_x\\ \epsilon_y\\ \gamma_{xy}\end{bmatrix}=[D]\{\epsilon\}$$

(A.8)

For plane stress we shall have by taking

$$\sigma_z=\tau_{yz}=\tau_{xz}=0$$

(A.9)

the following stress strain relations

$$\sigma_x=E_1(1-\eta\nu_1{}^2)^{-1}\{\epsilon_x+\eta\nu_1\epsilon_y\}$$

$$\sigma_y=E_1(1-\eta\nu_1{}^2)^{-1}\{\eta\nu_1\epsilon_x+\eta\epsilon_y\}$$

$$\tau_{xy}=G_1\gamma_{xy}$$

(A.10)

The Finite Element method.

The solution of any stress analysis problem can be approached via the formulation of the governing differential equations or by the use of various energy theorems. Essentially the finite element procedure is based on the latter, and uses the well known principle of minimum total potential energy. If U denotes the strain energy expressed as a function of displacements $\{\delta\}$ and if $\{P\}$ is the load system associated with these displacements then the total potential energy is

$$\phi=U-\{\delta\}^t\{P\} \tag{A.11}$$

and has to be minimized in the region considered. Matrix notation will be used to allow for any load system applied.

If now a displacement system throughout the region is specified by giving displacement values at each of the nodes such that a particular node affects only the displacements in adjacent elements, (figure 45), then an approximate solution can be obtained by differentiating the potential energy with respect to the nodal values, element by element, and adding the appropiate differentials of all elements to minimize the total potential energy.

In any element the displacements $\{\delta\}$ at any point can be written in terms of the nodal displacements $\{\delta^d\}$

$$\{\delta\}=[N]\ \{\delta^d\} \tag{A.12}$$

from which the strains at any point can be found as

$$\{\epsilon\}=[B]\ \{\delta^d\} \tag{A.13}$$

Then by Hooke's law the stresses are given as

$$\{\sigma\}=[D](\{\epsilon\}-\{\epsilon_o\}) \tag{A.14}$$

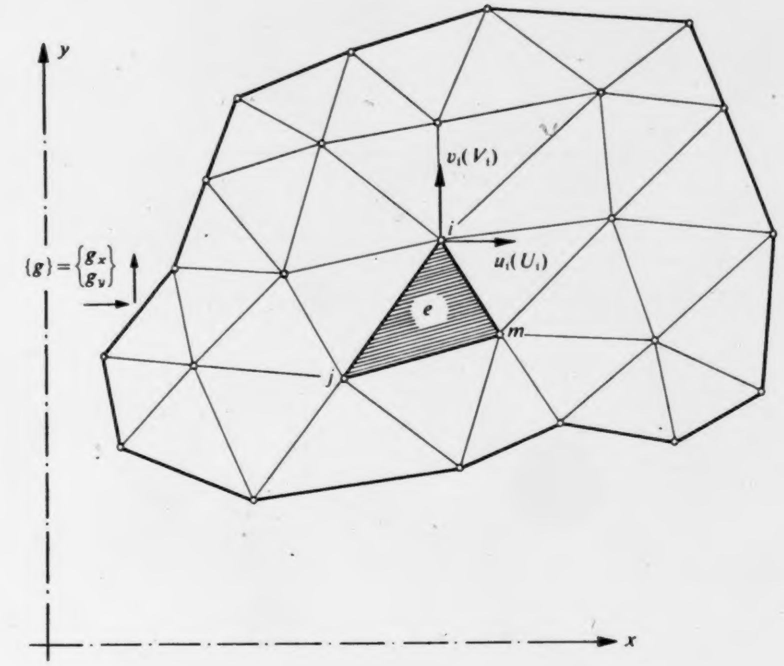

Figure 45.... Subdivision of a continium into finite elements

Now the strain change of an element due to a change $\Delta\{\delta^d\}$ may be expressed as

$$\Delta U^d=\Delta\{\delta^d\}^t\begin{bmatrix}\partial U^d/\partial\delta_i\\ \partial U^d/\partial\delta_j\\ \partial U^d/\partial\delta_k\end{bmatrix}=\int\int\Delta\{\epsilon\}^t\{\sigma\}d(\mathrm{vol}) \qquad (A.15)$$

with the integration taken over the volume of the element. Using equations (A.13) and (A.14)

$$\Delta(U^d)=\Delta\{\delta^d\}^t\{\int\int[B]^t[D][B]d(\mathrm{vol})\{\delta^d\}-\int\int[B]^t[D]\{\epsilon_0\}d(\mathrm{vol})\} \qquad (A.16)$$

In the same way, if the external loads {P} are divided into concentrated loads {C} associated with nodal displacements and distributed loads {c}, the variation of the loads in an element can be written as

$$\Delta(-\{\delta\}^t\{P\})=-\Delta\{\delta^d\}^t\begin{bmatrix}\partial\{\delta\}^tP/\partial\delta_i\\ \partial\{\delta\}^tP/\partial\delta_j\\ \partial\{\delta\}^tP/\partial\delta_k\end{bmatrix}$$

$$=\{\delta^d\}^t\{-\{C\}-\int\int[N]^t\{c\}d(\mathrm{vol})\} \qquad (A.17)$$

Thus the change in potential energy in any element can be expressed in terms of the nodal values of displacements associated with the element as

$$\begin{bmatrix} \partial\phi/\partial\delta_i \\ \partial\phi/\partial\delta_j \\ \partial\phi/\partial\delta_k \end{bmatrix} = [K]\{\delta^d\} - \{C\} - \int\int [N]^t \{c\} d(vol) - \int\int [B]^t [D] \{\epsilon_0\} d(vol) \tag{A.18}$$

in which

$$[K] = \int\int [B]^t [D][B] d(vol) \tag{A.19}$$

When equating the individual differentials of the total potential energy to zero to obtain its stationary value, the equations corresponding to a particular node, i, are set up by adding all the appropriate terms $K_{ij}\delta_j$ and the 'i' terms of the last three terms of equations (A.18) for each element.

This is the same process as if [K] were considered as a stiffness matrix of a structural element,

$$\begin{aligned} &\{C\}, \{C'\} = \int\int [N]^t \{c\} d(vol) \text{ and} \\ &\{C^o\} = \int\int [B]^t [D] \{\epsilon_0\} d(vol) \end{aligned} \tag{A.20}$$

as the loading contributions from each element to the equilibrium of a node, due to concentrated, distributed and initial stress forces respectively. Thus the resulting equation at a point 'i' due to equating the appropiate differentials to zero will then be

$$\{F_i\} = \Sigma C_i + \Sigma C'_i + \Sigma C^o_i = (\Sigma K_{i1})\delta_1 + (\Sigma K_{i2})\delta_2 + \cdots \tag{A.21}$$

The summation is taken throughout all the elements.

As δ_i affects only adjacents elements due to the choice of the displacement function many coefficients in the right hand side will be zero and the resulting system of equations

$$[S]\begin{bmatrix}\delta_1\\ \cdot\\ \cdot\end{bmatrix}=\begin{bmatrix}F_1\\ \cdot\\ \cdot\end{bmatrix} \tag{A.22}$$

will have a narrow band form which will be found of assistance in the numerical solution. In order to minimize this band width it is important to number the nodes across the narrow side of the model since the band determines the storage space (SS)

$$SS=Nm \tag{A.23}$$

were m is the maximum nodal difference on any element and N is the total number of nodes in the model. Therefore, the number of operations (NO) that have to be carried out to determine the stiffness of the model is of the order of

$$NO=Nm^2 \tag{A.24}$$

Once all the displacements have been determined, stresses in any element can be calculated by equation (A.14).

Up to this point the finite element description has been taken for a general case. For the problem of a continuous medium divided into triangular elements (figure 45), the displacement throughout the element with components u and v in the x and y directions can be defined as

$$\{\delta\}=\begin{bmatrix}u\\ v\end{bmatrix} \tag{A.25}$$

If the nodal displacements are listed as

$$\{\delta^e\}=\begin{bmatrix}\delta_i\\ \delta_j\\ \delta_k\end{bmatrix} \tag{A.26}$$

and the displacements within the element are assumed to vary as

$$\{\delta\}=\begin{bmatrix}a_1+a_2x+a_3y\\ a_4+a_5x+a_6y\end{bmatrix}=\begin{bmatrix}1 & x & y & 0 & 0 & 0\\ 0 & 0 & 0 & 1 & x & y\end{bmatrix}\begin{bmatrix}a_1\\ \cdot\\ \cdot\\ a_6\end{bmatrix} \tag{A.27}$$

then the six constants a can be determined by equating the six nodal displacement components with x and y coordinates taking an appropiate value as

$$\{\delta^d\}=\begin{bmatrix}u_i\\v_i\\u_j\\v_j\\u_k\\v_k\end{bmatrix}\begin{bmatrix}1 & x_i & y_i & 0 & 0 & 0\\0 & 0 & 0 & 1 & x_i & y_i\\1 & x_j & y_j & 0 & 0 & 0\\0 & 0 & 0 & 1 & x_j & y_j\\1 & x_k & y_k & 0 & 0 & 0\\0 & 0 & 0 & 1 & x_k & y_k\end{bmatrix}\begin{bmatrix}a_1\\a_2\\a_3\\a_4\\a_5\\a_6\end{bmatrix}=[A]\{a\} \qquad (A.28)$$

by equation (A.27)

$$\{\delta\}=\begin{bmatrix}1 & x & y & 0 & 0 & 0\\0 & 0 & 0 & 1 & x & y\end{bmatrix}[A]^{-1}\{\delta^d\}=[N]\{\delta^d\} \qquad (A.29)$$

The strains defined as

$$\{\epsilon\}=\begin{bmatrix}\epsilon_x\\\epsilon_y\\\tau_{xy}\end{bmatrix}=\begin{bmatrix}\partial u/\partial x\\\partial v/\partial y\\\partial u/\partial y+\partial v/\partial x\end{bmatrix}=\begin{bmatrix}0 & 1 & 0 & 0 & 0 & 0\\0 & 0 & 0 & 0 & 0 & 1\\0 & 0 & 1 & 0 & 1 & 0\end{bmatrix}[A]^{-1}\delta^d=[B]\{\delta^d\} \qquad (A.30)$$

define the [B] matrix of equation (A.13).

For calculating the stresses it is necessary to obtain the D matrix in the x and y coordinate system. In the form described by equations (A.9) and (A.10) the matrix is valid for a system in which the x is perpendicular to the strata. Calling [D'] the matrix in which a load system of coordinates exists defining

$$\{\sigma'\}=[D']\{\epsilon'\} \tag{A.31}$$

where

$$[D']=E_1(1+\nu_2)^{-1}(1-\nu_2-2\eta\nu_1^2)^{-1}\begin{bmatrix}(1-\nu_2^2) & \eta\nu_1(1+\nu_2) & 0\\ \eta\nu_1(1+\nu_2) & \eta(1-\eta\nu_1^2) & 0\\ 0 & 0 & G_1\end{bmatrix}$$

the [D] matrix can be obtained by an axis transformation. If the angle between the x' and the x axis is theta as shown in figure 2,

$$\{\sigma\}=\begin{bmatrix}\cos^2\theta & \sin^2\theta & -2\sin\theta\cos\theta\\ \sin^2\theta & \cos^2\theta & 2\sin\theta\cos\theta\\ \sin\theta\cos\theta & -\sin\theta\cos\theta & \cos^2\theta-\sin^2\theta\end{bmatrix}\{\sigma'\}$$

$$=[T]\{\sigma'\} \tag{A.32}$$

As the transformation of strains follows the constant work principle, i. e.

$$\sigma'^t\epsilon'=\sigma^t\epsilon \tag{A.33}$$

or from equation (A.32)

$$\{\sigma\}^t([T]^t)^{-1}\{\epsilon'\}=\sigma^t\{\epsilon\}$$

$\{\epsilon'\}=[T]'\{\epsilon\}$

$\{\sigma'\}=[T]^{-1}\{\sigma\}=[D'][T]'\{\epsilon\}$

$\{\sigma\}=[T][D'][T]'\{\epsilon\}$

therefore

$$[D]=[T][D'][T]' \tag{A.34}$$

The stiffness matrix given by equation (A.19), is dependent on [D] and [B] and neither of these matrices is dependent on the coordinates of integration, thus if an element of unit thickness is considered in

$$[K]=[B]'[D][B]\Delta \tag{A.35}$$

where Δ is the area of the triangle given in terms of the nodal coordinates as the determinant

$$\Delta=1/2\begin{vmatrix} 1 & x_i & y_i \\ 1 & x_j & y_j \\ 1 & x_k & y_k \end{vmatrix} \tag{A.36}$$

The nodal forces and body forces are simply computed from equation (A.20) with all the matrices there, now defined. For the element described the body forces are assumed constant throughout the element and the nodal forces are simply equal to total body force acting on the element assigned in three equal parts to each of the nodes (Zienkiewicz and Cheung, 1965).

Appendix B. Calculation of stress increments in porous media.

The description of stresses in porous media as mentioned in chapter 5, deals with the concept of effective stresses (Terzaghi, 1951). In order to be able to use the instability functions it is necessary to calculate the increments of these stresses when a change in the water content of the media is introduced. This involves the assumption that before any variation is introduced into the medium the model was stable, that is, no seismic movement occurs until the variation is made. The effective stress is then given by the relation:

$$\sigma_0=\sigma_n-P \tag{B.1}$$

where

σ_0= effective stress,

σ_n= neutral stress,

P = pore pressure.

We now recall the assumptions of consolidation theory (Biot, 1941), which were described in chapter 5 of this thesis,

1. Isotropy of the material.
2. Linear stress-strain relations.
3. The strains in the media are small.
4. The water contained in the pores is incompressible but may contain air bubbles.

5. The water flows through the porous skeleton according to Darcy's law. (If a load of water is applied over a sponge it will produce a gradual settling, depending on the rate at which the water is squeezed out of the voids).

Hooke's equation in the absence of fluid can be written as:

$$\epsilon_{ij}=(1+\nu)\sigma_{ij}E^{-1}-\nu\sigma_{kk}\delta_{ij}E^{-1} \tag{B.2}$$

$$\epsilon_{ij}=(\partial u_i/\partial x_j+\partial u_j/\partial x_i)/2$$

where ν is Poisson's modulus and E is Young's modulus.

If P is the pressure of the water contained in the pores of the media, and H describes the effect of the pressure combined with the previous assumptions, then it is possible to write.

$$\epsilon_{ij}=(1+\nu)\sigma_{ij}\nu^{-1}-\nu\sigma_{kk}\delta_{ij}E^{-1}+P/3H\delta_{ij} \tag{B.3}$$

From Biot (1941) we can write:

$$\theta=(\sigma_{xx}+\sigma_{yy}+\sigma_{zz})/H_1+P/R \tag{B.4}$$

where θ is defined as the increment of water per unit volume of the material. This equation following Biot (1941) can be written as:

$$\sigma_{ij}=2G(\epsilon_{ij}+(\eta-1)\epsilon)\delta_{ij}-\alpha\sigma \qquad (B.5)$$

$$\theta=\alpha\eta+\sigma/Q$$

where:

$\alpha=(1+\nu)G\{3H(1-2\nu)\}^{-1}$

$Q^{-1}=R^{-1}-\alpha/H$

$\eta=(1-\nu)/(1-2\nu)$

$G=E/(2+2\nu)$

$\epsilon=\nabla u$

$a=(1-2\nu)\{2G(1-\nu)\}^{-1}$

$a_1=a\{2G(1-\nu)\}^{-1}$

Introducing this notation equation (B.5) gives

$$G(\nabla^2 u_i+(2\eta-1)\epsilon_{ji})-\alpha\sigma_{ji}=0 \qquad (B.6)$$

knowing that Darcy's law for a non turbulent flow is:

$$v_i=-K\partial\sigma/\partial x_i \qquad (B.7)$$

Where K is the permeability of the material. We assumed that the water is incompressible, therefore the increase of water content in an element of the solid matrix equals the flow:

$$\partial\theta/\partial t=-\partial v_x/\partial x-\partial v_y/\partial y-\partial v_z/\partial z \qquad (B.8)$$

With (B.5),(B.6) and (B.8) we can now write

$$K\nabla^2\sigma-\alpha\partial\epsilon/\partial t+Q^{-1}\partial\sigma/\partial t=0 \qquad (B.9)$$

In order to solve equations (B.6) and(B.9) we will use the displacement functions of McNamee and Gibson (1960) following the method used by Withers (1976) and Withers and Nyland(1976,1978).

Taking the divergence of equation (B.6)

$$\nabla^2(2G\eta\epsilon-\alpha\sigma)=0$$

Now if ϵ is harmonic ($\nabla^2 S=0$) it follows

$$2G\eta\epsilon-\alpha\sigma=2G\partial S/\partial z$$

We can introduce the other scalar function 'E' of Mcnamee and Gibson (1960), that will satisfy this equation if

$$U=-\partial E/\partial x+z\partial S/\partial x$$

$$V=-\partial E/\partial y+z\partial S/\partial y$$

$$W=-\partial E/\partial z+z\partial S/\partial z-S$$

$$P=2G\alpha^{-1}(\partial S/\partial z-\eta\nabla^2 E)$$

$$v_z=-K2G\alpha^{-1}(\eta\partial\epsilon/\partial z+\partial^2 S/\partial z^2)$$

$$\epsilon=\nabla^2 E \tag{B.10}$$

Substituting (B.10) into equation (B.9) and time scaling t=tc, we get:

$$\nabla^4 E=d/dt(\nabla^2 E)-2a_1 d/dt(dS/dt) \tag{B.11}$$

and

$$\nabla^2 S=0 \tag{B.12}$$

where

$$a_1=G/(\alpha^2 Q+2G\eta)$$

Equations (B.11) and (B.12) are solved by Fourier transform in the x, y variables and Laplace transforming in time t. The notation used is

$$E_1(p,q,z,t)=\int\int E(x,y,z,t)\exp\{i(p_x+q_y)\}\cdot dxdy \tag{B.13}$$

$$E_2(p,q,z,s)=\int E(p,q,z,t)\exp(-st)\cdot dt \tag{B.14}$$

using

$$dE_2/dt=E_1(p,q,z,t=0)+sE_2p,q,z,s) \qquad (B.15)$$

In order to perform the Laplace transformation we will now introduce the following procedure.

The depth at t ($t_i \leq t \leq t_{i+1}$) is

$$z_2(p,q,s)=\int z_1(p,q,t)\exp(-st)\cdot dt$$

$$=z_2(p,q,t_i)+(t-t_i)\{z_2(p,q,t_{i+1})$$

$$-z_2(p,q,t_i)\}(t_{i+1}-t_i)^{-1} \qquad (B.16)$$

where $z_2(p,q,t)$ is the Fourier transform of the depth $z(x,y,z)$. The Laplace transform in t of this function is:

$$z_2(p,q,s)=\Sigma^m_{n=1}z_{n-1}\{\exp(-st_n)-\exp(-st_{n-1})\}$$

$$+(z_n-z_{n-1})(t_n-t_{n-1})^{-1}\{(t_{n-1}\exp(-st_{n-1})-t_n\exp(-st_n))s^{-1}$$

$$-(\exp(-st_n-\exp(-st_{n-1}))s^{-1}\}+s^{-1}\exp(-st_nh) \qquad (B.17)$$

where: s is the Laplace transform parameter, z_1 is the Fourier transform of the depth at the time, t_n is the nth time at which a depth is known, and m the total number of loading points.

We now have a formula that will allow us to determine $z_2(p,q,s)$ once the Fourier transforms of the load at a finite number of times has been calculated. These Fourier transforms are done by using the advanced mathematical library subroutines of the array processor (AP).

The AP-190L is a high speed peripheral arithmetic array processor, which works in parallel to the main computer. Computation of fast Fourier tranforms can be overlapped with data memory access time.

And as indicated in chapter 5, the use of the AP permits us to deal with the 2 dimensional transforms of the load at a given time as a vector and determine the change of stresses up to that time. The inverse transforms are made without using complicated algorithms and are less time-consuming in the computer than the approach followed by Withers (1977) and Nyland And Withers (1976, 1978). The AP is particularly well suited to the large numbers of multiplications and additions required for matrix arithmetic due to its highly parallel structure.

Clearly we need to discretize the S dependence of the problem. We evaluate Laplace transform explicitly at $s_i=1/t_i$. Thus we determine the parameters A(p,q,s), B(p,q,s) and C(p,q,s) involved in the calculation of the displacement functions of McNamee and Gibson (1960). From these the effective stress components can be obtained.

The condition imposed by the use of the Laplace transform, that we start calculations at time t=0, implies that there is no initial compression and no excess pressure, this means that the result will reflect the effects of the anomalous load alone.

For t=0 we have

$$\frac{d}{dz} S_1(t=0)=0 \tag{B.18}$$

Now the equations (B.11) and (B.12) simplify to

$$(-\mu+d^2/dz^2)(-k^2+d^2/dz^2)E=-2a_1SdS_2/dz$$

$$-K^2+d^2S_2/dz^2=0 \tag{B.19}$$

where $\mu^2=k^2+S$ and $k^2=p^2+q^2$

The solution must be bounded at infinity so by the method of variation (Butkov, 1968, p126) we may write

$$E=A\cdot\exp(-kz)+B\cdot\exp(-\mu z)+a_1zC\cdot\exp(-kz)$$

$$S=C\cdot\exp{-kz} \tag{B.20}$$

The constants A, B and C can be determined from the boundary conditions: at z=0 $\sigma_{xz}=\sigma_{yz}=0$, and at the surface σ_{zz} is the weight of the water alone, which is represented by the compressive load $-T_2(p,q,0,s)$ such that:

$$-T_2/2G=kB(\mu-k)+Ck(1-a_1) \tag{B.21}$$

Sustituting E and S into equation (B.10) it gives the following relations:

$$\alpha P/2G=-(\mu^2+k^2)B+2a_1\eta-1)kC$$

$$B=-(a_4T_2+\alpha P_2)\{2G\eta(\mu+\lambda)(\mu+\lambda)\}^{-1}$$

$$=\Lambda\{2G\eta(\mu+\lambda)(\mu+\lambda)\}^{-1}$$

$$C=(2a_1\eta-1)^{-1}k^{-1}\{\alpha P_2/2G+\eta(\mu^2-k^2)B\}$$

$$kA=-\mu B+a_1C \tag{B.22}$$

$$\Lambda=-(a_4T_2-\alpha P_2)$$

$$\lambda=(\eta+a_4)k\eta^{-1}$$

$$a_4=(2a_1\eta-1)(1-a_1)$$

The excess presure in the pores of the rock is then:

$$P_2/2G=Ck(2a_1\eta-1)\exp(-kz)-\eta B(\mu^2-k^2)\exp(-\mu z) \tag{B.23}$$

The effective stress components are now:

$$\sigma_{xx}/2G=(\partial^2/\partial x^2-\nabla^2)E+z\partial^2S/\partial x^2+\partial S/\partial z$$

$$\sigma_{yy}/2G=(\partial^2/\partial y^2-\nabla^2)E+z\partial^2S/\partial y^2+\partial S/\partial z$$

$$\sigma_{zz}/2G=(\partial^2/\partial z^2-\nabla^2)E-z\partial^2S/\partial z^2+\partial S/\partial z \tag{B.24}$$

Once the stresses have been determined for each s (s is the Laplace transform variable) by means of the procedure described earlier it is necessary now to go back to the time domain, the inverse Fourier transforms are done in the same way as the direct ones but in order to perform the inverse Laplace transform we used the following algorithm.

If the loading history can always be represented by a curve formed by several segments of exponential form, then the time variation in any of the components of stress will also be represented by another curve consisting of segments of exponential form.

Thus once we have the values of the transforms of the stresses at the desired location for each s, corresponding to each of the times of the known load history. We actualy have the necessary information to construct a curve for which inverse Laplace transform will give us the behaviour of one of the components of stress at any time.

This procedure applied to the three principal directions of stress will allow us to calculate at any moment all the required functions to develop the instability criteria at a particular location with respect to a plane of weakness.

In order to illustrate let us consider a loading history formed by only one segment. The curve will then be represented by

$$f(t)=b\{1-\exp(-at)\} \qquad (B.25)$$

and 'a' and 'b' are determined by a least squares technique from known values of f. Then the transform is

$$f(s)=\int_{0}^{t_i}\{1-\exp(-at)\}\exp(-st)dt$$

$$=b\{s^{-1}\exp(-st)+(s+a)^{-1}(\exp(-st-at)\}_{0}^{t_i}$$

$$F=f(s)=b\{s^{-1}-(a+s)^{-1}\} \tag{B.26}$$

When $(F)(s)(s+a)=b(a+s-s)=ba$ we can write

calling: $B=-ba$

$$B+aFs+s^2F=0 \tag{B.27}$$

Given some values of F it is routine to determine B, a and hence b.

The inclusion of several segments in the loading history curve can be done applying the superposition principle (depends on having linear constitutive equations). Thus after the inverse Fourier transform is performed in the AP for a given component of stress the resulting values at some X, Y, Z, are the Laplace transform in discrete form of the change in time of one component of stress. We can divide each of the resulting curves into exponential segments and determine the constants a and b that represent each of these segments. Taking the inverse Laplace transform of each of the segments involved in one of the curves and adding them up, the shape of the variation of a component of stress can be determined for all times.

The proof of the previous statements is as follows:

If f(t)is given as:

$$f(t)=b\cdot\exp(-at)+c \qquad t_1<t<t_2 \tag{B.28}$$

and knowing that the translation of a Laplace transform (Mathews and Walker, 1964) by:

$$L\{f(t-t_1)\}=\exp(-t_2s)L\{f(t)\} \tag{B.29}$$

Then

$$L(s)=\{\exp(-t_1s)-\exp(-t_2s)\}L\{f(t)\}$$

$$L(s)=\{\exp(-t_1s)-\exp(-t_2s)\}(a+s)^{-1}b \tag{B.30}$$

Generalizing (B.30) for $t_2=t_n$ and $t_1=t_{n-1}$

$$L(s)=\{\exp(-t_{n-1}s)-\exp(-t_ns)\}(a_n+s)^{-1}b_n \tag{B.31}$$

Therefore, the Laplace transform of any of the components of stress is given by the previous equation and the variation in time of the component of stress is given as

$$f_n(t)=b_n\exp(-a_nt)+c_n \qquad t_{n-1}\leq t\leq t_n \tag{B.32}$$

where t_n is the nth break point in the loading history.

To test the previous procedure we calculated the double Fourier-Laplace transformation of several shapes of reservoirs and combined them with different loading histories, then performed the inverse transforms in the way described and as result we obtained the curve that we fed in as the loading history. For example the resulting curve (figure 46) is in good agreement with the input that originated it (Table 4).

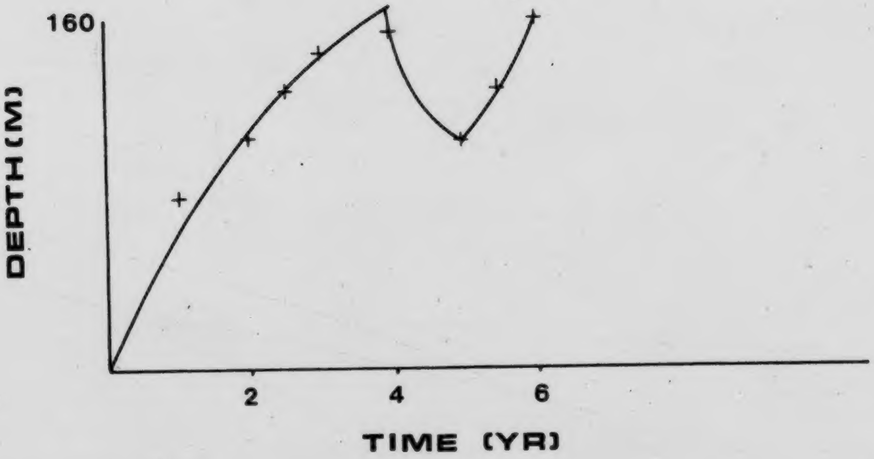

Figure 46.... Resulting curve from an input with several exponential segments

Depth of Water(mts.)	Time(yrs.)
80	0.5
110	1.0
125	2.0
140	2.5
150	3.0
155	4.0
125	5.0
140	5.5
160	6.0

Table 4.... Input data that originated Figure 46 using the procedure described by equations (B.25) to (B.32).